ADDIS ABABA UNIVERSITY
ADDIS ABABA INSTITUTE OF TECHNOLOGY
SCHOOL OF CIVIL AND ENVIRONMENTAL ENGINEERING

BUCKLING RESPONSE ANALYSIS OF CONCRETE CIRCULAR DOMES

A THESIS WORK IN STRUCTURAL ENGINEERING

By Birku Fentaw Ayeru

Addis Ababa
March 2023

Buckling Response Analysis of Concrete Circular Domes

By

Birku Fentaw Ayeru

A thesis submitted to the School of Graduate Studies in Partial Fulfillment of the Requirements for the Degree of Master of Science in Civil Engineering (Structures)

Advisor

Shifferaw Taye (Dr.)

March 2023

The undersigned have examined the thesis entitled ‘‘**Buckling response analysis of concrete circular domes**” presented by **Birku Fentaw**, a candidate for the degree of Master of Science, and hereby certify that it is worthy of acceptance.

By

Birku Fentaw Ayeru

Approved by the Board of Examiners:

Shifferaw Taye (Dr.)	_____	_____
Advisor	Signature	Date
_____	_____	_____
Internal Examiner	Signature	Date
_____	_____	_____
External Examiner	Signature	Date
_____	_____	_____
Chairperson	Signature	Date

UNDERTAKING

I certify that the research work titled "**Buckling response analysis of concrete circular domes"** is my work. The work has not been evaluated elsewhere. When material from other sources was used, it was properly acknowledged/ referred to.

Signature of Student

Birku Fentaw

ABSTRACT

Concrete circular dome roofs are widely used on large-diameter churches, mosques, houses, schools, storage and business facilities, industrial and commercial buildings, football-filled roofs and basketball stadiums, and so on, as they provide high strength for very limited amounts of material: buckling normally controls the design. The purpose of this study is to investigate the linear buckling behaviour of a circular concrete shell with a constant span of 40m. To do so, the linear buckling response of a concrete circular dome under dead load, live load, seismic action, and combinations of these, the linear buckling response of a concrete spherical dome with pinned and fixed support conditions when subjected to the horizontal component of earthquake load, the linear buckling response of a concrete circular dome with variable thickness and rise are investigated. For analysis, analytical and SAP2000 version-21 finite element software is used. In this scenario, five distinct radius-to-thickness ratios are used to determine the linear buckling responses of a circular concrete shell under the action of dead load and the horizontal component of seismic action, and the effect of different dome support conditions is considered. The buckling behaviour of the circular shell roof changes as the radius-to-thickness ratio and span-to-raise ratio change. The numerical value of buckling pressure decreases as the radius-to-thickness ratios and span-to-thickness ratios increase, and vice versa. Different dome structures with different geometry designations are used to make results more reliable. Software results are almost the same as empirical results. Hence, the findings are reliable and valid.

Keywords; Circular concrete shell roof, buckling pressure, Span rise ratio, radius to thickness ratio, buckling load factor, boundary condition

ACKNOWLEDGMENTS

First and foremost, I'd like to thank the Everlasting God and his mother Virgin Merry for their unimaginable patience from the beginning to the end of this paper. Second, I wanted to express my gratitude to the Ethiopian Road Authority (ERA) for providing me with a scholarship to participate in this incredibly educational and experiential journey. My heartfelt gratitude goes to my advisor, Dr Shifferaw Taye, for your patience, guidance, and support. Your wealth of knowledge has been a tremendous blessing to me. I am extremely grateful that you accepted me as a student and continued to believe in me over the years. Finally, I am grateful to my parents for their unfailing love and support, which keeps me motivated and hopeful. My accomplishments and success are the results of their acceptance of me.

Finally, I would like to thank all my friends for sharing reference books and vital information.

TABLE OF CONTENTS

ABSTRACT ..... **IV**

ACKNOWLEDGMENTS ..... **V**

TABLE OF CONTENTS ..... **VI**

LIST OF TABLES ..... **IX**

LIST OF FIGURES ..... **X**

CHAPTER 1 INTRODUCTION **1**

1.1 Back Ground 1

1.2 Main Objectives of the Study 3

1.2.2 Specific Objectives: 3

1.3 Methodology 3

1.4 Scope of the Thesis 4

1.5 Significance of the study 4

CHAPTER 2 LITERATURE REVIEW **6**

2.1 Introduction: 6

2.2 Previous Studies 6

2.3 Shells 8

2.3.1 Definition of Shells 8

2.3.2 Merits and demerits of Concrete Shell Structures 9

2.3.3 Classifications of shells 10

2.4 Assumptions of Classical Theories of Thin Shells 11

2.4.1 General Equations of Forces in Classical Shell Theory 14

2.4.2 The Bond between Strain and Displacement in Thin Shell 19

2.4.3 Stress-Strain Relationships of Thin Shell 20

2.4.4 Force-Displacement Relationship Equations 21

2.4.5 Governing Equation for Membrane Theory Simplifications 21

2.4.6 Limitation of Membrane Theory of Thin Shells 22

2.5 Elastic Stability of Thin Shells 23

2.5.1 Boundary condition of circular shells 28
2.5.2 Initial Geometric imperfection of circular dome 29
CHAPTER 3 CIRCULAR CONCRETE DOME ANALYSIS 31
3.1 Introduction 31
3.2 Analysis of Membrane Forces on a Concrete Circular Dome 31
3.2.1 Axisymmetric Loading Membrane Force Analysis 31
3.2.2 Analysis of Membrane Forces Under Self-weight 35
3.2.3 Analysis of Membrane Forces under Live Load 36
3.2.4 Membrane Force Analysis of a Spherical Shell under Earthquake Action 37
3.2.5 Strains and Displacements from Membrane Theory of Spherical Shells ... 39
3.3 Analysis of Spherical Dome-Ring Beam 42
CHAPTER 4 MATERIALS AND LOAD DETERMINATION 43
4.1 Action Combinations Based on Euro-Codes 43
4.1.1 Materials Based on Euro code Standards 43
4.1.2 The geometry of the Required Models 43
4.2 Load Determination 45
4.2.1 Self-weight 45
4.2.2 Live Load 47
4.2.3 Earthquake (Seismic Action) 47
4.2.4 Determination of Natural Frequency 47
4.2.5 Horizontal Component of Seismic Action 48
4.2.6 Peak Ground Acceleration (PGA) 50
4.3 SAP2000 Finite Element Method for Concrete Dome Buckling 51
4.3.1 Steps of the Finite Element Method 51
4.3.2 Implementation of the Finite Element Method 56
4.3.3 Finite Element Analysis Software SAP200 56
CHAPTER 5 RESULT AND DISCUSSION 59
5.1 Classical Theory Critical Buckling Load Results 59

5.2 Linear buckling analysis Using SAP2000 60
5.3 Comparison between Classical buckling Equation and SAP2000 Results 63
5.4 Effect of Support Conditions 67
5.5 Buckling Analysis of the Effect of a Horizontal Component of Seismic Actions on a Concrete Spherical Shell 68
5.6 Effect of Geometric Imperfection 74
CHAPTER 6 CONCLUSIONS AND RECOMMENDATIONS 75
6.1 Conclusions 75
6.2 Recommendations 76
REFERENCES 77
APPENDIX A 78
APPENDIX B 81

LIST OF TABLES

Table 4-1: The geometrical dimensions of the required models with a thickness (h) =0.1m. 45
Table 4-2:The geometrical dimensions of the required models with a thickness (h) =0.12m. 45
Table 4-3:The geometrical dimensions of the required models with a thickness (h) =0.15m. 45
Table 4-4: The ratio of peak ground acceleration to acceleration due to gravity..... 48
Table 4-5: The value of the parameters describing the recommended Type-I elastic response spectra for ground type B for the horizontal component of seismic action**…..**50
Table 5-1: Critical buckling load and shallowness parameter of each model dome cap with a thickness of 0.1m. 59
Table 5-2: Critical buckling load and shallowness parameter of each model dome cap with a thickness of 0.12m. 59
Table 5-3: Critical buckling load and shallowness parameter of each model dome cap with a thickness of 0.15m. 59
Table 5-4: Critical buckling result in SAP200 V21.1.0 due to the applied load of 3.65kN/m^2. 62
Table 5-5: Critical buckling result in SAP200 V21.1.0 due to the applied load of 4.15kN/m^2. 62
Table 5-6: Critical buckling result in SAP200 V21.1.0 due to the applied load of 4.90kN/m^2.... 62
Table 5-7: Comparisons of classical buckling pressure with SAP200 results in case of 3.65kN/m^2 63
Table 5-8: Comparisons of classical buckling pressure with SAP200 results in case of 4.15kN/m^2 63
Table 5-9: Comparisons of classical buckling pressure with SAP200 results in case of 4.90kN/m^2 64
Table 5-10: Comparison between fixed and pinned support conditions of buckling pressures in SAP200 results..... 67
Table 5-11: Comparison between the effect of seismic action only and Earthquake load plus self-weight of a circular dome on linear buckling load of shells. 70
Table5-12: Analytical result for linear and nonlinear buckling pressure 74

LIST OF FIGURES

Figure2-1 : Normal stresses in 3D thin shell deferential elements:.....12
Figure 2-2: differential thin shell elements.....15
Figure 2-3 Stress (Force) components in differential shell element.....15
Figure 2-4: Moment components of differential shell elements.....16
Figure 2-5: Behavior of shell differential shell element after deformation.....19
Figure 2-6: Structural failure due to buckling or strength.....24
Figure2-7: Behavior of axially compressed elastic columns.....25
Figure 2-8: Effect of initial imperfection.....28
Figure 2-9: Effect of boundary conditions.....29
Figure 3-1: A differential element of a spherical concrete shell surface in polar coordinates.....31
Figure 3-2: Membrane forces and the coordinate system in double curvature spherical shell element. 32
Figure 3-3Reinforced concrete dome shell equilibrium due to the integral load R.....34
Figure 3-4: Concrete spherical dome under its own self-weight.....35
Figure3-5 Spherical concrete dome under imposed or live load 36
Figure 3-6: Seismic surface loading condition on the concrete spherical shell in x-y pane view.....38
Figure 4-1: The geometry of circular shell……...44
Figure 4-2:Seismic hazard map in terms of peak design ground acceleration in Ethiopia…….....49
Figure 4-3: Shape of the elastic response spectrum…….....50
Figure 4-4:Simple line two-node elements typically used to represent a bar or a beam element……..52
Figure4-5: Simple two-dimensional elements used to represent plan stress/strain…..…52
Figure4-6: Simple three-dimensional elements used to represent 3-dimensional stress...52
Figure4-7:Simpleaxisymmetricelement……...53
Figure 5-1: Sample of FE idealization of the first model loaded 3.65kn/m^2 uniform load……61
Figure5-2:The linear eigenvalue buckling load factor in the first mode failure (mode one)……..61

Figure 5-3: The effect of radius to thickness ratio at the applied uniform pressure of 3.65kN/m^2.....64
Figure5-4: The effect of radius to thickness ratio at the applied uniform pressure of 4.15kN/m^2.....65
Figure5-5: The effect of radius to thickness ratio at the applied uniform pressure of 4.90kN/m^2.....65
Figure5-6: The effect of span to raise ratio at the applied uniform pressure of 3.65kN/m^2 66
Figure5-7: The effect of span to raise ratio at the applied uniform pressure of 4.90kN/m^2 66
Figure5-8: The effect of span to raise ratio at the applied uniform pressure of 4.15kN/m^2 66
Figure5-9; Sample for seismic action loading on spherical dome models 68
Figure5-10: The eigenvalue buckling load factor in the first mode failure of the dome under seismic action (mode one) 69
Figure5-11: The eigenvalue buckling load factor in the first mode failure of the dome under seismic action and its self-weight (mode one).....69
Figure5-12: The effect of radius to thickness ratio at the applied uniform pressure of seismic action of 1.5kN/m^2.....71
Figure 5-13: The effect of radius to thickness ratio at the applied uniform pressure of seismic action of 1.8kN/m^2.....71
Figure5-14: The effect of radius to thickness ratio at the applied uniform pressure of seismic action of 1.5kN/m^2.....72
Figure5-15: The effect of span to raise ratio at the applied uniform pressure a seismic action of 1.5kN/m^2.....72
Figure5-16: The effect of span to raise ratio at the applied uniform pressure a seismic action of 1.8kN/m^2.....73
Figure5-17: The effect of span to raise ratio at the applied uniform pressure a seismic action of 1.8kN/m^2.....73

LIST OF SYMBOLS

ε_x Is the strain along the X-axis

ε_y Is the strain along the Y-axis

ε_y Is the strain along the Z-axis

$E_x = E_y = E_z = E$ Is an elastic module of concrete material

$v_{XY} = v_{XZ} = v_{yz} = v$ Is poison's ratio of concrete material

σ_x Is normal stress along the X-axis

σ_y Is normal stress along the Y-axis

σ_z Is normal stress along the Z-axis

γ_{xy} Is shear strain in the XY-plane

γ_{XZ} Is shear strain in the XZ-plane

γ_{yz} Is shear strain in YZ-plane

τ_{XY} Is shear stress in XY-plane

τ_{xz} Is shear stress in XZ-plane

τ_{yz} Is shear stress in YZ-plane

G_{XY} Is the shear modulus of rigidity in XY-plane

G_{XZ} Is the shear modulus of rigidity in XZ-plane

G_{yz} Is the shear modulus of rigidity in YZ-plane

N_x Is internal hoop stress (or force) along X- the direction

N_y Is an internal hoop stress (or force) along the y- direction

N_{XY}; N_{YX} Are internal in-plane shear stresses (forces)

Q_x Is an internal in-plane shear stress (force)

Q_y Is internal out-of-pane shear stress (force)

σ_x ; σ_y; σ_z; Is normal stresses along X, Y, and Z direction respectively.

τ_{xy} ; τ_{yx}; τ_{xz}; Is shear stress along the XY, YX, and XZ-planes

M_x; M_y Is an internal bending moment (or force).

M_{xy}; M_{yx} Is an internal twisting moment (or force).

h Is the thickness of a thin shell

r_x Is the principal radius of a thin shell along the X-direction

$\boldsymbol{r_y}$ Is the principal radius of the thin shell along the Y-direction

ε_{xo} Is an extensional shear strain along the X direction

ε_{yo} Is extensional shear strain along the Y direction

γ_{xy} Is angular shear strain in radian

X_x Is strain due to a change in curvature of the shell element in case of bending along the X

X_y Is strain due to a change in curvature of the shell element in case of bending along the Y

$2X_{xy}$ Is angular shear strain due to bending

$\emptyset_x$; $\emptyset_y$ Is rotation of the middle surface along X and Y direction in radian.

u; v and w are displacements along X; Y and Z respective

P_{cr} Is the classical analysis of buckling load, in $\frac{N}{m^2}$

E Is the Modulus of elasticity, in Mpa

a Is the Radius of the circular dome, in m

$\boldsymbol{v}$ Is Poisson's ratio

H Is the rise of the dome cap

λ Is the shallowness parameter of a spherical dome

r_o Is the radius of a spherical dome cap

∅ Is the meridional angle or cutting angle

$N'_{\emptyset}$ Is the internal membrane force in the meridian direction

N'_{θ} Is internal hoop force in the direction of a parallel circle

$N'_{\emptyset\theta}$ Is the in-plane shear force in the concrete spherical shell

$\boldsymbol{r_1}$ Is the radius of curvature at any point on the meridian

r_2 Is the radius of curvature for the surface from the axis of revolution

∅ Is meridional angle from the axis of revolution

θ Is circumferential angle (or hoop angle)

P_z Is external distributed load applied on the surface of the shell in radial direction per unit area

P_θ Is external distributed load applied on the surface of the shell in hoop direction per unit area

$P_\emptyset$ Is external distributed load applied on the surface of the shell in a meridian direction per unit area

R Is the total vertical load acting along the axis of symmetry

q Is a self-weight or a dead load of a spherical shell

P Is represents the live load on a spherical concrete dome

a_v Is the horizontal seismic acceleration

g Is acceleration due to gravity

γ_c Is the unit weight of concrete

P_s Is earthquake action per unit area distributed over the shell surface

$\boldsymbol{\varepsilon_\theta}$ Is the extensional circumferential strain

$\varepsilon_\emptyset$ Is the extensional meridional strain

$\Delta_{\boldsymbol{H}}$ Is the horizontal translation at the edge of a spherical dome

$\Delta_\emptyset$ Is the rotation at the edge of a spherical dome

$D^D{}_{10}$ Is horizontal deformation due to membrane forces

$\mathrm{D}^{\mathrm{D}}{}_{20}$ Is rotational deformation due to membrane forces

α Is half of the central angle

C Is an integral constant

u Is the displacement tangent to the meridian

w Is the displacement normal to the meridian

G_K is permanent gravity load (self-weight and additional dead load)

Q_K Is live load (variable; imposed load)

E_X Is the horizontal component of seismic action along X-axis

q Is a self-weight or a dead load of spherical dome

r_c is the unit weight of concrete

γ_p is the unit weight of plastering mortar

h_p is 0.05m is the thickness of plastering and painting

K Is represents the stiffness matrix

M Is represents the mass matrix of the structure

ω Is the natural frequency of the structure in rad per second.

λ Is modal vibration or eigenvector

n Is the number of degrees of freedom

T Is the fundamental period of a structure

C_t= 0.05 is the recommended value Euro code-8 of all structures

f Is the fundamental cyclic frequency

$S_e(T)$ Is the horizontal component of the earthquake elastic response spectrum

a_g Is the design ground acceleration on type A ground ($a_g = \gamma_1 * a_{gR}$)

T_B Is the lower limit of the period of the constant spectral acceleration branch

T_C Is the upper limit of the period of the constant spectral acceleration branch

T_D Is the value defining the beginning of the constant displacement response range of the spectrum

S Is soil factor

η Is the damping correction factor with a reference value of $\eta = 1$ for 5% viscous damping

γ_1 Is importance factor

{f} is the vector of nodal element forces,

[k] is the element stiffness matrix and

{d} is the vector of the degrees of freedom or generalized displacements.

{F} is the vector of global nodal forces,

[K] is the structure global or total stiffness matrix, and

{d} is the vector of known and unknown degrees of freedom or generalized displacements

K is the stiffness matrix,

G(r) is the geometric (P-delta) stiffness due to the load vector r,

λ Is the diagonal matrix of eigenvalues,

φ Is the matrix of corresponding eigenvectors (mode shapes)

P_{EX} Is a critical buckling load in SAP2000

P_o Is the load applied in the initial state

λ Is Load factor or eigenvalue

Q is the applied load or perturbation load

CHAPTER 1 INTRODUCTION

1.1 Background

Shells are spatially curved surfaces that support externally applied loads without the use of internal columns and can cover large construction areas with fewer materials than other framed structures. Shells can be found in a variety of natural structures, including eggs, plants, leaves, skeletal bones, and geological forms (Farshad, 2013).

Man has been building shell structures since the beginning of time. In ancient times, humans constructed a shell out of masonry and stone. These shells can still be found in some parts of the world, including Ethiopia. A shell can be named circular (spherical), conical, cylindrical, hyperbolic paraboloid, elliptical shells, or any combination of these. These shells are classified as revolution shells, translation shells, ruled surface shells, and composite shells (Farshad, 2013).

The concrete circular dome with a span length of 40m was the main focus of this thesis. For more than two thousand years, the circular dome, also known as spherical dome shells, has been used as a roof all over the world. From the Middle East to the Roman Empire, and many other cultures in between, those structures were used as the roofs of their most important buildings, making them an iconic symbol of the ancient and modern worlds.

Nowadays, many countries can construct dome structures out of concrete. Ethiopia is currently one of the countries that have constructed a concrete spherical dome. Most of the time, this type of structure is used as the roof of churches, mosques, and large assembly homes in Ethiopia. Large crowds gather in these areas for worship and meetings.

Thus, structural engineers are responsible for the design of concrete shell structures, particularly in earthquake-prone areas. Concrete shells have high structural efficiency and can thus be built very thinly.

Because of their geometry configuration, the internal forces of compression and tension are organized in such a way that the structure can withstand large loads with optimum

performance. Because of their lightweight nature, the earthquake force induced in these thin structures is relatively low.

However, they like any structure do not have infinite resistance, and their geometry, specifically their thickness and rise, is the source of their failure. As a result, unexpected horizontal components of earthquake-induced forces cause bending stresses in concrete thin shell structures. These stresses have the potential to cause structural instability or failure (or damage). The collapse of the structure could result in mass human deaths and property damage.

Before construction, an appropriate design will be made to reduce this type of risk or complete collapse of structures. Buckling analysis of spherical shells under external pressure is a critical problem for proper shell structure design. It is well known that the buckling loads obtained by traditional methods are significantly higher than the experimental results. As a result, this paper focused on the buckling response analysis of concrete circular domes under earthquake action to avoid the loss of lives due to the collapse of structures in earthquake-prone areas. The main realistic cause of reinforced concrete dome shell collapse is structural instability or linear or nonlinear buckling (Peerdeman, 2008).

Experimentation on self-weight, live load and especially seismic action response of full-scale concrete structures is extremely limited, particularly in concrete circular shells. As a result, developing an appropriate numerical method that allows for valuable different loading condition parameters is critical. So, the primary goal of this research is to investigate the effect of dead load, live load, and seismic actions on the instability or linear buckling of concrete circular dome shells with a 40m constant span, two different support conditions, and distinct thickness and dome rise.

For this investigation of the bucking response of domes under various types of applied loading conditions, the variables that affect their behaviour are kept to a minimum; primarily dome shape, thickness, constant span length, cutting angles, and height. Domes may be located in seismic zones in Ethiopia, exposing them to dynamic loads. Although dynamic forces on a concrete dome rarely influence the design, seismic actions are the most destructive force that can be applied to a dome in earthquake-prone areas.

1.2 Main Objectives of the Study

1.2.1 General Objectives:

The general objectives of this study are:

- Investigate the linear buckling response of the concrete circular domes under dead load, live load, seismic action, and combinations of them.
- Examine the linear buckling response of a concrete spherical dome with pinned and fixed support conditions when subjected to the horizontal component of earthquake action.

1.2.2 Specific Objectives:

The specific objectives of this particular case study are:

- Examine the effect of a variety of parameters on the linear buckling response of circular dome shells, including radius-to-thickness ratio, span-to-rise ratio, and boundary conditions.
- Will present the analysis results in tabular and graphical form, displaying geometric variables against the structure's response at the analysis stage.

1.3 Methodology

To achieve the aforementioned goals, ninety models (fifteen models for each loading and support condition) were analyzed one at a time in static loading conditions in SAP2000.v.21 for dead, live, and earthquake load cases. The variable parameters are thickness h; rise H; cutting angle; and radius of the shell a, while the constants are span 2r o = 40 m, Poisson's ratio v= 0.2, dead load q = 3.65 kN/m^2 for models 1 up to 5, q = 4.15 kN/m^2 for models 6 up to 10, 4.15 kN/m^2 for models 1 up to 5, are used for fixed or pinned support condition state, Earthquake loads, ρ_s = 1.5 kN/m^2 for models 1-5, ρ_s= 1.8 kN/m^2 for models 6-10, and ρ_s= 2.25 kN/m^2 for models 11-15. A concrete class must have a grade of C30/37MPa, cylinder compressive strength of concrete f_{ck} = 30MPa, normal weight γ_c = 25kN/m^3, and modulus of elasticity E= 33GPa.

1.4 Scope of the Thesis

The general purpose of this paper is to investigate the linear buckling response behaviour of circular concrete domes under dead load, live load, and seismic action in fixed and pinned support conditions concerning their radius-to-thickness ratio and span-to-rise (height) ratio.

To accomplish the objective of the study, classical theory and finite element software can be used to analyze the circular dome shells SAP2000. V.21 computer software was used for the linear buckling analysis, which was dominated by axisymmetric and asymmetric static loads, as well as theoretically by different shell parameters. Each model was created by assuming and selecting the appropriate shell geometry, support condition, loading condition, materials, and other required parameters from manuals, codes, and standards.

The 40 m constant span and variable thickness (0.1m; 0.12m and 0.15m); different height H; cutting angle ∅ and radius of the shell of the dome, which is located in the earthquake-sensitive area of, zone five in Ethiopia. Normally, this paper has the following limitations:

- It is limited to linear buckling response analysis using membrane theory, which means it does not provide an absolute analysis of all forces required for a complete design.
- It is also limited to linearly elastic materials, i.e. it does not take into account geometric and material nonlinearity, creep, and cracking effects.
- It is not considered all the requirements of the designed purpose procedures; which means the paperwork focused on the analysis part of the dome.

1.5 Significance of the study

The study mainly targeted the linear buckling response behaviour of concrete circular domes with a constant span, of 40m. As it is known, shell structures have high structural efficiency due to their thinness during construction as compared to other framed structures and they have very good geometric configurations, because of this their internal forces of compression and tension are well organized in such a way that they allow the structure withstand (resist) large external applied loads with optimum

performance. In addition, due to their lightweight nature, the seismic force induced on thin shell structures is relatively very low.

However, like any structure, they do not have infinite resistance, due to their geometry, more specifically their thickness and rise (height), which are the source of their failures. So, an expected external force induced on them produced bending stresses on the thin shell structures. These stresses lead to structural instability or failure (or damage). The failure of a circular dome may cause mass death of human beings and property damage.

To minimize these types of risks or complete collapse of structures appropriate design will be made before construction. For proper design of shell structures buckling analysis of a circular dome under an externally applied load is a crucial problem. It is widely known that the buckling loads obtained by classical methods are much higher than experimental results. Hence, this paper mainly focused on showing the relationship of linear buckling response on the geometric effect of a concrete dome, more specifically on the radius of curvature, span (base radius of the dome) thickness (h) and rise (H). So, it is very important to give a clue to structural engineers on the buckling behaviour of circular concrete dome shells concerning their geometric parameters.

CHAPTER 2 LITERATURE REVIEW

2.1 Introduction:

This chapter contains previously developed theories and investigations related to this thesis concept.

It is mandatory to provide a general explanation of thin shells, shell forms, shell classification, their merit, limitations, and behaviour of thin concrete shell elements under self-weight and lateral loadings in the first part of this unit before moving on to the research problem (Earthquake actions). The foundation of the thesis problem has been established based on this explanation of thin shell elements. The theories' general ideas suggest that predicting the behaviour of reinforced concrete circular domes is present. These theories are known as the thin shell theory and the buckling theory (or instability).

2.2 Previous Studies

Buckling assessment of analyzed concrete spherical shells can be extremely sensitive to slight deviations from their ideal parameters such as initial geometry, boundary conditions, and so on. Initial geometrical imperfections and non-linearity tend to prevent the most realistic structures from achieving their unrealistically high failure loads. The nonlinear analysis would be performed to obtain a more precise answer, taking into account geometrical imperfections, material nonlinearity, edge effects that cause bending, and so on, provided the shell is less prone to buckling failure (Mekjavić, 2011).

The other investigation paper carried out by (J. Michael Rotter et al., 2016), on the spherical dome buckling with edge ring support under uniform external pressure; studied both the stresses and classical buckling resistance and the effects of shell thickness; the dome subtended angle and the cross-sectional size of eaves rings; as a consequence; they concluded as the size of the edge ring has been shown to have a very significant effect on the membrane and bending stresses in the shell, but surprisingly little on the elastic critical buckling pressure. This finding contradicts conventional wisdom about shell buckling, which holds that peak membrane stresses control buckling resistance. For

almost all geometries and ring sizes, the elastic critical buckling pressure can be conservatively estimated at 0.81 of the classical elastic critical pressure.

Another study, conducted by Verwimp et al. (2015), concluded that buckling behaviour is highly dependent on geometrical imperfections, and more specifically on the imperfection shape, i.e. the assumed buckling modes.

The study on the buckling of shallow spherical concrete domes under gravity and earthquake loads conducted by, Zarghamee and Sarawit, (2020), concluded that the buckling strength of spherical shells is very sensitive to imperfections in their constructed geometry, and the minimum snap-through buckling strength of shallow caps occurs with shallowness parameter λ = 4 over an area with diameter d = $4.3\sqrt{R_o h}$ and the imperfections observed in the constructed concrete domes are consistent with this imperfection; the geometric imperfection considered in this study was in the form of a shallow cap with λ=4 over an area with diameter d and a radius of curvature of $\sqrt{2}.R_o$.

Zolqadr (2017) conducted a study on the buckling behaviour of spherical concrete dome shells with various dome configurations and geometry. The findings revealed that geometric non-linearity primarily affects the buckling resistance capacity of a spherical shell, and the horizontal component of an earthquake load has a significant effect on buckling pressure.

Madueno et al. (2020) investigated the effect of an earthquake's horizontal component on the buckling of concrete spherical shells, the given final decisions comparing the snap-trough buckling (nonlinear analysis) with the bifurcation buckling (linear analysis), a reduction of around 72% in the buckling capacity is always found; buckling capacity of spherical shells fixed at the base are lower compared to those that are pinned; the effect of the horizontal component of the earthquake on the buckling capacity of the dome structure increases as the radius-to-thickness ratios decrease; a similar behaviour is also observed for low dome rise/base diameter ratios; and the horizontal component of the earthquake could lead to a reduction of up to 4.36% in the buckling capacity of the structure.

2.3 Shells

2.3.1 Definition of Shells

Shells are a type of spatial structural element distinguished by their thinness in comparison to the other dimensions (radii of curvatures). Shell structures are used in the construction of large space structures in which a large span is realized without the use of supporting columns. The primary function of these concrete shell elements is to support applied loads by developing membrane in-plane stresses and bending moments at the same time.

This behaviour results from the geometrical features of shells, which distinguish the internal force system in shells from that of other types of civil engineering framed structures. Internal force distributions in shells are typically three-dimensional, i.e. spatial. This implies that the shell structure bears the applied loads primarily through membrane forces, whereas other framed structures bear the applied forces through bending mechanisms. As a result, in addition to their construction method, shells' unique behaviour is taken into account in their design.

The force distribution system of a shell is three-dimensional (or spatial forces), and as a result, the formulations to correctly represent them have always been complex in the mechanics of material strength. The complexity of the formulation of space forces has actuated numerous researchers who have attempted to study it for many years.

The investigators' system has practical ideas for studying these complex structures by reducing the general problem to simpler specific cases. In this regard, the general spatial shell problem is divided into two groups of shell elements based on their thickness, commonly referred to as thick shells and thin shells.

According to the above-mentioned concept, the shell surface that passes through the mid-thickness of the shell at each point is referred to as the shell's middle surface. If the thickness (h) of the shell is very small in comparison to the radius curvature (a) of the shell middle, the shell surface is referred to as a thin shell; otherwise, it could be referred to as a thick shell.

In general, for engineering perfection, a shell may appear thin if the condition 20≤ α/h ≤100 is met, α is the radius of a spherical dome and ***h*** is the thickness of a spherical dome (Varghese, 2010).

2.3.2 Merits and Demerits of Concrete Shell Structures

Man has been building shell structures since the beginning of time. In ancient times, humans constructed a shell out of masonry and stone. This type of shell structure can still be found in some parts of the world, including Ethiopia (Farshad, 2013).

Shell structures have been used to build churches, mosques, houses, schools, storage and business facilities, industrial and commercial buildings, football-filled roofs and basketball stadiums, and so on. Thin concrete shells have the following benefits in general (Wilson, 2005):

Merits:

- Thin shell concrete structures are extremely stiff in comparison to other framed structures.
- Thin shell concrete structures have a very high strength-to-weight ratio.
- Low-cost thin-shell concrete structures are used over a large area.
- Thin-shell concrete structures are easier to model and design than other structures and have greater strength.
- Thin-shell concrete structures have a continuous structural design that allows loads to be transferred in multiple directions. Thin shell concrete structures are appealing and are commonly found in churches and mosques.
- Compressive, shear, and tensile stresses/forces carry the load applied to the shell structures to the ground.
- By reducing the foundation and overall support systems, the dead load in the shell structure can be reduced.

Demerits:

- It is not possible to build a floor above thin concrete shell structures.
- Thin concrete shell construction requires more labour than other framed structures.

- Greater precision in formwork is required for the construction of thin concrete shell structures.
- The construction of thin concrete shell structures necessitated skilled labour and close supervision.

2.3.3 Classifications of shells

According to the differential geometry, the definition of Gaussian curvature based on the numerical value of $K= K_1*K_2$ is negative, zero, and positive at the planes intersection point (where, $K_1 = \frac{1}{r_x r_y}$ and $K_2 = \frac{1}{r_y R_x}$ and are maximum and minimum values of a radius of curvature respectively and r x and r are principal radii of curvatures, are measures of how the shell curves in the hoop and meridional directions). Thin shell structures could be Anticlastic surface (negative), Synclastic surface (positive), or Zero Gaussian curvature at that point based on this value. The circular reinforced concrete dome is one of the positive (or Synclastic) double-curved curvature thin shells according to the Gaussian classification of thin shells.

The following description of shell surface classification is based on their geometrical development ability. According to this distinction, the thin shell surfaces are either developable or non-developable. Developable shell surfaces are those that can be developed into a plane form without cutting or stretching their middle surface. The non-developable shell surface, on the other hand, must be cut or stretched to develop into a planar form. Because of this, thin shells with double curvature are commonly referred to as non-developable. As a result, the reinforced concrete circular dome is one of the non-developable surface shells. Because they require more external energy, non-developable thin shells are stronger and more stable than developable surface shells.

Surface classification of shell structure surfaces includes a surface of revolution, translational surfaces, and ruled surfaces. This shell classification is crucial for shell analysis and design (Farshad, 2013).

The surface of revolution is obtained by rotating the plane curve around an axis that lies within the plane curve. This is known as the meridian, and its plane is known as the meridian plane. Shell's concrete spherical domes can be classified as having positive Gaussian curvature and shells of revolution or rotational shells based on this explanation (Billington, 1982).

2.4 Assumptions of Classical Theories of Thin Shells

The following are the fundamental classical shell theories that can be used for the analysis and design of various types of thin shell structures:

- The shell is assumed to be thin, which means that its thickness is small in comparison to its representative minimum radius of curvature or lateral dimensions.
- Because the displacements and strains are so small, their higher powers can be ignored.
- The stress components normal to the shell mid-surface are insignificant in comparison to other stress components and can be ignored.
- Plane sections that were originally normal to the mid-surface of the shell remain plane and perpendicular to the deformed mid-surface. The latter assumption entails ignoring shear deformations.
- Compile the complete formulation by combining the force-displacement and equilibrium equations (11 equations with 11 unknowns).

According to Hook's presentation, the second assumption of classical shell theory is about small displacements and strains. In this regard, the displacements and strains are so small that their higher-ordered powers of the equations can be ignored. The material considered for the three-dimensional element of the shell should be linearly elastic, with the general equations of strain with its corresponding stress expressed as:

$$\varepsilon_x = \frac{1}{E}[\sigma_x - v(\sigma_y + \sigma_z)] \tag{2.1}$$

$$\varepsilon_y = \frac{\sigma_y}{E_y} - \frac{v_{yx}}{E_x}\sigma_x - \frac{v_{yz}}{E_z}\sigma_y \tag{2.2}$$

$$\varepsilon_z = \frac{\sigma_z}{E_z} - \frac{v_{zx}}{E_z}\sigma_x - \frac{v_{xz}}{E_z}\sigma_y \tag{2.3}$$

$$\gamma_{xy} = \frac{\tau_{xy}}{G_{xy}} \tag{2.4}$$

$$\gamma_{xz} = \frac{\tau_{xz}}{G_{xz}} \tag{2.5}$$

$$\gamma_{yz} = \frac{\tau_{yz}}{G_{yz}} \tag{2.6}$$

Because the material used in this study is concrete, the elastic modulus of concrete (E) and the poison's ratio (v) is the same on the entire structure's system. So, $E_x=E_y=E_z=E$ and $v_{xy}=v_{yx}=v_{yz}=v$ concerning this concept, the following equation could be used:

$$\varepsilon_x = \frac{1}{E}[\sigma_x - v(\sigma_y + \sigma_z)] \tag{2.7}$$

$$\varepsilon_y = \frac{1}{E}[\sigma_y - v(\sigma_x + \sigma_z)] \tag{2.8}$$

$$\varepsilon_z = \frac{1}{E}[\sigma_z - v(\sigma_x + \sigma_y)] \tag{2.9}$$

$$\gamma_{xy} = \frac{2(1+v)}{E}\sigma_{xy} \tag{2.10}$$

$$\gamma_{xz} = \frac{2(1+v)}{E}\sigma_{xz} \tag{2.11}$$

$$\gamma_{yz} = \frac{2(1+v)}{E}\sigma_{yz} \tag{2.12}$$

In the case of a polar coordinate system, the differential element's position is defined by the angle $\boldsymbol{\theta}$ and $\emptyset$. At the notation for stresses, resultant forces, and resultant moments, the subscripts $\boldsymbol{\theta}$ and $\emptyset$ replaced by X and Y, respectively.

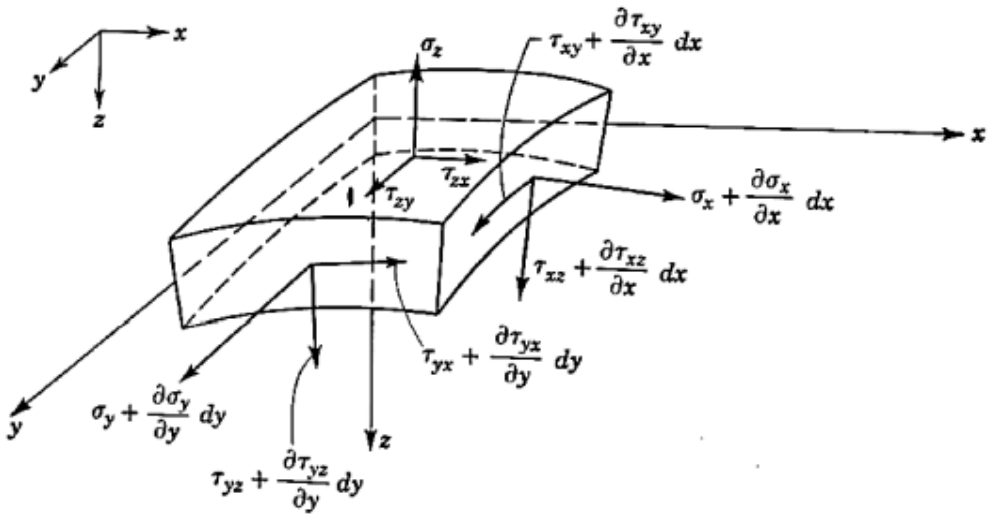

Figure 2-1: Normal stresses in 3D thin shell deferential elements (Farnsworth, 1999).

One of the postulates of Kirchhof law mentioned above states that the differential of thin shell elements with small thickness is related to beam theory, which states that straight lines normal to the middle surface before deformation remain normal after deformations. Because the in-plane displacements vary linearly throughout the thickness of the shell, all strain components normal to the middle surface should vanish.

$$\varepsilon_z = \gamma_{xz} = \gamma_{yz} = 0 \quad (2.13)$$

Finally, Kirchhof's hypothesis discovered that for thin shells, the transverse normal stress is trivial (or ignored) when compared to the in-plane normal stress.

$$\sigma_z = 0 \quad (2.14)$$

Based on this concept, the equation for strains along the X and Y directions (2.1-2.6) could be:

$$\varepsilon_x = \frac{\sigma_x}{E_x} - \frac{v_{xy}}{E_y}\sigma_y \quad (2.15)$$

$$\varepsilon_y = \frac{\sigma_y}{E_y} - \frac{v_{yx}}{E_x}\sigma_x \quad (2.16)$$

$$\gamma_{xy} = \frac{\tau_{xy}}{G_{xy}} \quad (2.17)$$

$$\varepsilon_z = \gamma_{xz} = \gamma_{yz} = \sigma_z = 0 \quad (2.18)$$

Kirchhoff's Equations (2.7-2.12) become according to the assumptions stated above.

$$\varepsilon_x = \frac{1}{E}[\sigma_x - v\sigma_y] \quad (2.19)$$

$$\varepsilon_y = \frac{1}{E}[\sigma_y - v\sigma_x] \quad (2.20)$$

$$\gamma_{xy} = \frac{2(1+v)}{E}\sigma_{xy} \quad (2.21)$$

Where:

ε_x Is the strain along the X-axis

ε_y Is the strain along the Y-axis

ε_y Is the strain along the Z-axis

$E_x = E_y = E_z = E$ Is an elastic module of concrete material

$v_{XY} = v_{XZ} = v_{yz} = v$ Is poison's ratio of concrete material

σ_x Is normal stress along the X-axis

σ_y Is normal stress along the Y-axis

σ_z Is normal stress along the Z-axis

γ_{xy} Is shear strain in the XY-plane

γ_{XZ} Is shear strain in the XZ-plane

γ_{yz} Is shear strain in YZ-plane

τ_{XY} Is shear stress in XY-plane

τ_{xz} Is shear stress in XZ-plane

τ_{yz} Is shear stress in YZ-plane

G_{XY} Is the shear modulus of rigidity in XY-plane

G_{XZ} Is the shear modulus of rigidity in XZ-plane

G_{yz} Is the shear modulus of rigidity in YZ-plane

2.4.1 General Equations of Forces in Classical Shell Theory

Many researchers have been presented to explain the formulation of forces, stresses, and moments in thin shell structures. Billington (1982) stated that the formulation of general shell theory must go through the five steps listed below:

- Find the equilibrium equations for a shell element (five equations with eight unknowns).
- Define the strain-displacement relationships (six equations with three unknowns).
- Assume material properties (three equations with six unknowns) and then derive force-strain equations to establish stress-strain relationships (six equations with three unknowns).
- Convert the force-strain equations into force-displacement equations (six equations with six unknowns).
- Compile the complete formulation by combining the force-displacement and equilibrium equations (11 equations with 11 unknowns).

The equilibrium forces of the shell element are established based on the six conditions stated by Billington (1982) based on the differential thin shell element and stress resultants illustrated in Figure 2.2:

1) $\sum F_X = 0,$
2) $\sum F_Y = 0$
3) $\sum \mathbf{F_Z} = \mathbf{0}$ 2-22
4) $\sum M_X = 0$
5) $\sum M_Y = 0$
6) $\sum M_Z = 0$

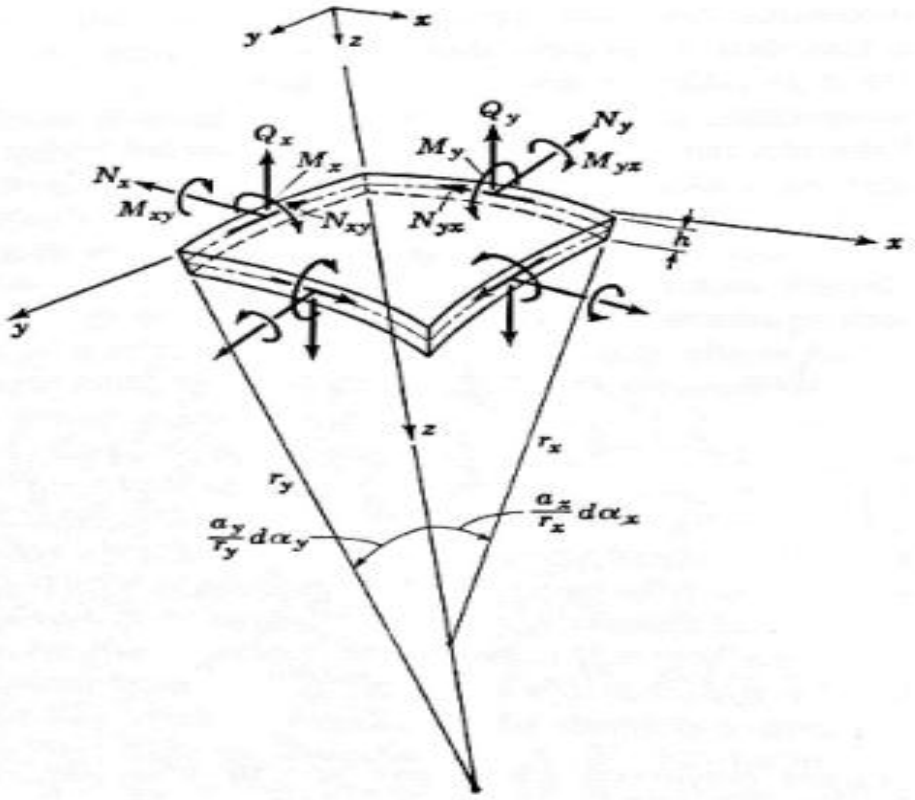

Figure 2-2: differential thin shell elements (Farnsworth, 1999).

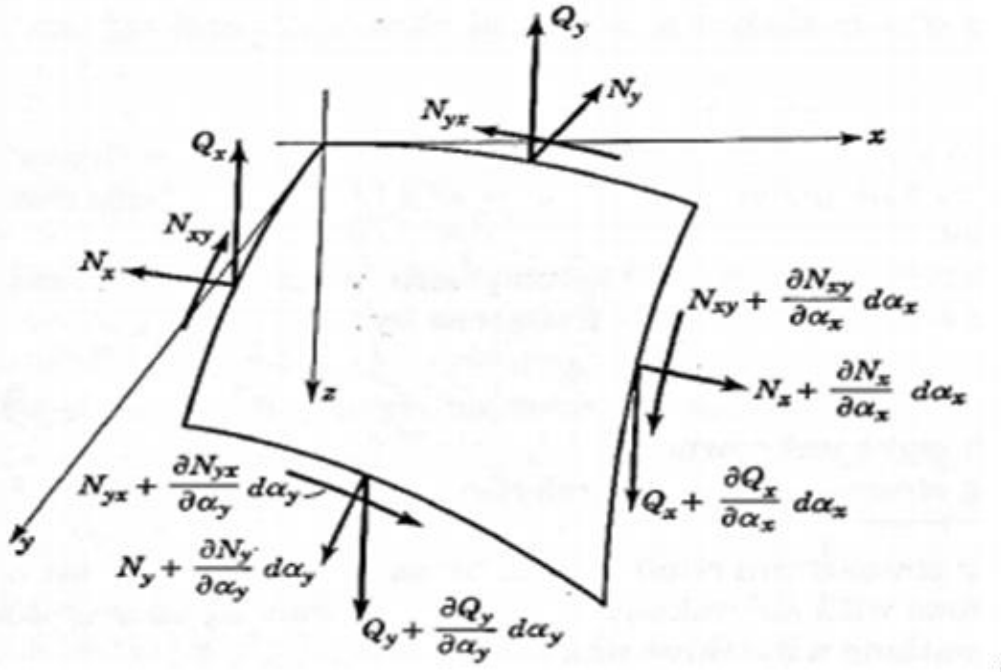

Figure 2-3 Stress (Force) components in differential shell element (Farnsworth, 1999)

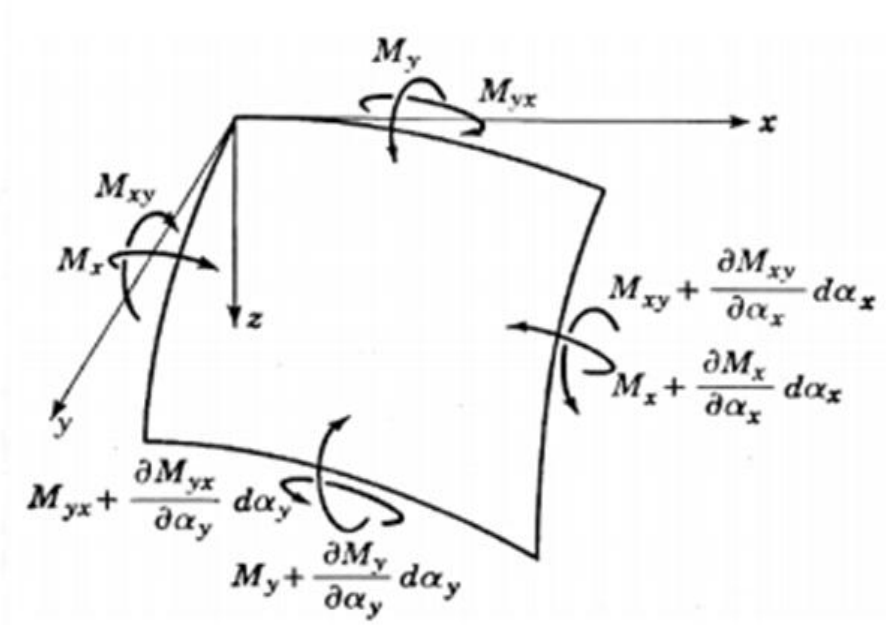

Figure 2-4: Moment components of differential shell elements (Farnsworth, 1999).

Figures 22.3 and 2.4 above show the internal force system of forces (or stresses) and moments over thickness (h) acting on the differential of thin shell elements. The following are the outcomes of stresses and moments:

$$N_X = \int_{-\frac{h}{2}}^{\frac{h}{2}} \sigma_x \left(1 - \frac{z}{r_y}\right) dz \tag{2.23}$$

$$N_Y = \int_{-\frac{h}{2}}^{\frac{h}{2}} \sigma_y \left(1 - \frac{z}{r_x}\right) dz \tag{2.24}$$

$$N_{XY} = \int_{-\frac{h}{2}}^{\frac{h}{2}} \tau_{xy} \left(1 - \frac{z}{r_y}\right) dz \tag{2.25}$$

$$N_{YX} = \int_{-\frac{h}{2}}^{\frac{h}{2}} \tau_{yx} \left(1 - \frac{z}{r_x}\right) dz \tag{2.26}$$

$$Q_X = \int_{-\frac{h}{2}}^{\frac{h}{2}} \tau_{xz} \left(1 - \frac{z}{r_y}\right) dz \tag{2.27}$$

$$Q_Y = \int_{-\frac{h}{2}}^{\frac{h}{2}} \tau_{yz} \left(1 - \frac{z}{r_x}\right) dz \tag{2.28}$$

$$\mathrm{M_X} = \int_{-\frac{\mathrm{h}}{2}}^{\frac{\mathrm{h}}{2}} \sigma_{\mathrm{x}} \left(1 - \frac{\mathrm{z}}{\mathrm{r_y}}\right) \mathrm{dz} \tag{2.29}$$

$$\mathrm{M_Y} = \int_{-\frac{\mathrm{h}}{2}}^{\frac{\mathrm{h}}{2}} \sigma_{\mathrm{y}} \left(1 - \frac{\mathrm{z}}{\mathrm{r_x}}\right) \mathrm{dz} \tag{2.30}$$

$$\mathrm{M_{XY}} = -\int_{-\frac{\mathrm{h}}{2}}^{\frac{\mathrm{h}}{2}} \tau_{\mathrm{xy}} \left(1 - \frac{\mathrm{z}}{\mathrm{r_y}}\right) \mathrm{dz} \tag{2.31}$$

$$\mathrm{M_{YX}} = \int_{-\frac{\mathrm{h}}{2}}^{\frac{\mathrm{h}}{2}} \tau_{\mathrm{yx}} \left(1 - \frac{\mathrm{z}}{\mathrm{r_x}}\right) \mathrm{dz} \tag{2.32}$$

Where:

N_x Is internal hoop stress (or force) along X- the direction

N_y Is an internal hoop stress (or force) along the y- direction

N_{XY}; N_{YX} Is internal in-plane shear stress (forces)

Q_x Is an internal in pane shear stress (forces)

Q_y Is an internal out-of-pane shear stress (force)

σ_x ; σ_y; σ_z; Is normal stresses along X, Y, and Z direction respectively.

τ_{xy} ; τ_{yx}; τ_{xz}; Is shear stress along the XY, YX, and XZ-planes

M_x; M_y Is an internal bending moment (or force).

M_{xy}; M_{yx} Is an internal twisting moment (or force).

h Is the thickness of a thin shell

r_x Is the principal radius of a thin shell along the X direction

$\boldsymbol{r_y}$ Is the principal radius of the thin shell along the Y direction

As we saw in the axioms of thin shell theory, the thickness (h=z) of a shell is very small in comparison to the principal radii r x and r y; thus, the expressions z/r x and z/r y can be ignored when using the arithmetic operation of addition or subtraction from unity. This assumption leads to:

$$\tau_{xy} = \tau_{yx} \quad (2.33)$$

$$N_{xy} = N_{yx} \quad (2.34)$$

$$M_{xy} = -M_{yx} \quad (2.35)$$

Minimize the general equilibrium equations into five with eight unknowns using Equation (2.33-2.35) and leaving $\sum M_Z = 0$ among the six equilibrium equations. As a

result, Billington (1982) derived the complete formulations of the equilibrium by the following forms:

$$\frac{\partial}{\partial \alpha_x}\left(N_x a_y\right) - N_y \frac{\partial a_y}{\partial \alpha_x} + N_{xy} \frac{\partial a_x}{\partial \alpha_y} + \frac{\partial}{\partial \alpha_y}\left(N_{yx} a_x\right) - Q_y \frac{a_x a_y}{r_{xy}} - Q_x \frac{a_x a_y}{r_x} + p_x a_x a_y = 0 \quad (2.36)$$

$$\frac{\partial}{\partial \alpha_y}\left(N_y a_x\right) - N_x \frac{\partial a_x}{\partial a_y} + N_{yx} \frac{\partial a_y}{\partial \alpha_x} + \frac{\partial}{\partial \alpha_x}\left(N_{xy} a_y\right) - Q_x \frac{a_x a_y}{r_{xy}} - Q_y \frac{a_x a_y}{r_y} + p_y a_x a_y = 0 \quad (2.37)$$

$$\frac{\partial}{\partial \alpha_y}\left(N_y a_x\right) - N_x \frac{\partial a_x}{\partial a_y} + N_{yx} \frac{\partial a_y}{\partial \alpha_x} + \frac{\partial}{\partial \alpha_x}\left(N_{xy} a_y\right) - Q_x \frac{a_x a_y}{r_{xy}} - Q_y \frac{a_x a_y}{r_y} + p_y a_x a_y = 0 \quad (2.38)$$

$$-\frac{\partial}{\partial \alpha_y}\left(M_y a_x\right) + M_x \frac{\partial a_x}{\partial \alpha_y} - M_{yx} \frac{\partial a_y}{\partial \alpha_x} + \frac{\partial}{\partial \alpha_x}\left(M_{xy} a_y\right) + Q_y a_x a_y = 0 \quad (2.39)$$

$$-\frac{\partial}{\partial \alpha_x}\left(M_x a_y\right) + M_y \frac{\partial a_y}{\partial \alpha_x} + M_{xy} \frac{\partial a_x}{\partial \alpha_y} - \frac{\partial}{\partial \alpha_y}\left(M_{yx} a_x\right) + Q_x a_x a_y = 0 \quad (2.40)$$

Where, p_x ; p_y and p_z are represent the externally applied load on the shell, r_x and r_y are the radii of curvature of the shell, a_x and a_y the changes in the arc length of the shell are called lame parameters, α_x and α_y are the curvilinear coordinates for the corresponding sides.

2.4.2 The Bond between Strain and Displacement in Thin Shell

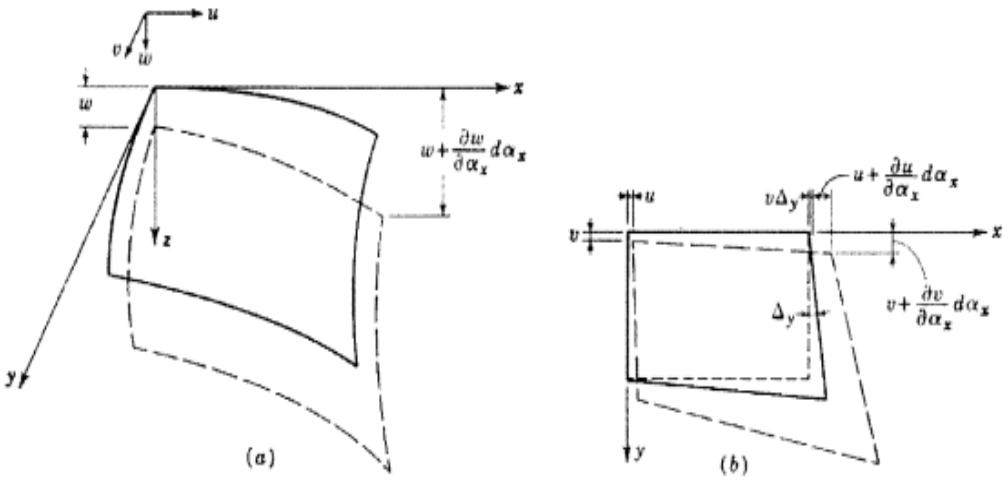

Figure 2-5: Behavior of shell differential shell element after deformation (Farnsworth, 1999).

Determine the interrelationship between strain and displacement of a thin shell defined by the following forms, where $\boldsymbol{\varepsilon_{xo}}$, $\boldsymbol{\varepsilon_{yo}}$ and $\boldsymbol{\gamma_{xyo}}$ are called extensional shear strains at the middle surface and angular shear strains, respectively, based on Figure 2.5.

$$\varepsilon_{xo} = \frac{1}{a_x}\frac{\partial u}{\partial \alpha_x} + \frac{v}{a_x a_y}\frac{\partial a_x}{\partial \alpha_y} - \frac{w}{r_x} \tag{2.41}$$

$$\varepsilon_{yo} = \frac{1}{a_y}\frac{\partial v}{\partial \alpha_y} + \frac{u}{a_x a_y}\frac{\partial a_y}{\partial \alpha_x} - \frac{w}{r_y} \tag{2.42}$$

$$\gamma_{xyo} = \frac{1}{a_x}\frac{\partial v}{\partial \alpha_x} + \frac{1}{a_y}\frac{\partial u}{\partial \alpha_y} - \frac{u}{a_x a_y}\frac{\partial a_x}{\partial \alpha_y} - \frac{v}{a_x a_y}\frac{\partial a_y}{\partial \alpha_x} - \frac{2w}{r_{xy}} \tag{2.43}$$

The strains caused by the effect of bending on the change in curvature of the shell element are explained as follows:

$$X_x = \frac{1}{a_x}\frac{\partial \emptyset_x}{\partial \alpha_x} + \frac{\emptyset_y}{a_x a_y}\frac{\partial a_x}{\partial \alpha_y} \tag{2.44}$$

$$X_y = \frac{1}{a_y}\frac{\partial \emptyset_y}{\partial \alpha_y} + \frac{\emptyset_x}{a_x a_y}\frac{\partial a_y}{\partial \alpha_x} \tag{2.45}$$

$$2X_{xy} = \frac{1}{a_y}\frac{\partial \emptyset_x}{\partial \alpha_y} + \frac{1}{a_x}\frac{\partial \emptyset_y}{\partial \alpha_x} - \frac{\emptyset_x}{a_x a_y}\frac{\partial a_x}{\partial \alpha_y} - \frac{\emptyset_y}{a_x a_y}\frac{\partial a_y}{\partial \alpha_x} \tag{2.46}$$

Note that the displacements for X, Y, and Z are represented by u, v, and w respectively, and that $\boldsymbol{\emptyset_x}$ and $\boldsymbol{\emptyset_x}$ designate the rotation of the middle surface, which is defined as:

$$\emptyset_x = \frac{u}{r_x} + \frac{\partial w}{a_x \partial \alpha_x} + \frac{v}{r_{xy}} \tag{2.47}$$

$$\emptyset_y = \frac{v}{r_y} + \frac{\partial w}{a_y \partial \alpha_y} + \frac{u}{r_{xy}} \quad (2.48)$$

Where:

ε_{xo} Is an extensional shear strain along the X direction.

ε_{yo} Is extensional shear strain along the Y direction

γ_{xy} Is angular shear strain in radian

X_x Is strain due to a change in curvature of the shell element in case of bending along the X

X_y Is strain due to a change in curvature of the shell element in case of bending along the Y

$2X_{xy}$ Is angular shear strain due to bending

$\emptyset_x$; $\emptyset_y$ Is rotation of the middle surface along X and Y direction in radian.

u; v and w are displacements along X; Y and Z respectively.

2.4.3 Stress-Strain Relationships of Thin Shell

Because the displacements are small in comparison to the shell's transverse characteristics dimension, the equilibrium equation can be formulated using the initial undeformed geometry, and the shell's deformation parameter can be ignored. The following equations are used to express the small terms of a thin shell:

$$\varepsilon_x = \varepsilon_{xo} - 2X_x \quad (2.49)$$
$$\varepsilon_y = \varepsilon_{yo} - 2X_y \quad (2.50)$$
$$\gamma_{xy} = \gamma_{xyo} - 2zX_{xy} \quad (2.51)$$

Hook's assumption states that the material must be linearly elastic, isotropic, and homogeneous. In this sense, the shell element's stress-strain relationship with Young's modulus E and Poisson's ratio V can be defined as:

$$\sigma_x = \frac{E}{1-v^2}(\varepsilon_x + v\varepsilon_y) \quad (2.52)$$
$$\sigma_y = \frac{E}{1-v^2}(\varepsilon_y + v\varepsilon_x) \quad (2.53)$$

$$\tau_{xy} = \frac{E}{2(1-\nu^2)}\gamma_{xy} \quad (2.54)$$

Now, replaced (2.49-2.51) into (2.52-2.54) and then the outcome of (2.52-2.54) into (2.23-2.28) and (2.29-2.32) respectively, then the resultant of forces and moments could be:

$$\mathrm{N_x} = \mathrm{K}(\varepsilon_{\mathrm{xo}} + \mathrm{v}\varepsilon_{\mathrm{yo}}) \quad (2.55)$$

$$\mathrm{N_y} = \mathrm{K}(\varepsilon_{\mathrm{yo}} + \mathrm{v}\varepsilon_{\mathrm{xo}}) \quad (2.56)$$

$$\mathrm{N_{xy}} = \mathrm{Gh}\gamma_{\mathrm{xyo}} \quad (2.57)$$

$$\mathrm{M_x} = -\mathrm{D}(\mathrm{X_x} + \mathrm{vY_y}) \quad (2.58)$$

$$\mathrm{M_y} = -\mathrm{D}(\mathrm{X_y} + \mathrm{vY_x} \quad (2.59)$$

$$\mathrm{M_{xy}} = -\mathrm{M_{yx}} = \mathrm{D}(1-\mathrm{v})\mathrm{X_x} \quad (2.60)$$

Where, The extensional rigidity of the shell

$$\mathrm{K} = \frac{\mathrm{E}}{1-\mathrm{v}^2} \quad (2.61)$$

The shear modulus rigidity of the shell

$$\mathrm{G} = \frac{\mathrm{E}}{2(1+\mathrm{v})} \quad (2.62)$$

The bending rigidity of the shell

$$\mathrm{D} = \frac{\mathrm{Eh}^3}{12(1-\mathrm{v}^2)} \quad (2.63)$$

h = The thickness of the shell,

2.4.4 Force-Displacement Relationship Equations

This topic discusses the force-displacement relationship, which is derived from the strain-displacement equations. As a result, the resulting force formulation is described as:

$$N_x = K[\frac{1}{a_x}\frac{\partial u}{\partial \alpha_x} + \frac{v}{a_x a_y}\frac{\partial a_x}{\partial \alpha_y} - \frac{w}{r_x} + v\left(\frac{1}{a_y}\frac{\partial V}{\partial \alpha_y} + \frac{u}{a_x a_y}\frac{\partial a_y}{\partial \alpha_x} - \frac{w}{r_y}\right)] \quad (2.64)$$

$$N_y = K[\frac{1}{y}\frac{\partial V}{\partial \alpha_y} + \frac{u}{a_x a_y}\frac{\partial a_y}{\partial \alpha_x} - \frac{w}{r_y} + v\left(\frac{1}{a_x}\frac{\partial u}{\partial \alpha_x} + \frac{V}{a_x a_y}\frac{\partial a_x}{\partial \alpha_y} - \frac{w}{r_x}\right)] \quad (2.65)$$

$$N_{xy} = N_{yx} = Gh(\frac{1}{a_x}\frac{\partial V}{\partial \alpha_x} + \frac{1}{a_y}\frac{\partial u}{\partial \alpha_y} - \frac{u}{a_x a_y}\frac{\partial a_x}{\partial \alpha_y} - \frac{V}{a_x a_y}\frac{\partial a_y}{\partial \alpha_x} - \frac{2w}{r_{xy}} \quad (2.66)$$

$$M_x = -D[\frac{1}{a_x}\frac{\partial \emptyset_x}{\partial \alpha_x} + \frac{\emptyset_y}{a_x a_y}\frac{\partial a_x}{\partial \alpha_y} + v\left(\frac{1}{a_y}\frac{\partial \emptyset_y}{\partial \alpha_y} + \frac{\emptyset_x}{a_x a_y}\frac{\partial a_y}{\partial \alpha_x}\right)] \quad (2.67)$$

$$M_y = -D[\frac{1}{a_y}\frac{\partial \emptyset_y}{\partial \alpha_y} + \frac{\emptyset_x}{a_x a_y}\frac{\partial a_y}{\partial \alpha_x} + v\left(\frac{1}{a_y}\frac{\partial \emptyset_x}{\partial \alpha_x} + \frac{\emptyset_y}{a_x a_y}\frac{\partial a_x}{\partial \alpha_y}\right)] \quad (2.68)$$

$$\mathrm{M_{xy}} = -\mathrm{M_{yx}} = \frac{\mathrm{D}(1-\mathrm{v})}{2}(\frac{1}{\mathrm{a_y}}\frac{\partial \emptyset_{\mathrm{x}}}{\partial \alpha_{\mathrm{y}}} + \frac{1}{\mathrm{a_x}}\frac{\partial \emptyset_{\mathrm{y}}}{\partial \alpha_{\mathrm{x}}} - \frac{\emptyset_{\mathrm{x}}}{\mathrm{a_x a_y}}\frac{\partial \mathrm{a_x}}{\partial \alpha_{\mathrm{y}}} - \frac{\emptyset_{\mathrm{y}}}{\mathrm{a_x a_y}}\frac{\partial \mathrm{a_y}}{\partial \alpha_{\mathrm{x}}}) \quad (2.69)$$

2.4.5 Governing Equation for Membrane Theory Simplifications

The shell element's equations of equilibrium typically have ten unknowns - the stress resultants and stress couples - and six equations. As a result, the system is statistically indeterminate. As a result, to find a solution, deformation must be considered. By

reducing the number of unknowns from ten to four, the Membrane Theory avoids the complexities associated with solving the statically indeterminate system. As a result, the system is statically determined and can be solved directly. This is accomplished by ignoring all normal shears, bending moments, and twisting moments in the shell. This system simplification is based on the shell's proclivity to resist loading by utilizing hoop and meridional forces.

$$\frac{\partial}{\partial\alpha_x}\left(N'_x a_y\right) - N'_y \frac{\partial a_y}{\partial\alpha_x} + N'_{xy} \frac{\partial a_x}{\partial\alpha_y} + \frac{\partial}{\partial\alpha_y}\left(N'_{yx} a_x\right) + P_x a_x a_y = 0 \qquad (2.70)$$

$$\frac{\partial}{\partial\alpha_x}\left(N'_y a_x\right) - N'_x \frac{\partial a_x}{\partial\alpha_x} + N'_{xy} \frac{\partial a_y}{\partial\alpha_x} + \frac{\partial}{\partial\alpha_y}\left(N'_{yx} a_y\right) + P_y a_x a_y = 0 \qquad (2.71)$$

$$\frac{N'_x}{r_x} + \frac{N'_{xy}}{r_{xy}} + \frac{N'_{yx}}{r_{yx}} + \frac{N'_y}{r_y} + P_z = 0 \qquad (2.72)$$

2.4.6 Limitation of Membrane Theory of Thin Shells

The acceptability of the results obtained by the membrane theory is dependent on some conditions, including the shell geometry, boundary conditions, appropriate loading, and edge constraints.

In membrane theory, a thin concrete shell bears an existing external loading by internal forces (or stress resultants); bending and twisting moments. Incompatible loading and boundary conditions; on the other hand, the effect of bending and twisting moments is either zero or so small as to be negligible. Because shells have a high resistance to membrane stresses, those that cannot be bent extensionally are usually very stiff. In general, the membrane theory is valid only for shells that cannot be bent extensionally or for shells with very small bending moments.

The general conditions under which the membrane theory is valid are now presented without proof. These conditions are shown to be both necessary and sufficient for the existence of the moment less state of stress in thin shells, and they correspond to the minimum strain energy stored by a shell during straining. These are the conditions (Varghese, 2010):

- The shell's boundaries are free of transverse shear forces and moments. Loads applied to the shell boundaries must be in planes tangent to the shell's middle surface.

- The normal displacements and rotations at the shell edges are unconstrained: that is, these edges can displace freely in the direction of the normal to the middle surface.
- A shell's surface must be smoothly varying and continuous.
- Surface and edge load components must also be smooth and continuous functions of the coordinates.

2.5 Elastic Stability of Thin Shells

The previous topic discussed the formulation of stresses, displacements, and strains using classical thin shell theory and numerical analysis results.

The current topic has addressed the stability and instability identified by less well-defined behaviour, which is still relevant in design. This virtue cannot be predicted as easily or precisely as that derived from traditional assumptions. When applied to thin-shell concrete structures, shell designers must accept the classical theory's limitations.

The classical theory was based on an elastic, isotropic, thin shell with small deflections. As a result, the three general questions that must be considered in the design behind classical stress analysis are the shell geometry and imperfections, concrete crack and steel yielding, creep, and large deflections (Billington, 1982).

When the designers considered all of the requirements of good design for designing shell structures, they realized that concrete shells have high structural efficiency and can thus be built very thinly. Because of their relatively lightweight nature, the internal forces of compression and tension are organized in such a way that they allow the structure to withstand large loads with optimum performance; the collapse force induced in this thin structure is relatively low. However, they, like any other structure, do not have infinite resistance, which means they can fail due to long-term or short-term loading conditions.

Shell structures may fail due to large deformation caused by material degradation or a combination of the two. Buckling instability is one failure mechanism and strength failure is Figure 2.6 depicts the difference between these mechanisms' failures.

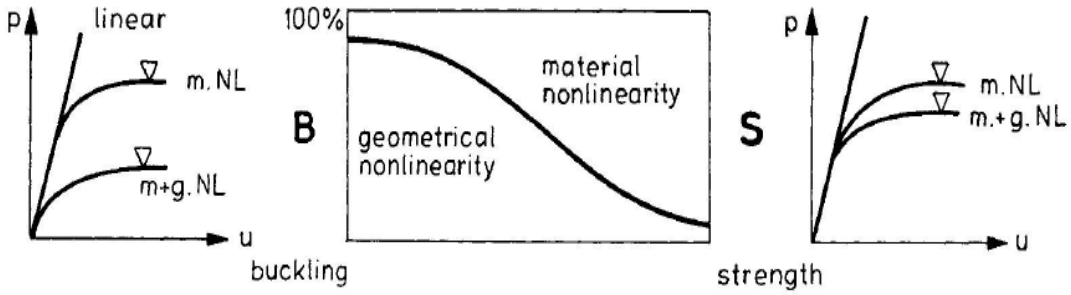

Figure 2-6: Structural failure due to buckling or strength (Peerdeman, 2008).

Regardless, the shell structure failed due to both failure mechanisms, but this research only focused on buckling instability. Under certain conditions, structures may fail due to insufficient stability rather than high stresses on the material's strength. Buckling is a type of equilibrium instability (Peerdeman, 2008).

According to Popov and Medwadowski, there are five types of loss stability due to buckling. These are bifurcation buckling, limitation buckling, inelastic buckling, creep buckling, and dynamic buckling. Bifurcation and Limitation buckling are examples of elastic instability failure, whereas the others are examples of inelastic loss of structural stability (Peerdeman, 2008).

This thesis work concentrated on the elastic instability of circular concrete domes, with a particular emphasis on bifurcation buckling. The bifurcation of the equilibrium state is a prominent feature of static elastic instability, i.e., buckling. It describes a situation in which a body is subjected to increased loading. There are two possible paths of equilibrium at the point of buckling bifurcation: the primary path up to the critical buckling load and the secondary path, which is the post-buckling portion of a structure. After buckling, the primary path becomes unstable, which means that a small perturbation causes large deformation, whereas the secondary path represents a stable state condition beyond the bifurcation point. Both paths intersect at the buckling point, also known as the bifurcation point, and states of equilibrium can exist for the same load at that point. Figure 2.7 depicts a representative "load-deflection" diagram for Euler stability columns of perfect geometric form and loaded by in-plane compressive forces p[11].

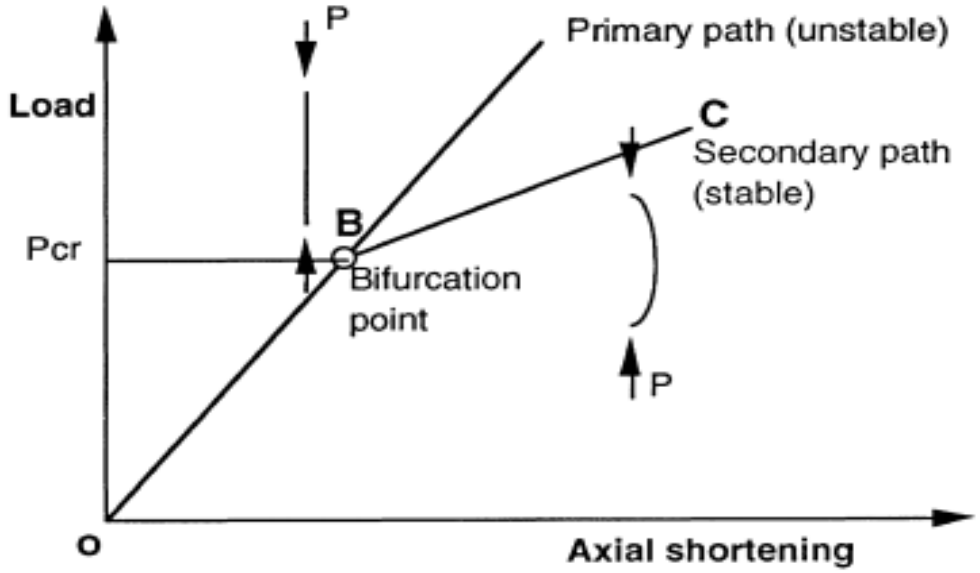

Figure 2-7: Behavior of axially compressed elastic columns (Farshad, 2013).

The bifurcation equilibrium is characterized by the existence of two equilibrium paths and the fact that the structure chooses its own buckled shape beyond the bifurcation point. As a result, the bifurcation buckling point is also known as the classical buckling load. The classical buckling load in a concrete circular dome is defined as follows:

$$P_{cr} = \frac{2E(\frac{h}{a})^2}{\sqrt{3(1-v^2)}} \quad (2.73)$$

Where,

P_{cr} Is the classical analysis of buckling load, in $\frac{N}{m^2}$

E Is the Modulus of elasticity, in Mpa

h Is the thickness of the shell or circular dome, in m

a Is the Radius of the circular dome, in m

$\boldsymbol{v}$ Is Poisson's ratio

The magnitude of the uniform compressive stressσ, for the circular concrete shell under uniform external pressures q, is expressed as:

$$\sigma = \frac{q*a}{2h} \quad (2.74)$$

The equilibrium relationship of the circular concrete shell's theoretical buckling pressure, P_{cr}, and corresponding internal compressive membrane stress, σ_{cr}, is defined as follows:

$$P_{cr} * \pi a^2 = \sigma_{cr} 2\pi a \quad (2.75)$$

By substituting equation (2.73) for equation (2.75), the general formula for the internal compressive membrane stress, $\boldsymbol{\sigma_{cr}}$, which corresponds to the classical buckling stress, can be obtained and expressed as follows:

$$\sigma_{cr} = \frac{E}{\sqrt{3(1-V^2)}} \left(\frac{h}{a}\right) \quad (2.76)$$

When a uniform external pressure, q, exceeds the classical buckling stresses value, P cr, as defined in equation (2.73), the system becomes unstable, that is, $q > P_{cr}$. If $q = P_{cr}$, the spherical shell is in neutral equilibrium for small displacements. If q is less than P cr, the spherical shell is stable.

The critical stress value defined by equation (2.76), which is based on the small displacement theory, does not match the experimental data very well, but the true critical stress value is much lower.

The most frequently observed experimental result has been a critical pressure of tested value as slow as 10% of the classical pressure predicted by the small deflection theory (J. Michael Rotter et al., 2016).

Numerous researchers have studied over the centuries, and a large number of spherical shells with various materials and geometries have been fabricated and tested, resulting in the disappointing phenomenon that most tested buckling loads were significantly lower than classical theory prediction.

According to (Zolqadr and An, 2017), the experimental elastic buckling load is approximately equal to one-fourth of the classical buckling load (P_{cr}), as defined in equation (2.73).

The theoretical buckling pressure for initially perfect spheres formed from flat plates has been compared with the test sample buckling load, which differs from the test result due to variations in thickness and residual stresses, as well as unfavourable boundary conditions.

The experimentally obtained buckling pressure is lower than the classical value for three reasons: the possibility of unsymmetrical, disturbance in the uniform membrane stress caused by edge support conditions, and an imperfection in the fabrication or construction of the spherical shape.

Many researchers have attempted to explain the difference between the experimental and theoretical buckling loads by introducing nonlinear, large deflection shell equations, whose expressions for the classical buckling pressures take the same general form as equation (2.73) ((Zolqadr and An, 2017).

The difference between the experimental test buckling pressure and the theoretically predicted stress gives rise to the concept of the knockdown factor (KDF), which is defined as the tested buckling load divided by the classical buckling load.

$$\mathrm{KDF} = \frac{\mathrm{P_{test}}}{\mathrm{P_{cr}}} \qquad (2.77)$$

Where, $\mathrm{P_{test}}$ Is the Actual buckling load obtained from SAP200 software results

P_{cr} Is Classical theory prediction buckling load

Zarghamee and Sarawit (2020), first investigated the imperfection sensitivity of spherical shells under experimental pressure; they also discovered a post-buckling state with lower energy, resulting in the difference between the theoretical buckling load and the actual experimental building load.

In addition, Zarghamee and Sarawit (2020) investigated the initial geometric imperfection and discovered that they are one of the main causes of the buckling load knockdown effect for spherical shells.

A spherical shell influenced by radial external stress will buckle abruptly or "oilcan" by leaping to a lower state of energy at a pressure less than the theoretical value (Rotter et al., 2016).

According to the discovery of Timoshenko and Gere (1963), $400 \leq \frac{\mathrm{a}}{\mathrm{h}} \leq 2000$ and $20 \leq \theta \leq 60^0$, for the practical application of the empirical formula for calculating the classical buckling pressure is given by:

$$P_{cr} = (1 - 0.175\frac{\theta - 20^0}{20^0})(1 - \frac{0.07a}{\frac{h}{400}})(0.3E)(\frac{h}{a})^2 \quad (2.78)$$

There is no single budding coefficient that can be used in the theoretical buckling pressure to calculate the strength of the spherical shells with varying degrees of initial imperfection shown in Figure 2.8 below.

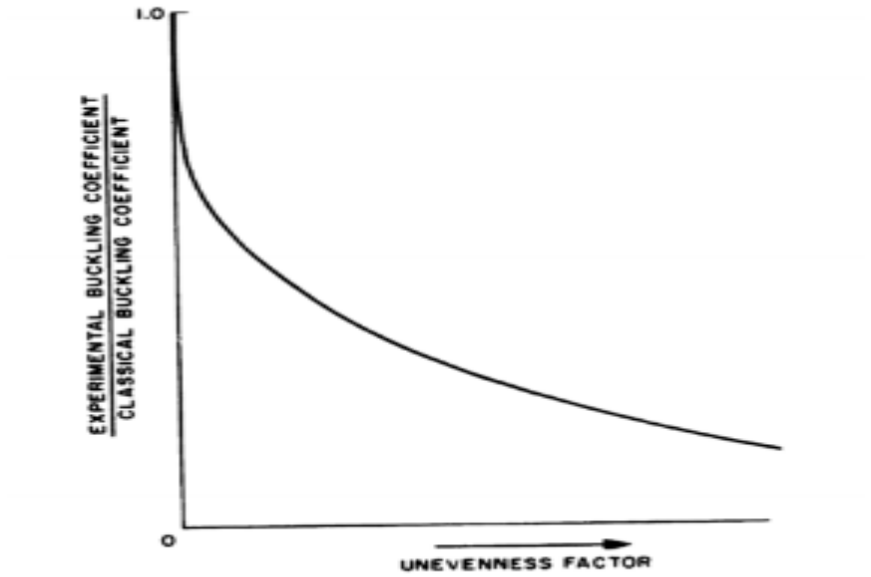

Figure 2-8: Effect of initial imperfection ((Zolqadr and An, 2017).

Based on the experimental test results of (Zolqadr and An, 2017), an empirical equation for near-perfect spheres was developed to predict collapse at about 0.7 times the theoretical pressure. As a result, the empirical equation for elastic buckling pressure, P, for a near-perfect sphere is as follows:

$$P = 0.7 * P_{cr} = \frac{1.4E(\frac{h}{a})^2}{\sqrt{3(1-\nu^2)}} \quad (2.79)$$

2.5.1 Boundary condition of circular shells

According to (Zolqadr and An, 2017), the classical buckling of the clamped spherical shell is less than that of a shell with radially free boundary conditions. The buckling load of the radially free boundary shell should be calculated conservatively when compared to a clamped shallow shell with an identical radius of curvature. Figure 2.9 depicts the effect of the boundary condition on the buckling load of a spherical shell with clamped (fixed), pined (hinged), or free displaced radially.

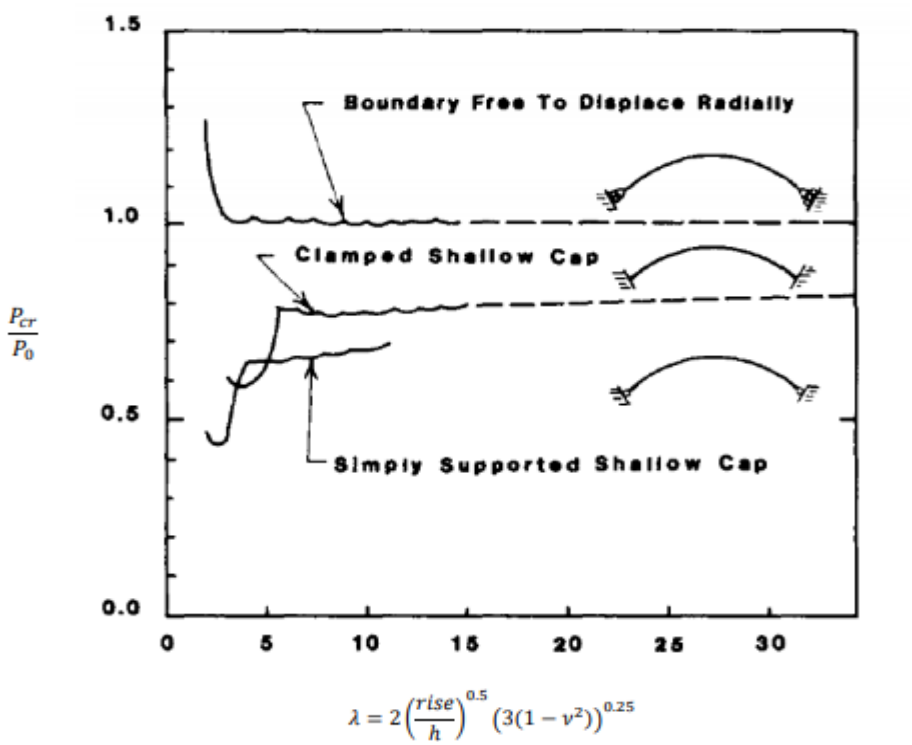

Figure2-9: Effect of boundary conditions (Zolqadr and An, 2017)

2.5.2 Initial Geometric imperfection of circular dome

The bucking load defined in equation (2.73) was created using a complete spherical shell. To facilitate the analysis of the sample elements, the problem was idealized as a spherical cap with a claimed edge. This analysis method was insufficient for shells with varying boundary conditions. Due to the inadequacy of this technique, the spherical cap introduced a new parameter that was not considered in the complete sphere problem with the edge. The new parameter is known as the shape or shallowness parameter, and it is expressed as follows in Figure2.9:

$$\lambda=[3(1-\nu^2)]^{\frac{1}{4}} * \mathbf{2}(\frac{\boldsymbol{rise}}{\boldsymbol{h}})^{\frac{1}{2}} = [3(1-\nu^2)]^{\frac{1}{4}} * \mathbf{2}(\frac{\boldsymbol{H}}{\boldsymbol{h}})^{\frac{1}{2}} \quad (2.80)$$

For small angles,∅

$$\lambda = \sqrt[4]{12(1-\nu^2)} * \sqrt{\frac{a}{h}} * 2\sin\frac{\emptyset}{2} \quad (2.81)$$

For very small angles,∅ and the base radius of a spherical cap,r_o, it becomes:

$$\lambda = \sqrt[4]{12(1-\mathrm{v}^2)} * \frac{\mathrm{r_o}}{\sqrt{\mathrm{ah}}} \quad (2.82)$$

Where:

H Is the rise of the dome cap

h Is the thickness of the spherical dome cap

λ Is the shallowness parameter of a spherical dome

$\emptyset$ Is the meridional angle or cutting angle

$\boldsymbol{v}$ Is the poison's ratio of concrete material

r_o Is the radius of a spherical dome cap

Previous researchers proposed that the buckling pressure behaviour of a spherical cap for the value of the shallowness parameter can be summarized as follows:

- The classical load of a spherical cap with λ value of less than seven was far from the complete spherical shell.
- At the value of $\lambda < 3.5$, the structure does not show an instability failure.
- The value of $\lambda=4$ is shown a snap-through buckling but there is no bifurcation buckling.
- The value of $\lambda > \mathbf{7}$, the pre-buckling behaviour is more linear and more similar to the value of bifurcation buckling.
- In the region of $5.5 < \lambda \leq 7$, makes non-axisymmetric buckling.

CHAPTER 3 CIRCULAR CONCRETE DOME ANALYSIS

3.1 Introduction

A circular concrete dome can be defined as a shell with positive Gaussian curvature and a surface of revolutions. A surface of revolution is obtained by rotating a plane curve known as a meridional curve through a full circle around a vertical axis and producing a parallel circle known as a hoop or circumferential curve (Farshad, 2013).

The circular or spherical concrete thin shell is most commonly found on the roofs of churches, mosques, schools, storage structures, water tanks, stadiums, and nuclear containments.

Furthermore, the theoretical analysis of axisymmetric loadings such as a dome loading with self-weight and live loads will be discussed in this chapter, as well non-axisymmetric loading conditions, particularly earthquake action; displacement, and deformations of a concrete circular dome in the case of axisymmetric loading.

3.2 Analysis of Membrane Forces on a Concrete Circular Dome

3.2.1 Axisymmetric Loading Membrane Force Analysis

Figure 3.1 depicts the general shell of the revolution. The angles ∅ and θ and the radius $r_o$are used to position the element ABCD on the shell surface. It is bound by two meridians and two parallel sections with principal radii r_1 andr_2.

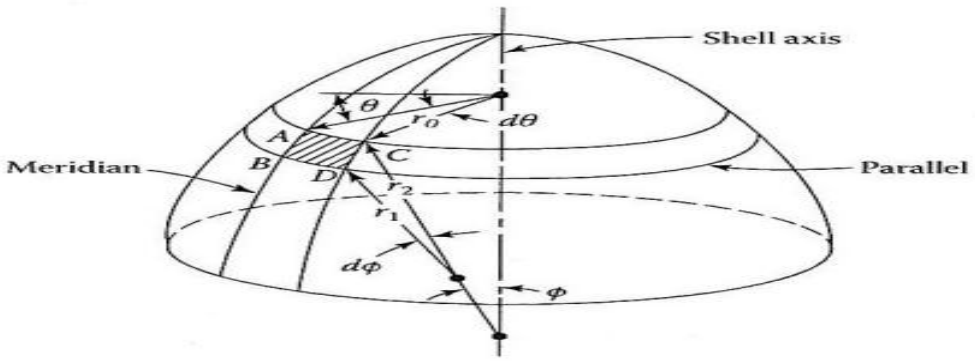

Figure 3-1: A polar differential element of a spherical concrete shell surface (Farnsworth, 1999).

As we saw in the previous chapter, the governing equation of membrane theory can be obtained directly from the equation of general shell theory by ignoring the effects of bending and twisting moments, as well as transverse shear forces, on the stress and strain states of thin shells. As a result, for the membrane theory of thin concrete shells, we can assume that the membrane forces in the polar coordinate system are as follows: $M_{\emptyset}$= M_{θ}= $M_{\emptyset\theta}$= $M_{\theta\emptyset}$= $Q_{\emptyset}$= Q_{θ}= 0. Furthermore, because a given load does not change in the circumferential direction, the governing equation of membrane theory for an axisymmetric loaded shell of revolution can be simplified by assuming the derivative of membrane forces and displacements for is zero.

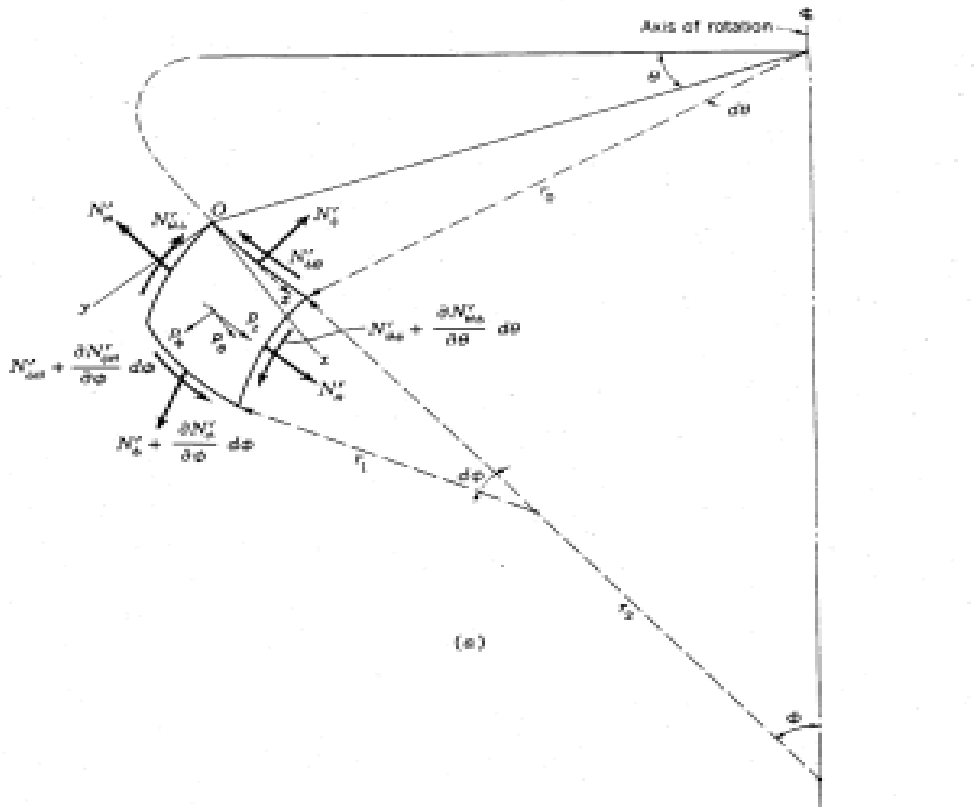

Figure 3-2: Membrane forces and the coordinate system in double curvature spherical shell element (Billington, 1982).

As shown in Figure 3.2 above, the membrane forces can be defined on the differential element in the polar coordinate system. Based on this figure, the governing equilibrium equations of membrane theory in the concrete spherical shell concerning hoop

(circumferential) or; tangent to the meridional ($\emptyset$) and radial ($\boldsymbol{r_o}$) directions are as follows, and recall that from the previous chapter equation (2.70-2.72)

where; $a_x = r_o$; $a_y = r_1 = r_2 = a$; $\alpha_x = \theta$; $\alpha_y = \emptyset$; $N'_x = N'_\theta$; $N'_y = N'_\emptyset$; $N'_{XY} = N'_{\theta\emptyset}$ and $r_o = r_2 \sin\emptyset = a \sin\emptyset$ become:

$$\frac{\partial}{\partial\emptyset}(N'_\emptyset r_o) - N'_\theta \frac{\partial r_o}{\partial\emptyset} + \frac{\partial N'_{\theta\emptyset}}{\partial\theta} r_1 + P_\emptyset r_o r_1 = 0 \quad (3.1)$$

$$\frac{\partial N'_\theta}{\partial\theta} r_1 + N'_{\theta\emptyset} \frac{\partial r_o}{\partial\emptyset} + \frac{\partial}{\partial\emptyset}(N'_{\emptyset\theta} r_o) + P_\theta r_o r_1 = 0 \quad (3.2)$$

$$\frac{N'_\theta}{r_2} + + \frac{N'_\emptyset}{r_1} + P_z = \frac{N'_\emptyset + N'_\theta}{a} = 0 \quad (3.3)$$

Because the loading condition in the concrete spherical shell is symmetrical about its rotational axis, the partial derivative for θ and vanish, and the expression $\partial\emptyset$ can now be written as a total differential $d\emptyset$ because nothing varies with. The axiom of $P_\theta$is very small and will be assumed to be zero. Shear forces are also zero along the meridional and circumference (hoop). As a result, equations (3.1-3.3) are written in the following format:

$$\frac{d}{d\emptyset}(N'_\emptyset r_o) - N'_\theta \frac{dr_o}{d\emptyset} + P_\emptyset r_o r_1 = 0 \quad (3.4)$$

$$\frac{N'_\theta}{r_2} + + \frac{N'_\emptyset}{r_1} + P_z = \frac{N'_\emptyset + N'_\theta}{a} = 0 \quad (3.5)$$

The following expressions evaluate the solutions of the meridional force ($N'_\emptyset$) and the hoop force (N'_θ) in the membrane theory, as expressed in Equations (3.4-3.5) above:

$$N'_\theta = -\frac{r_o}{\sin\emptyset}\left(\frac{N'_\emptyset}{r_1} + P_z\right) \quad (3.6)$$

$$N'_\emptyset = -\frac{1}{2\pi r_o \sin\emptyset}\int_0^\emptyset (P_\emptyset \sin\emptyset + P_z \cos\emptyset)\, 2\pi r_o r_1 d\emptyset \quad (3.7)$$

If R=$\int_0^\emptyset (P_\emptyset \sin\emptyset + P_z \cos\emptyset)\, 2\pi r_o r_1 d\emptyset$; then

$$N'_\emptyset = -\frac{R}{2\pi r_o \sin\emptyset} \quad (3.8)$$

$$\boldsymbol{N'_\theta = \frac{R}{2\pi a \sin^2\emptyset} - P_z \frac{r_o}{\sin\emptyset}\, r_1 = r_2 = a} \text{ or} \quad (3.9)$$

$$N'_\theta = aP_z - N'_\emptyset$$

The integral value of R=$\int_0^\emptyset (P_\emptyset \sin\emptyset + P_z \cos\emptyset)\, 2\pi r_o r_1 d\emptyset$ represents the total vertical load above the parallel circle defined by $\emptyset$.

Where:

$N'_{\emptyset}$ Is the internal membrane force in the meridian direction

N'_{θ} Is internal hoop force in the direction of a parallel circle

$N'_{\emptyset\theta}$ Is the in-plane shear force in the concrete spherical shell

$\boldsymbol{r_o}$ Is the radius of a parallel circle or half of the dome span

$\boldsymbol{r_1}$ Is the radius of curvature at any point on the meridian

r_2 Is the radius of curvature for the surface from the axis of revolution

$r_1 = r_1 = a$ Is the radius of curvature of the dome from the rotational axis

$\emptyset$ Is meridional angle from the axis of revolution

θ Is circumferential angle (or hoop angle)

P_z Is external distributed load applied on the surface of the shell in radial direction per unit area

P_θ Is external distributed load applied on the surface of the shell in hoop direction per unit area

$P_\emptyset$ Is external distributed load applied on the surface of the shell in a meridian direction per unit area

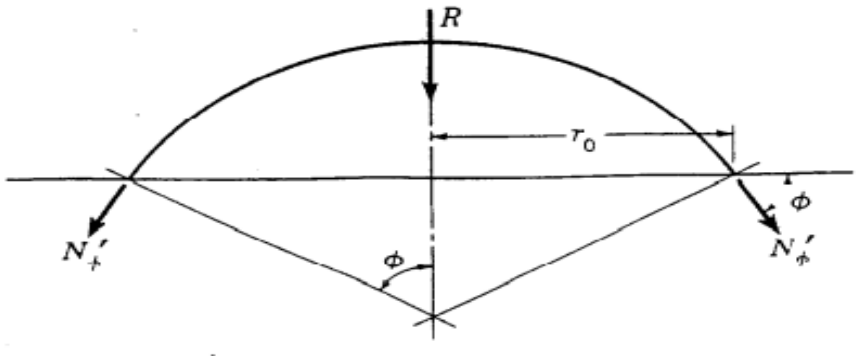

Figure 3-3 The integral load R causes concrete dome shell equilibrium (Billington, 1982).

3.2.2 Analysis of Membrane Forces Under Self-weight

Based on Figure 3.4; the analysis of membrane forces described in the previous subtopic when the reinforced concrete dome with constant thickness is uniformly loaded over its surface by its self-weight (q) with $r_1 = r_2 = a$; $P_\emptyset = q \sin \emptyset$; $P_z = q \cos \emptyset$ and $P_\theta = 0$ are written in the following ways:

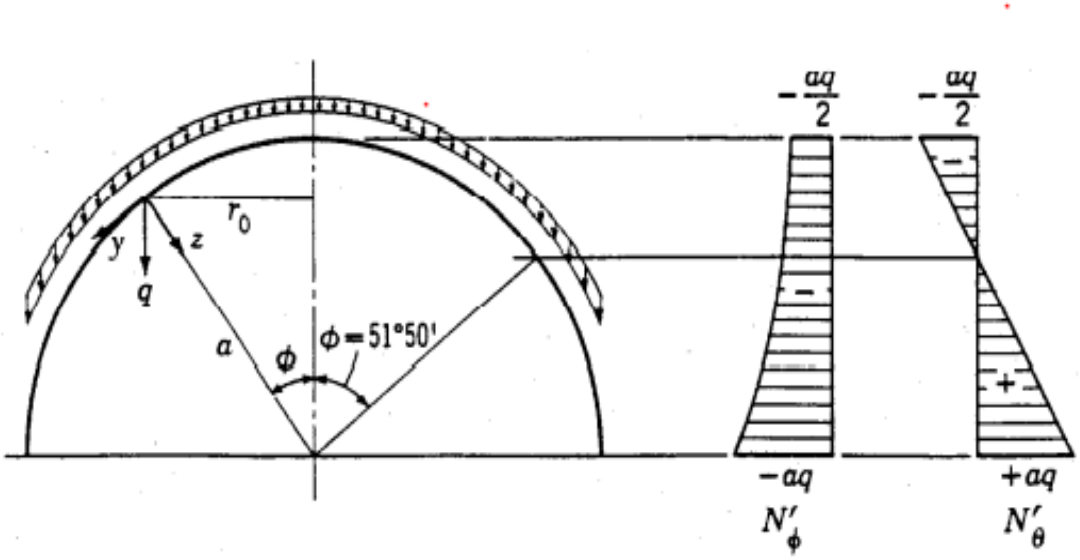

Figure 3-4: Self-weighted concrete spherical dome (Billington, 1982).

Thus, the integral value of R=$\int_0^\emptyset (P_\emptyset \sin \emptyset + P_z \cos \emptyset)\, 2\pi r_o r_1 d\emptyset$ due to self-weight is

R=$2\pi a^2 q \int_0^\emptyset \sin \emptyset d\emptyset = 2\pi a^2 q(1 - \cos \emptyset)$

The meridional and hoop forces mentioned in equations (3.8) and (3.9) due to the self-weight (q) of a concrete dome are expressed using the value of R as:

$$N'_\emptyset = -aq\left(\frac{1}{1+\cos \emptyset}\right) \quad (3.10)$$

$$N'_\theta = aq\left(\frac{1}{1+\cos \emptyset} - \cos \emptyset\right) \quad (3.11)$$

Where:

R Is the total vertical load acting along the axis of symmetry.

a Is the radius of a spherical shell

q Is a self-weight or a dead load of a spherical shell

$\emptyset$ Is the meridional angle for the axis of revolution/symmetry

It is critical to note that the expression (3-10) always produces negative values for $N'_{\emptyset}$ throughout the shell due to the dome's self-weight. Figure 3.4 depicts the distributions of the two membrane forces (force/unit length). Compressive meridian values ($N'_{\emptyset}$) an increase from the crown to the edge. Hoop values (N'_{θ}) the decrease from a maximum compression(-) at the crown to zero at some point in the hemisphere, 51° 50', then becomes tension (+) and increases to a maximum at the edge.

3.2.3 Analysis of Membrane Forces under Live Load

Consider a constant thickness spherical dome of radius (a) upon by live load (P) which is uniformly distributed over a horizontal projection of the dome surface illustrated in Figure 3.5 below. In this case;$P_z = P\,cos^2\,\emptyset$; $P_{\emptyset} = P \sin\emptyset \cos\emptyset$ and $P_{\theta} = 0$.

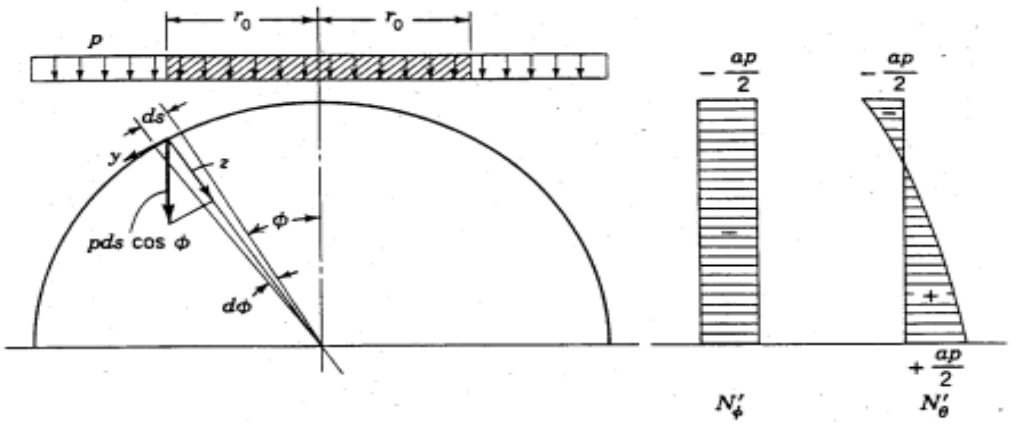

Figure 3-5 Spherical concrete dome subjected to imposed or live load (Billington, 1982).

Thus; the integral value of R=$Pa^2\pi sin^2\emptyset$ and

$$N'_{\emptyset} = -\frac{aP}{2} \tag{3.12}$$

$$N'_{\theta} = -a\left(P\,cos^2\,\emptyset - \frac{aP}{a}\right) = -\frac{aP}{2}(2cos^2\emptyset - 1) \text{ or} \tag{3.13}$$

$$N'_{\theta} = -\frac{aP}{2}\cos 2\emptyset$$

Where:

P Is represents the live load on a spherical concrete dome

a Is the radius of the spherical dome

The distribution of membrane force values due to living load shown in Figure 3.5 suggests that where the meridian force $N'_{\emptyset}$ is constant compression, the hoop force N'_{θ} value changes from compression at the apex to tension at the edge. The value of hoop force N'_{θ} become zero at $\cos 2\emptyset = 0$ or $\mathbf{2}\emptyset = 90^0$ or $\emptyset = 45^0$.

3.2.4 Membrane Force Analysis of a Spherical Shell under Earthquake Action

An earthquake or seismic load is another dynamic force frequently simulated by a static representation. Actual or simulated earthquake records are typically available in the form of two horizontal components (N-S) and (E-W), as well as a vertical component. The vertical component is an axisymmetric loading, and horizontal components are usually assumed to be out of phase (peak acceleration effects from two directions do not occur at the same instant on the structure). Because spherical domes are axisymmetric structures, it is sufficient to consider only the stronger of the two components, as shown in Figure 3.6.

A FEM or special purpose dynamic analysis of a shell is too time-consuming and expensive for most other types of structures when a membrane theory approach is adequate. The following set of assumptions is critical for analyzing the spherical dome under earthquake action, particularly in membrane theory [2].

- Due to the lack of anti-symmetric membrane equilibrium equations, equations are derived based on equilibrium conditions for the axisymmetric structure.
- Seismic loading on the shell is applied as a body load per square foot of surface area.
- The shear is not equal to zero.
- The thickness of the shell is constant.

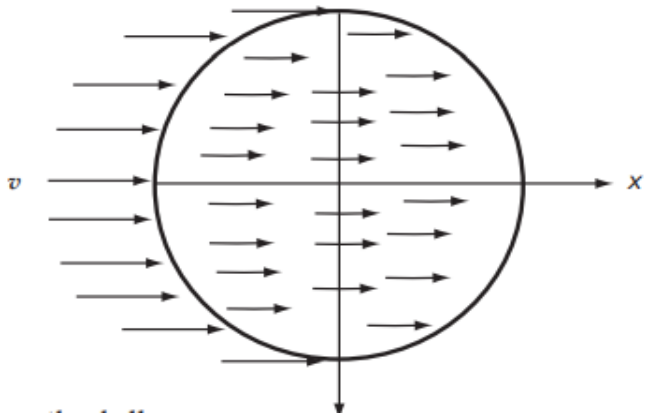

Figure 3-6: Seismic surface loading condition on the concrete spherical shell in x-y pane view (Wilson, 2005).

As an approximation for earthquake loading on a spherical shell, we can use horizontal loading in one direction equal to the dead weight times the $\frac{a_v}{g}$.ratio**.**

$$P_s = \upsilon = \frac{a_v}{g} * h * \gamma_c \quad (3.14)$$

The earthquake load components on the concrete circular dome's surface are as follows:

$$P_z = P_s \cos\theta \sin\emptyset \quad (3.15)$$

$$P_\emptyset = -P_s \cos\theta \sin\emptyset \quad (3.16)$$

$$P_\theta = P_s \sin\emptyset \quad (3.17)$$

The membrane forces on the circular dome shell caused by seismic loads are given by:

$$N'_\emptyset = \frac{a_v * a * h * \gamma_c \cos\theta}{g sin^3\emptyset}(sin^2\emptyset + 2cos^2\emptyset - 2\cos\emptyset) \quad (3.18)$$

$$N'_\theta = \frac{a_v * a * h * \gamma_c \cos\theta}{g sin^3\emptyset}(2\cos\emptyset - sin^4\emptyset - cos^2\emptyset - 1) \quad (3.19)$$

$$N'_{\emptyset\theta} = \frac{a_v * a * h * \gamma_c \sin\theta}{g sin^3\emptyset}(\cos\emptyset\, sin^2\emptyset + 2\cos\emptyset - 2) \quad (3.20)$$

Where:

a_v Is the horizontal seismic acceleration

g Is acceleration due to gravity

h Is the thickness of the concrete spherical dome shell

γ_c Is the unit weight of concrete

P_s Is earthquake action per unit area distributed over the shell surface

$r_1 = r_1 = a$ Is the radius of a spherical shell

$N'_{\emptyset}$ Is the meridian (radial) force due to earthquake action which is computed at $\theta = 0^0$

N'_{θ} Is the hoop (circumferential) force due to earthquake action which is computed at $\theta = 0^0$

$N'_{\emptyset\theta}$ Is the shear force due to earthquake action which is computed at $\theta = 90^0$

3.2.5 Strains and Displacements from Membrane Theory of Spherical Shells

- Strains;

The simplified extensional strains in the meridional and circumferential directions corresponding to the value of meridional and hoop forces in the spherical concrete shell with constant thickness are given by:

$$\varepsilon_{\theta} = \frac{1}{Eh}(N'_{\theta} - vN'_{\emptyset}) \quad (3.21)$$

$$\varepsilon_{\emptyset} = \frac{1}{Eh}(N'_{\emptyset} - vN'_{\theta}) \quad (3.22)$$

Where:

$\boldsymbol{\varepsilon_{\theta}}$ Is the extensional circumferential strain

$\varepsilon_{\emptyset}$ Is the extensional meridional strain

E Is the elastic modulus of concrete material

h Is the thickness of the spherical dome

v Is the poison's ratio of the concrete material

$\emptyset$ Is the meridional angle from the axis of revolution/symmetry

$N'_{\emptyset}$ Is the internal membrane force in the meridian direction

N'_{θ} Is internal hoop force in the direction of a parallel circle

- Displacements of a spherical concrete shell

The displacements from the Membrane Theory for spherical shells subjected to axisymmetric loading can be calculated by first determining the extensional strains and

then calculating the displacements. These are denoted as horizontal translation and rotation, and they are derived from the strain equations in (2.29-2.31) as:

$$\Delta_H = D^D{}_{10} = \frac{a \sin \emptyset}{Eh}(N'_\theta - vN'_\emptyset) \quad (3.23)$$

$$\Delta_\emptyset = D^D{}_{20} = \frac{\cot \emptyset}{Eh}[(N'_\emptyset - N'_\theta)(1+v)] - \frac{1}{a}\frac{d}{d\emptyset}\left(\frac{\Delta_H}{\sin \emptyset}\right) \quad (3.24)$$

Where:

Δ_H Is the horizontal translation at the edge of a spherical dome

$\Delta_\emptyset$ Is the rotation at the edge of a spherical dome

a Is the radius of the spherical dome

$\emptyset$ Is the meridional angle for the axis of revolution/symmetry

$D^D{}_{10}$ Is horizontal deformation due to membrane forces

$D^D{}_{20}$ Is rotational deformation due to membrane forces

The horizontal and rotational displacements for any given membrane loading condition can be calculated using equations 3.23 and 3.24. The displacements at the edge of a constant-thickness spherical concrete shell are calculated by substituting the values of $N'_\emptyset$ and N'_θ expressed in the previous section due to any loading conditions. As a result, the displacements at the dome's edge will be expressed as follows:

- Displacements due to self-weight (or dead load)

$$\Delta_H = D^D{}_{10} = \frac{a^2 q}{Eh}\left(\frac{1+v}{1+\cos \emptyset} - \cos \emptyset\right) \sin \emptyset \quad (3.25)$$

$$\Delta_\emptyset = D^D{}_{20} = -\frac{aq}{Eh}(2+v) \sin \emptyset \quad (3.26)$$

Where; α = is the radius of a spherical shell.

q = is a self-weight or a dead load of a spherical shell

$\emptyset$ = is the meridional angle for the axis of revolution/symmetry

- Displacements due to living load (or imposed load)

$$\Delta_H = D^D{}_{10} = \frac{a^2 P}{2Eh}(v - \cos 2\emptyset) \sin \emptyset \quad (3.27)$$

$$\Delta_\emptyset = D^D{}_{20} = -\frac{aP}{2Eh}(3+v) \sin \emptyset \quad (3.28)$$

Where:

P Is represents the live load on a spherical concrete dome

a Is the radius of the spherical dome

h Is the thickness of the spherical dome

v Is the poison's ratio of the concrete material

- Displacements due to Earthquake action (or seismic load)

$$\Delta_H = D^D{}_{10} = \frac{aP_s \cos\theta}{Ehsin^2\emptyset}(K_3 - vK_4) \quad (3.29)$$

Where; $K_3 = (\cos\emptyset - \frac{1}{3}cos^2\emptyset - \cos\emptyset sin^4\emptyset - \frac{2}{3})$ and $K_4 = (\frac{2}{3} - \cos\emptyset + \frac{1}{3}cos^3\emptyset)$

$$\Delta_\emptyset = \mathrm{D}^{\mathrm{D}}{}_{20} = 0 \quad (3.30)$$

Where:

P_s Is earthquake action per unit area distributed over the shell surface

E Is the elastic modulus of concrete material

h Is the thickness of the spherical dome

v Is the poison's ratio of the concrete material

$\emptyset$ Is the meridional angle from the axis of revolution/symmetry

Because the rotational displacement caused by an earthquake action is so small and negligible, the displacement for seismic loading conditions has been set to zero.

Finally, using membrane theory, the displacements tangent and normal to the meridian of a spherical concrete shell under the action of its weight can be calculated as follows:

$$u = \frac{a^2q(1+v)}{Eh}\sin\emptyset[\ln(1+\cos\emptyset) - \frac{1}{1+\cos\emptyset}] + C\sin\emptyset \quad (3.31)$$

Where;

$$C = \frac{a^2q(1+v)}{Eh}\sin\emptyset[\frac{1}{1+\cos\alpha} - \ln(1+\cos\alpha)] \quad (3.32)$$

$$w = -\frac{a^2q}{Eh}\left(\frac{1}{1+\cos\emptyset} - \cos\emptyset\right) + \frac{a^2q}{Eh}\cos\emptyset\,[\ln(1+\cos\emptyset) - \frac{1}{1+\cos\emptyset}] + C\cos\emptyset \quad (3.33)$$

Where:

E is the elastic modulus of concrete material

h Is the thickness of the spherical dome

$\boldsymbol{\nu}$ Is the poison's ratio of the concrete material

$\emptyset$ Is the meridional angle from the axis of revolution/symmetry

α Is half of the central angle

C Is an integral constant

u Is the displacement tangent to the meridian

w Is the displacement normal to the meridian

q Is a self-weight or a dead load of a spherical shell

3.3 Analysis of Spherical Dome-Ring Beam

The majority of domes have an edge ring beam at their lower edges and/or an edge ring beam somewhere along their parallel circles.

Edge ring beams reinforce the shell and/or provide lateral support for the shell structure. The lateral support action of the edge ring beams is especially important when there are only vertical supports and the lateral forces must be occupied by the structure itself.

Several concrete domes are supported tangentially at the meridian edge. A fixed dome is usually not possible or desirable for providing a fixed support to the meridian at the edge. In most cases, a dome is supported by vertical bearings that can move horizontally. To prevent large horizontal displacements at the dome edge, lateral constraints are required. A structural engineer is usually charged with some kind of lateral restraint, such as a ring beam, cylinder wall, or a combination of the two.

The size of the edge ring beam has been shown to have a very meaningful effect on the membrane and bending stresses in shells, but surprisingly small results on the elastic critical buckling pressure; as a result, this paper is not considered the elastic buckling analysis of ring beam at the edge of a circular dome.

CHAPTER 4 MATERIALS AND LOAD DETERMINATION

4.1 Action Combinations Based on Euro-Codes

For this investigation, the basic load union (combination values of variable action) is used to demonstrate the ultimate limit state design. The selected load combination and load factor values $\boldsymbol{\gamma_f}$ for ultimate limit, state design of effective design situation and unfavourable load case of roof based on Euro code 0:2001 are as follows **(**prEN 1990:2001**).** Note, the seismic action along the x-direction is considered.

$$1.35G_k \quad (4.1)$$

$$1.35G_k + 1.5Q_k \quad (4.2)$$

$$G_k + 1.0\,EQ_X \quad (4.3)$$

$$1.0G_K + 0.3Q_k + EQ_X + 0.3EQy \quad (4.4)$$

Where:

G_K is permanent gravity load (self-weight and additional dead load)

Q_K Is live load (variable; imposed load)

EQ_X Is the horizontal component of seismic action along X-axis

4.1.1 Materials Based on Euro Code Standards

In this study, plain concrete with quartzite aggregates with properties of characteristic 28-day compressive cylinder strength of concrete (f_{CK}) =30Mpa of C30/37, unit weight of concrete (γ_c) value of 25kN/m2 and design value of elastic modulus of concrete (E_C) of 33GPa is used. Poisson's ratio (v) is 0.2 for non-cracked concrete and 0 for cracked concrete, as specified in Euro code 2 part 1-1 section 3 clause 3.1.3. (Logan, 2022).

4.1.2 The Geometry of the Required Models

In this study, a wide range of spherical shell arrangements are considered with the goal of analyzing the effect of geometry on buckling behaviour. To achieve this effect, 15 different geometric configurations are used, which are obtained by varying the cutting angle, thickness, and principal radius of the circular concrete thin shell with a constant span of 40m. Furthermore, the effects of dead load, live load, seismic action, and boundary conditions on each model's buckling behaviour will be discussed later.

For the complete design of concrete circular domes the geometric parameters, in particular, their thicknesses can be selected based on shell classifications, collapse mechanism, membrane theory, theory of shell under point load (Koitor's Equation) and material selection. But this paper mainly focused on the analysis part of structures. Therefore, for this study, a 100mm minimum thickness of a spherical dome (h) roof was chosen as a baseline; thin shells are defined as shells with a radius-to-thickness ratio between 20 and 1000, as determined by shell classifications and collapse mechanism of structures (radius-to thickness ratio greater than or equal 336.4) (Varghese, 2010). The radius of curvature (α) was chosen using thin shell theory. The geometrical dimension of a cutting angle or half central angle ∅ of each model can be obtained by applying the following mathematical expressions; all of the remaining values of the geometrical parameters of the dome cap listed in Table4.1, Table4.2, and Table4.3 have been calculated using equations 4.5 and 4.6, which are defined below.

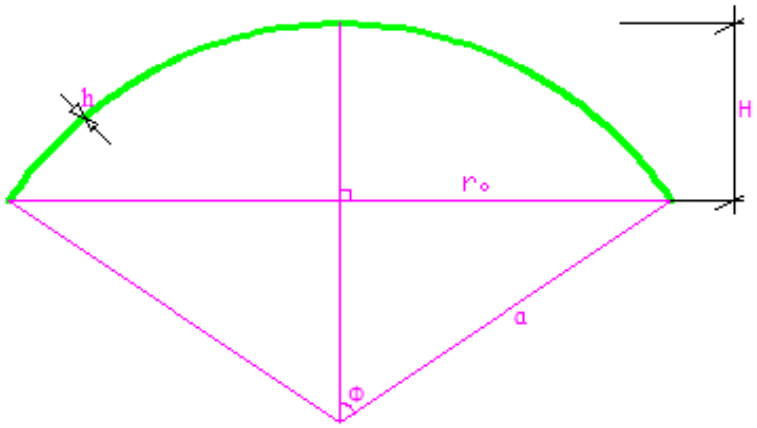

Figure 4-1: The geometry of the circular shell

$$\sin \emptyset = \frac{r_o}{a} \quad (4.5)$$

$$H = a(1 - \cos \emptyset) \quad (4.6)$$

Where;

a Is the principal radius of each model

$r_o = \frac{2r_o}{2}$ Is the base radius or half of the given span

$\emptyset$ Is cutting angle or half central angle or half of included angle

H Is the rise of the model of spherical dome caps

Table 4-1**:** The required models' geometrical dimensions with a thickness (h) of 0.1m

Number of models	Radius ($\boldsymbol{a}$) in (m)	Cutting angle (∅) in degree.	Rise(H) in (m)	The ratio of ($\boldsymbol{a}$ /h)	The ratio of ($\boldsymbol{a}$ /H)
1	40	30.0000	5.3590	400	7.4641
2	35	34.8499	6.2772	350	6.3723
3	30	41.8103	7.6393	300	5.2361
4	25	53.1301	10.0000	250	4.0000
5	20	90.0000	20.0000	200	2.0000

Table 4-2**:** The required geometrical dimensions with a thickness (h) of 0.12m

No. of models	Radius ($\boldsymbol{a}$) in (m)	Cutting angle (∅) in degree.	Rise(H) in (m)	The ratio of ($\boldsymbol{a}$ /h)	The ratio of ($\boldsymbol{a}$ /H)
1	40	30.0000	5.3590	333.3333	7.4641
2	35	34.8499	6.2772	291.6667	6.3723
3	30	41.8103	7.6393	250.0000	5.2361
4	25	53.1301	10.000	208.3333	4.0000
5	20	90.0000	20.000	166.6667	2.0000

Table 4-3: The required geometrical dimensions with a thickness (h) of 0.15m

No. of models	Radius ($\boldsymbol{a}$) in (m)	Cutting angle (∅) in degree.	Rise(H) in (m)	The ratio of ($\boldsymbol{a}$ /h)	The Ratio of ($\boldsymbol{a}$ /H)
1	40	30.0000	5.3590	266.6667	7.4641
2	35	34.8499	6.2772	233.333	6.3723
3	30	41.8103	7.6393	200.000	5.2361
4	25	53.1301	10.000	166.666	4.0000
5	20	90.0000	20.000	133.333	2.0000

4.2 Load Determination

For this investigation, the circular concrete shell structure is accounted for separately for dead, live, and seismic loads and their combination is based on European Code Standard EN 1990:2001 to determine each load for the required models.

4.2.1 Self-weight

The structure self-weight can be represented by a single characteristic value and calculated using the nominal dimensions and mean unit masses, as specified in EN 1991-1-1.

The self-weight of construction works should be classified as a permanently fixed action, according to EN 1990, 1.5.3 and 4.1.1.

Action that is likely to act over a given reference period and whose magnitude variation with time is negligible, or whose magnitude variation is always in the same direction (monotonic) until the action reaches a certain limit value.

The total self-weight of structural and non-structural members should be considered in action combinations as a single action.

As a result, dead load q is calculated by adding the self-weight of the shell as well as plastering and painting finishing. According to European Code Standard EN 1991-1-1 table A-1, concrete has a specific weight of 25kN/m2 and cement plastering mortar has a specific weight of 23kN/m3. Thus, the surface of each model is obtained by multiplying the unit weight of the material by the thickness of the required material; this concept is mathematically expressed as follows:

$$q = (r_c * h_i) + (r_p * h_p) \qquad (4.7)$$

Where;

q Is a self-weight or a dead load of spherical dome

r_c is the unit weight of concrete

h_i is the thickness of spherical shells; i=1; 2; 3

γ_p is the unit weight of plastering mortar

h_p is 0.05m is the thickness of plastering and painting

This study employs three different shell thicknesses to determine the effect of shell thickness on the buckling load of each model. So, within the variable thickness of the shell, the dead load of the model is given by:

At $h_1 = 0.1m$; $q_1 = \left(25\frac{KN}{m^3} * 0.1m\right) + \left(23\frac{KN}{m^3} * 0.05m\right) = 3.650\frac{KN}{m^2}$

At $h_2 = 0.12m$; $q_2 = \left(25\frac{KN}{m^3} * 0.12m\right) + \left(23\frac{KN}{m^3} * 0.05m\right) = 4.150\frac{KN}{m^2}$

At $h_3 = 0.15m$; $q_2 = \left(25\frac{KN}{m^3} * 0.15m\right) + \left(23\frac{KN}{m^3} * 0.05m\right) = 4.900\frac{KN}{m^2}$

4.2.2 Live Load

According to Euro code 1 part1-1 (2002) of section 6 clause 6.3.4.1(1) table 6.10 characteristic imposed load Q_k for roof category H (i.e. Roofs not accessible except for normal maintenance and repair.) is equal to $0.4\frac{KN}{m^2}$.

4.2.3 Earthquake (Seismic Action)

Earthquakes are caused by faults in the earth's crust rupturing, landslides, and volcanic eruptions. An earthquake can also be caused by man-made activities such as large explosions. Normally, earthquakes occur near the boundaries of tectonic plates. Because these plates are constantly moving, stresses build up and release energy through the earth's crust, causing the ground to shake. As a result, the majority of seismic hazards in Ethiopia occur in zone five. As a result, this paper focused on the circular concrete shell that was constructed in this zone.

4.2.4 Determination of Natural Frequency

As is the case, the fundamental frequency of a structure corresponds to the structure's lowest natural frequency. The determination of these frequencies is very interesting in this study for each model, to find out the corresponding maximum spectral response acceleration of the structure.

The study presents a linear perturbation action that can solve the eigenvalue problem for symmetric mass and stiffness matrices, yielding the frequency and mode shape for each case. A classical eigenvalue un-damped finite element model is defined by the following mathematical expressions:

$$\{[\mathrm{K}] - \omega^2{}_{\mathrm{n}}[\mathrm{M}]\} * \lambda = 0 \qquad (4.8)$$

Where;

K Is represents the stiffness matrix

M Is represents the mass matrix of the structure

$\omega = \frac{2\pi}{T} = 2\pi f$ Is the natural frequency of the structure in rad per second

λ Is modal vibration or eigenvector

n Is the number of degrees of freedom

$T = C_t x H^{3/4}$ Is the fundamental period of a structure

C_t=0.05 is the recommended value Euro code-8 of all structures

H is the height of the dome models

$f = \frac{1}{T}$ Is the fundamental cyclic frequency

The fundamental frequencies for free vibration analysis can be obtained using Euro code-8 at 4.3.3.2.2. (3). Table A.1 in Appendix A lists the frequencies and their corresponding periods for each model.

4.2.5 Horizontal Component of Seismic Action

The European designs standard code EN1998-1:2004 is used in this study to determine the magnitude of the horizontal component of earthquake action.

Structures in seismic zones must be analyzed and built to meet damage limitations and no collapse requirements. Thus, to meet this requirement and obtain the corresponding earthquake parameters in structural analysis, the ground class and structure locations must first be determined. In this study, a type-1 elastic response spectrum ground class-B with 5% damping is chosen as recommended by EN1998-1:2004, and the study location is classified as one of the highest seismic zones in Ethiopia's seismic hazard mapping project, which is near the rift Valley.

In Ethiopia, seismic hazard mapping is currently divided into five zones, with the ratio of the design peak ground acceleration (a_g) to the acceleration of gravity (g) equal to α_o for the corresponding zones shown in Table 4.3 below.

Table 4-4:The ratio of peak ground acceleration to acceleration due to gravity

Zones	0	1	2	3	4	5
$\boldsymbol{\alpha_o = \frac{a_g}{g}}$	0	0.04	0.07	0.10	0.15	0.20

The value of the above table is taken based on the following Ethiopian seismic hazard mapping.

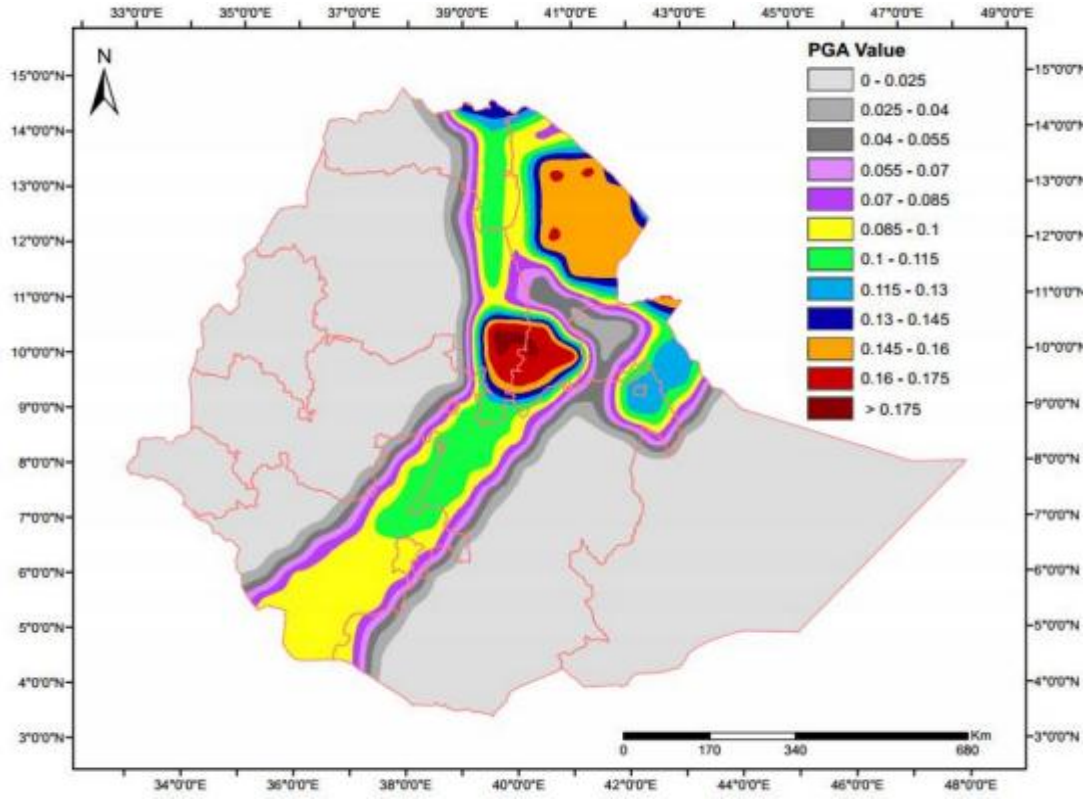

Figure 4-2: Ethiopian seismic hazard map in terms of peak design ground acceleration (EBSCEN, 2004).

Because the current investigation is not concerned with the structure's design, the values $\boldsymbol{\gamma_1}$=1 (Importance Factor) and R=1 (Response Modification Factor) were chosen for the spectral analysis.

The elastic spectrum S e (T) for the horizontal component of seismic action is defined by the following expression based on EN1998-1:2004: 3.2.2.2(1) P; the shape of the elastic response spectrum is shown in Figure 4.1.

$$0 \le T \le T_B: \quad S_e(T) = a_g * S * [1 + \frac{T}{T_B}(\eta * 2.5 - 1)]. \tag{4.9}$$

$$T_B \le T \le T_C: \quad S_e(T) = a_g * S * \eta * 2.5 \tag{4.10}$$

$$T_C \le T \le T_C: \quad S_e(T) = a_g * S * \eta * 2.5 * [\frac{T_C}{T}] \tag{4.11}$$

$$T_D \le T \le 4S: \quad S_e(T) = a_g * S * \eta * 2.5 * [\frac{T_C T_D}{T^2}] \tag{4.12}$$

Where:

$S_e(T)$ Is the horizontal component of the earthquake elastic response spectrum

T Is the vibration period of a single degree of freedom system

a_g Is the design ground acceleration on type A ground ($a_g = \gamma_1 * a_{gR}$)

T_B Is the lower limit of the period of the constant spectral acceleration branch

T_C Is the upper limit of the period of the constant spectral acceleration branch

T_D Is the value defining the beginning of the constant displacement response range of the spectrum

S Is soil factor

η Is the damping correction factor with a reference value of $\eta = 1$ for 5% viscous damping

γ_1 Is importance factor

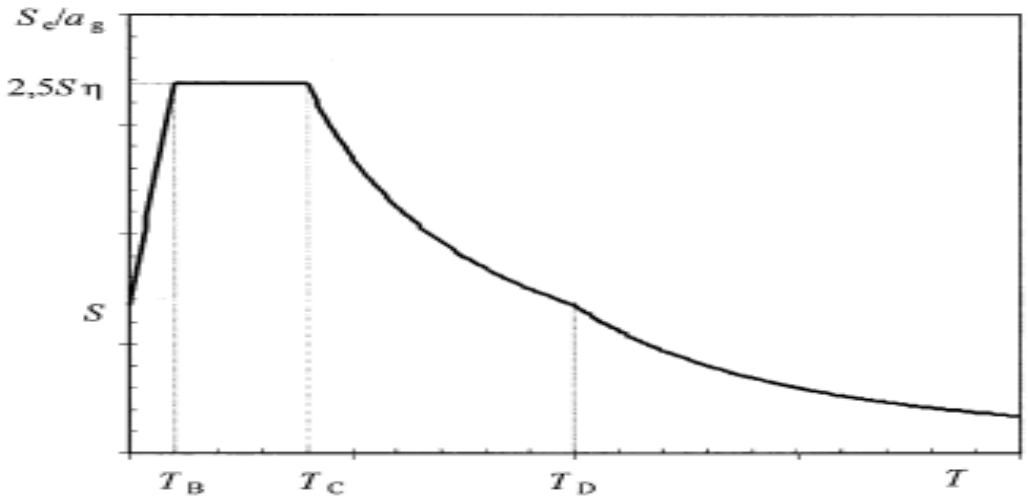

Figure 4-3: Shape of the elastic response spectrum (EBSCEN, 2004).

Table 4-5: The value of the parameters describing the recommended Type-I elastic response spectra for ground type B for the horizontal component of seismic action**.**

Ground Type	S	T_B in second(S)	T_C in second(S)	T_D in second(S)
B	1.2	0.15	0.5	2.0

4.2.6 Peak Ground Acceleration (PGA)

The maximum intensity, duration of the shock, peak ground acceleration (PGA), peak ground velocity (PGV), peak ground displacement (PGD), and several spectral accelerations are all regularly considered earthquake action parameters at a site. Peak

ground acceleration (PGA) is the most commonly used for structural engineering applications because it is traditionally and directly related to the induced seismic forces, which form the basis of current structural seismic design procedures.

As a result, based on seismic hazard zonation mapping for European countries, the peak ground acceleration (PGA) for action type I in zone 5 for ground soil type B is assumed to be 0.2g in the percentage of critical damping $\zeta = 5\%$.

4.3 SAP2000 Finite Element Method for Concrete Dome Buckling

The finite element method is a numerical method for calculating approximate solutions to partial differential equation boundary value problems. The basic idea behind this method is to divide a large problem into smaller, simpler parts (called finite elements) and connect them using points (called nodes) or/and edges or/and surfaces that they share. This process is commonly named "Discretization". It is possible to formulate an equation for each finite element and combine them to obtain a solution for the domain using this method. The finite element method has grown in popularity, especially when an analytical solution is difficult to achieve due to the complexity of the problem. Numerical methods provide approximate solutions to unknowns (called degrees of freedom) with a reasonable loss of accuracy. Some problems where the finite element method has been successfully applied include structural analysis, fluid dynamics, electromagnetic potential distribution, and heat transfer. Displacements and stresses are typically the problem's unknowns in structural analysis, which involves structures subjected to applied loads. Fluid pressures, electromagnetic potential, temperature, and other unknown values may be used in the nonstructural analysis.

4.3.1 Steps of the Finite Element Method

Now, present the steps used in the finite element method formulation and solution of a structural problem, along with any necessary explanations. The purpose of outlining these general steps now is to familiarize you with the procedure typically used in a finite element formulation of a problem. So, according to Logan's "A First Course in the Finite Element Method," the finite element method's main steps are as follows:

Step 1: Discretize and select the element types

Step one entails subdividing the body into a set of finite elements connected by nodes and selecting the element type that best models the body's real physical behaviour. The dimensions of such elements must be carefully chosen to achieve adequate solution accuracy while reducing computational time and effort. Large elements can be used to solve relative constant problems. When the properties of the body change quickly, however, the use of smaller elements becomes necessary. Furthermore, the type of elements used influences the accuracy of the result; thus, it must be determined based on the geometry of the body and the type of loading conditions. The most typical

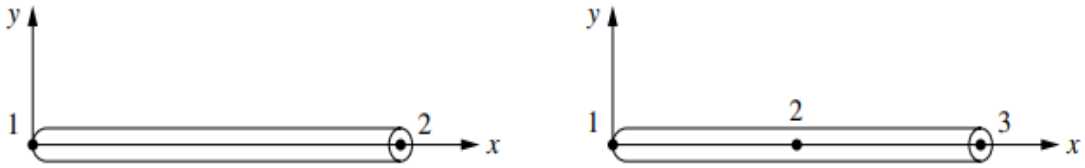

Figure 4-4: Simple two-node line elements are commonly used to represent a bar or beam element [4].

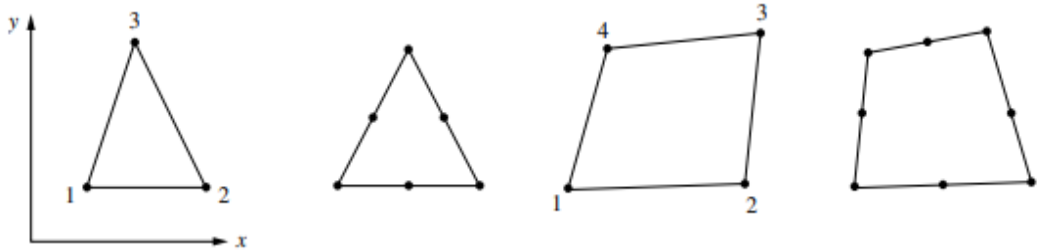

Figure 4-5: Simple two-dimensional elements used to represent plan stress/strain (Logan, 2022).

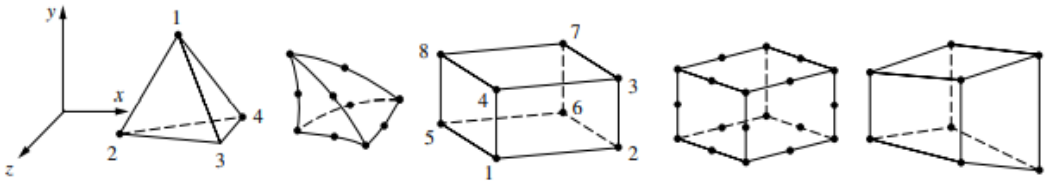

Figure 4-6: Simple three-dimensional elements used to represent 3-dimensional stress (Logan, 2022).

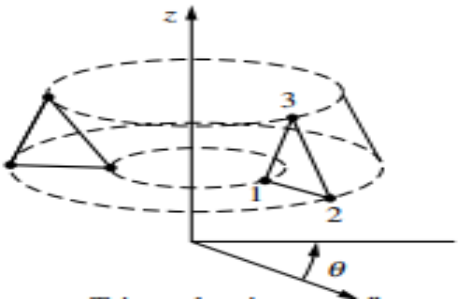

Figure 4-7: Simple axisymmetric element (Logan, 2022).

Step 2: Select a displacement function

The second step is to select a displacement function that is defined within the element using the nodal values of the element. Because of the simplicity of their formulation, linear, quadratic, and cubic polynomials work well with the finite element process in general. Other functions, such as trigonometric series, can also be used. Once the displacement function has been chosen, it can be used for each element repeatedly. Any continuous function of interest can be approximated by a series of piecewise-continuous functions defined within each finite domain or finite element using this method.

Step 3: Define the Strain/Displacement and Stress/Strain relationship.

The third step is to define the Strain/Displacement and Stress/Strain relationships to derive the equations for each finite element. For small strains, the strain ε_x in the X direction, related to the displacement u, is defined as: $\varepsilon_x = \frac{du}{dx}$ in the simplest case of one-dimensional deformation. Furthermore, the strain and stress must be linked by a constitutive law. Hooke's law is the most common and simplest constitutive law, and it is expressed in one dimension as $\sigma_x = E\varepsilon_x$ where E represents the modulus of elasticity and σ_x the stress in the x direction.

Step 4: Derive the element stiffness matrix and equations.

In step four, the direct equilibrium/stiffness method, the work/energy method, or the weighted residual method are used.

Direct equilibrium or stiffness method

The force equilibrium conditions for a single element are used in this method. The force/deformation relationship is used to provide stiffness matrix element equations that relate nodal forces to displacement (Logan, 2022).

Work or energy method

When developing the stiffness matrix and equations for two- and three-dimensional elements, the work or energy method is the best solution. The most popular methods for this purpose are the virtual work principle, the principle of minimum potential energy, and Castigliano's theorem. The first applies to any material, whereas the other two are only applicable to elastic materials.

Method of weighted residuals

When a function, such as potential energy, is not readily available, the weighted residuals method comes in handy. Galleria's method is the most well-known. Wherever the energy methods are applicable, this method produces the same results as the energy methods. Furthermore, employing them can be directly applied to any type of differential equation.

The goal of any of the methods mentioned above is to provide equations that describe the behaviour of each element. These equations can be written in a more compact form:

$$\{f\} = [K]\{d\} \qquad (4.13)$$

Where;

{f} is the vector of nodal element forces,

[k] is the element stiffness matrix and

{d} is the vector of the degrees of freedom or generalized displacements.

Step 5: Assemble the equations to obtain the global or total equations and introduce boundary conditions.

The fifth step focuses on combining the individual element nodal equilibrium equations to form the global nodal equilibrium equations. A more direct method, known as the "direct stiffness method," can also be used to obtain the global equations. This method implicitly assumes that the structure will remain intact (no tears occur anywhere within

the structure). The assembled or global equation can be written in matrix form as follows:

$$\{F\} = [K]\{d\} \tag{4.14}$$

Where:

{F} is the vector of global nodal forces,

[K] is the structure global or total stiffness matrix, and

{d} is the vector of known and unknown degrees of freedom or generalized displacements.

Step 6: Solve for the unknown degrees of freedom.

Step six entails resolving the unknown degrees of freedom using a set of algebraic equations that can be written in the following matrix form:

$$\begin{Bmatrix} F_1 \\ F_2 \\ \vdots \\ F_n \end{Bmatrix} = \begin{bmatrix} K_{11} & K_{12} & \dots & K_{1n} \\ K_{21} & K_{22} & \dots & K_{2n} \\ \vdots & & & \vdots \\ K_{n1} & K_{n2} & \dots & K_{nn} \end{bmatrix} \begin{Bmatrix} d_1 \\ d_2 \\ \vdots \\ d_n \end{Bmatrix}$$

Where: now n is the structure total number of unknown nodal degrees of freedom

Step 7: Solve for element strains and stresses.

Important secondary quantities of strain and stress (or moment and shear force) can be obtained for the structural stress-analysis problem because they can be directly expressed in terms of the displacements determined in steps three and six.

Step 8: Interpret the results.

Step eight entails interpreting the results, which necessitates critical thinking. The primary goal is to identify the locations where the structure experiences significant stresses or deformations to improve the design process. Postprocessor computer software

aids user comprehension by displaying results in a variety of graphical formats (Logan, 2022).

4.3.2 Implementation of the Finite Element Method

Both structural and nonstructural problems can be analyzed using the finite element method. Stress analysis, including truss and frame analysis, and stress concentration problems typically associated with holes, fillets, or other changes in geometry in a buckling body are examples of typical structural areas.

Vibration analysis Nonstructural problems include

- Heat transfer
- Fluid flow, including seepage through porous media
- Distribution of electric or magnetic potential

4.3.3 Finite Element Analysis Software SAP200

A linear finite element analysis for buckling of spherical concrete shells was performed in this investigation using a finite element computer program, SAP2000® Version 21.

Buckling occurs physically when a structure becomes unstable under a given loading arrangement, and mathematically when the solution to equations of static equilibrium bifurcates. Eigenvalue and Nonlinear buckling analyses are the two primary methods for performing buckling analysis. Buckling modes, unlike natural frequencies, are dependent on a given load pattern and must be explicitly evaluated for each set of loads considered.

Any number of load cases may be defined during buckling estimation, each of which should specify loading, convergence tolerance, and the number of modes to be found. Because the first few buckling modes may have similar factors, a minimum of six modes were considered in this study for each analysis.

SAP2000 supports incremental static loads, quasi-static cyclic loads (cyclic loads that vary slowly over time), combinations of horizontal and vertical seismic actions, inelastic dynamic analyses, and general-purpose hysteretic models.

To perform a nonlinear static analysis of the circular concrete dome shells with SAP2000, the domes must first be modelled as if they were linear-elastic static analysis

cases. The effect of material nonlinearity is not considered in the current analysis because only geometric nonlinearity is considered in the analysis of nonlinear cases.

Nonlinear static analysis can be used for a variety of purposes, including performing an initial P-delta or large-displacement analysis to determine the stiffness used for subsequent linear analyses.

Under a given set of loads, linear buckling analysis seeks the instability modes of a structure caused by the P-delta effect. Buckling analysis entails solving the generalized eigenvalue problem:

$$[K - \lambda G(r)]\varphi = 0 \qquad (4.15)$$

Where;

K is the stiffness matrix,

G(r) is the geometric (P-delta) stiffness due to the load vector r,

λ is the diagonal matrix of eigenvalues,

φ is the matrix of corresponding eigenvectors (mode shapes).

It is critical to understand that buckling modes are affected by the load. There is no single set of buckling modes for the structure, as there is for natural vibration modes. Buckling must be explicitly evaluated for each set of loads of concern.

In general, SAP2000 can account for geometric nonlinearity as P-delta effects or large-displacement/rotation effects. The elements' strains are assumed to be minor. In nonlinear static and direct-integration time-history analysis, geometric nonlinearity can be considered step by step and incorporated into the stiffness matrix for linear analysis.

Nonlinear static and nonlinear direct-integration time-history analysis may consider the following types of geometric nonlinearity:

- None: All equilibrium equations are taken into account in the structure's undeformed configuration.
- Only P-delta: The equilibrium equations take into account the structure's deformed configuration in part. Tensile forces tend to resist element rotation and

stiffen the structure, whereas compressive forces tend to promote element rotation and destabilize the structure. This could necessitate a moderate amount of iteration.

- Large displacements: All equilibrium equations are written in the deformed configuration of the structure. This may necessitate a large number of iterations; Newton-Raphson iterations are usually the most effective. Although large displacement and rotation effects are modelled, all strains are assumed to be small. P-delta effects are included (Wilson, 2015).

CHAPTER 5 RESULT AND DISCUSSION

5.1 Classical Theory Critical Buckling Load Results

Tables 5.1, 5.2, and 5.3 show the values of critical buckling load and shallowness parameters for each model. These values for the individual parameters of a circular dome cap are calculated using equations 2.73 and 2.80, respectively.

Table 5-1: Dome caps with a thickness of 0.1m have a critical buckling load and a shallowness parameter

No. models	Elastic Modulus (E_c) in Mpa	Poisson's ratio (v)	The radius of curvature (a) in (m)	Dome height (H) in m	Classical buckling load in kN/m^2	Shallowness parameter (λ)
1	33000	0.2	40	5.3590	243.065	19.0729
2			35	6.2772	317.473	20.6423
3			30	7.6393	432.116	22.7645
4			25	10.000	622.248	26.0540
5			20	20.000	972.262	36.8459

Table 5-2: Dome caps with a thickness of 0.12m have a critical buckling load and a shallowness parameter

No. Models	Elastic Modulus (E_c) in Mpa	Poisson's ratio (v)	The radius of curvature (a) in m	Dome height (H) in (m)	Classical buckling load in kN/m	Shallowness parameter (λ)
6	33000	0.2	40	5.3590	350.0145	17.4111
7			35	6.2772	457.1618	18.8437
8			30	7.6393	622.2480	20.7811
9			25	10.000	896.0371	23.7839
10			20	20.000	1400.058	33.6354

Table 5-3: Dome caps with a thickness of 0.15m have a critical buckling load and a shallowness parameter

No. Models	Elastic Modulus (E_c) in Mpa	Poisson's ratio (v)	The radius of curvature (a) in (m)	Dome height (H) in (m)	Classical buckling load in (kN/m^2)	Shallowness parameter (λ)
11	33000	0.2	40	5.3590	546.8987	15.5729
12			35	6.2772	714.3153	16.8543
13			30	7.6393	972.2625	18.5872
14			25	10.000	1400.058	21.2730
15			20	20.000	2187.590	30.0846

As shown in Tables 5.1, 5.2, and 5.3 above, the classical buckling load value of each model with constant span and identical thickness has an inverse relationship with the principal radius of a circular dome, which is measured from the axis of revolution.

All values of the shallowness parameter greater than seven are called deep spheres; thus, the pre-buckling behaviour can be more linear and more similar to the value of bifurcation buckling.

5.2 Linear buckling analysis Using SAP2000

The classical theory buckling formulation evaluates the bifurcation buckling of thin spherical shell structures; as defined in Equation 2.73 in chapter two, this type of buckling behaviour only occurs in deep perfect spherical shells; for shallow ones, axisymmetric snap-through buckling is expected.

Although to certify this theory and demonstrate the reliability of the proposed numerical technique, all models are subjected to an eigenvalue buckling analysis with linear elastic buckling behaviour and a perfect geometric condition to show the bifurcation buckling response of the models, covering a wide range of geometries commonly found in practice.

SAP2000 includes a "Buckling" integrated solution for structural analysis and a design analysis manual that allows for the determination of this specific type of linear buckling. The process is based on a classical eigenvalue problem, which is mentioned in Chapter 4 by equation 4.14 and is used to determine the loads for which the model stiffness matrix becomes singular.

In general, the bifurcation or linear buckling in this paper is calculated using SAP2000 using the following forms:

$$P_{Ex} = P_o + (\lambda Q) \qquad (5.1)$$

Where;

P_{EX} is a critical buckling load in SAP2000

P_o is the load applied in the initial state

λ Is Load factor or eigenvalue

Q is the applied load or perturbation load

Figure 5.1 depicts the Model 1 model, which is based on the geometry and material properties discussed in previous sections. No initial loading is considered for analysis; however, as shown in the figure, a uniform pressure normal to the surface equal to 3.56kN/m^2 is applied to the entire surface of a structure. As a result, the load factor or eigenvalue obtained directly from the analysis result, multiplied by the applied load, represents the structure's linear or classical buckling pressure. Figure 5.2 depicts this result, as well as the deformed shape of the structure in a bifurcation buckling state.

For all 15 models, an equivalent mechanism is handled; however, for clarity, only the finite element idealization of Model 1 is presented. Tables 5.4, 5.5, and 5.6 summarize the results of the SAP2000 finite element (FE) analysis.

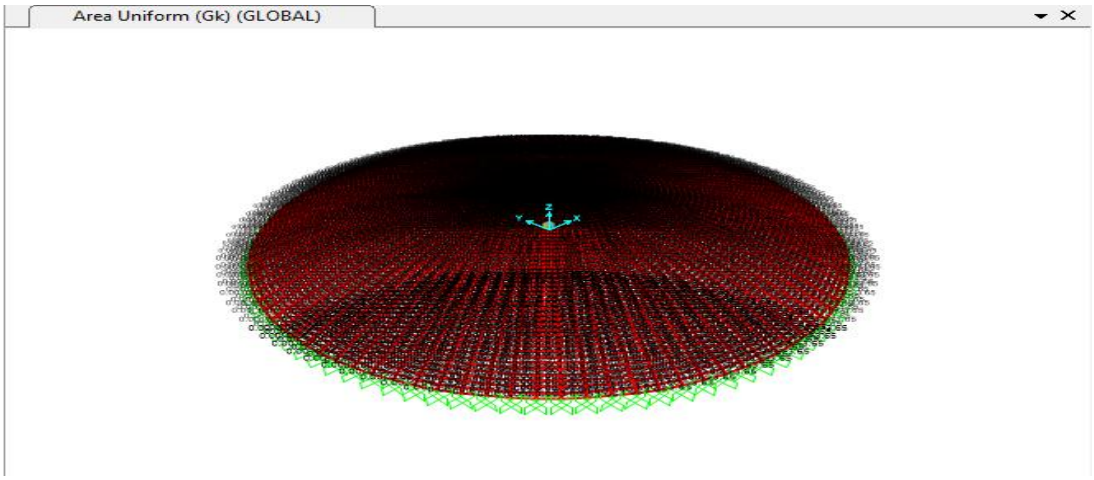

Figure 5-1: Sample of FE idealization of the first model loaded 3.65kn/m^2 uniform load.

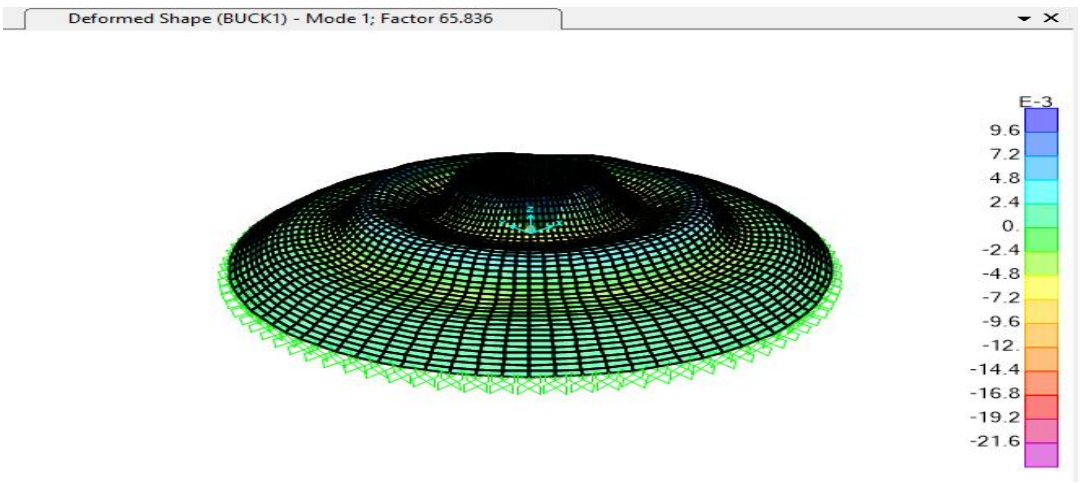

Figure5-2:The linear eigenvalue buckling load factor in the first mode failure (mode one)

Tables 5.4, 5.5, and 5.6 show the critical linear buckling pressure calculated from SAP200 for each model using a dead load of 3.65kN/m^2 for 1-5 models, 4.15 kN/m^2 for 6-10 models, and 4.90 kN/m^2 for 11-15 models.

Table 5-4: SAP200 V21.1.0 experienced critical buckling due to an applied load of 3.65kN/m^2 at h=0.1m

No. Models	Buckling load in SAP200 (kN/m^2)
1	240.3014
2	316.8189
3	432.8345
4	623.5110
5	972.2950

Table 5-5: SAP200 V21.1.0 experienced critical buckling due to an applied load of 3.65kN/m^2 at h=0.12m

No. Models	Buckling load in SAP200 (kN/m^2)
6	352.0449
7	344.9779
8	625.3079
9	899.6461
10	1401.7887

Table 5-6: SAP200 V21.1.0 experienced critical buckling due to an applied load of 3.65kN/m^2 at h=0.15m

No. Models	Buckling load in SAP200 (kN/m^2)
11	552.6318
12	543.2586
13	980.6380
14	1409.5242
15	2194.5655

The numerical values of an experimental linear buckling pressure are increased with increasing the thicknesses of the concrete dome; which are in the same geometric parameters; for example, model-1, model-6, and model-11 have identical geometric parameters. Furthermore, the linear buckling pressure of a circular concrete dome increases in value as the rise of the concrete dome increases.

5.3 Comparison between Classical buckling Equation and SAP2000 Results

The linear buckling result of SAP2000 was obtained by applying a dead load of 3.65 kN/m^2 to models 1-5, 4.15 kN/m^2 to models 6-10, and 4.90 kN/m^2 to models 11-15, while the classical buckling load was calculated using equation 2.73, as explained in chapter two. As a result, the comparison of their results is shown in percentages in Table 5.7, 5.8 and 5.9 below.

Table 5-7: In the case of 3.65kN/m^2, comparisons of classical buckling pressure with SAP200 results

Thickness, m	No. Model	Classical buckling load, kN/m^2	Buckling load from SAP2000, kN/m^2	Error in Percentages (%)
0.1	1	243.0656	240.3014	-1.1372
	2	317.4735	316.8187	-0.2063
	3	432.1167	432.8345	+0.1661
	4	622.2480	623.5110	+0.203
	5	972.2625	972.2950	+0.0033

Table 5-8: In the case of 4.15kN/m^2, comparisons of classical buckling pressure with SAP200 results

Thickness, m	No. Models	Classical buckling load, kN/m^2	Buckling load from SAP2000, kN/m^2	Error in Percentages (%)
0.12	6	350.0145	352.0449	+0.5801
	7	457.1618	344.9479	-24.5458
	8	622.2480	625.3079	+0.4915
	9	986.0372	899.6461	-8.7614
	10	1400.0580	1401.7887	+0.1236

Table 5-9: In the case of 4.90kN/m^2, comparisons of classical buckling pressure with SAP200 results

Thickness, m	No. Models	Classical buckling load, kN/m^2	Buckling load from SAP2000, kN/m^2	Error in Percentages (%)
0.15	11	546.8987	552.6318	+1.0483
	12	714.3153	543.2586	-23.9469
	13	972.2625	980.6380	+0.8614
	14	1400.0580	1409.5242	+0.6761
	15	2187.5906	2194.5655	+0.3188

The negative percentage denotes a decrease in the experimental linear buckling value from SAP2000 when compared to the theoretical values of perfect spherical dome caps. As shown in the tables, the maximum deviation occurs in the second model of a concrete dome cap, which is 25%. The percentage deviations of the concrete domes between the theoretical and experimental values of a buckling load are nearly identical.

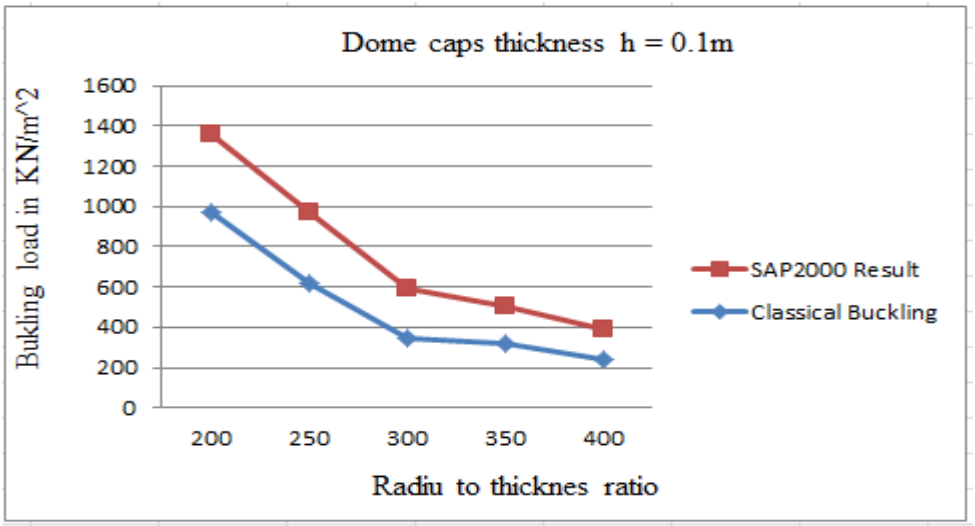

Figure 5-3: The effect of radius to thickness ratio at the applied uniform pressure of 3.65kN/m^2.

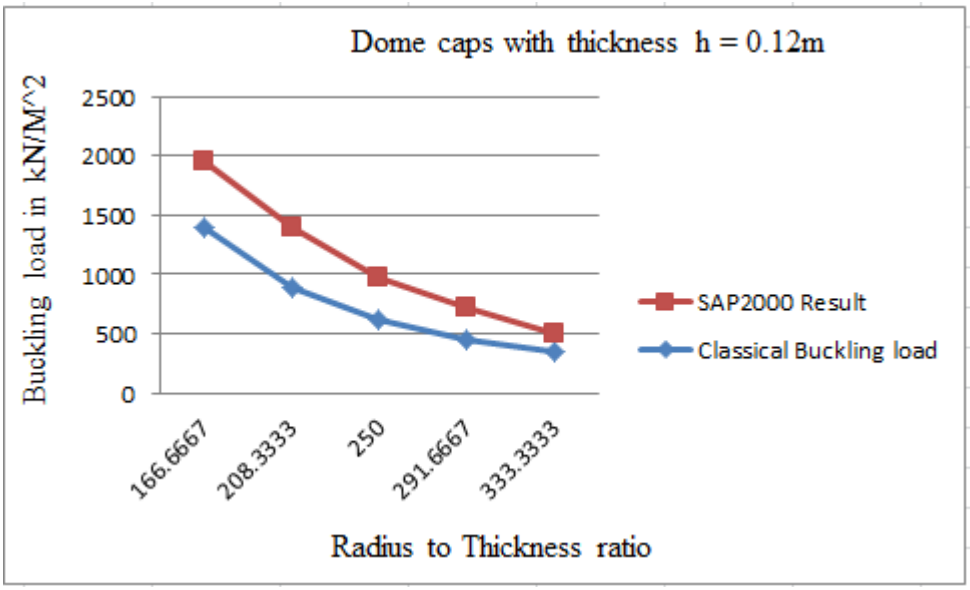

Figure5-4: The effect of radius to thickness ratio at the applied uniform pressure of $4.15kN/m^2$

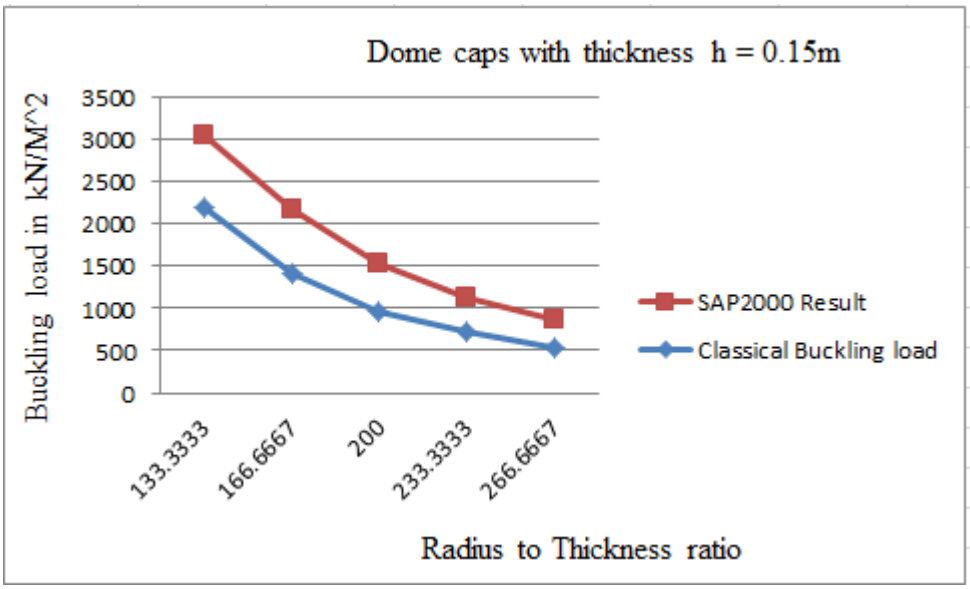

Figure5-5: The effect of radius to thickness ratio at the applied uniform pressure of $4.90kN/m^2$

The graphs in Figures 5.2, 5.3, and 5.4 depict the relationship between the classical and numerical buckling loads and the corresponding values of radius to thickness ratio; their correlation is inversely proportional when compared one to another. This implies that even if the concrete dome caps have the same geometry, the values of the radius-to-thickness ratio increase as the buckling pressure values decrease.

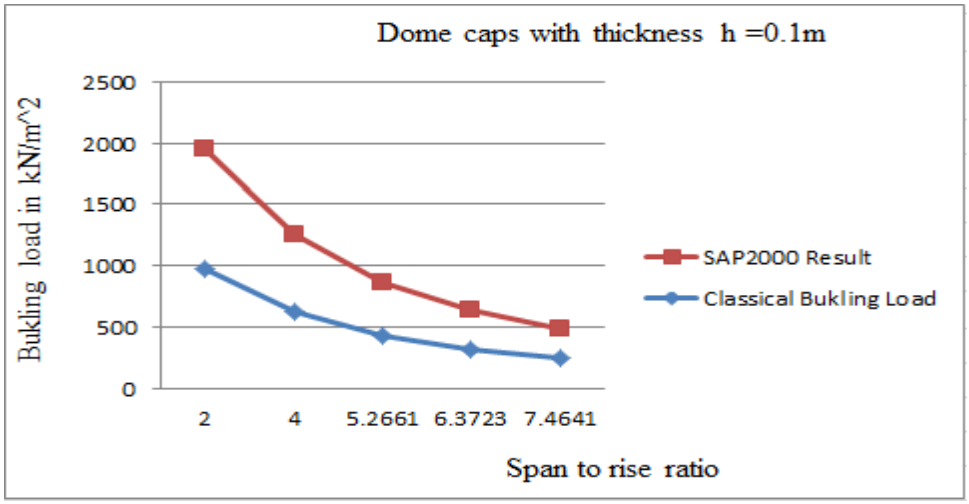

Figure5-6: The effect of span-to-rise ratio at the applied uniform pressure of 3.65kN/m^2

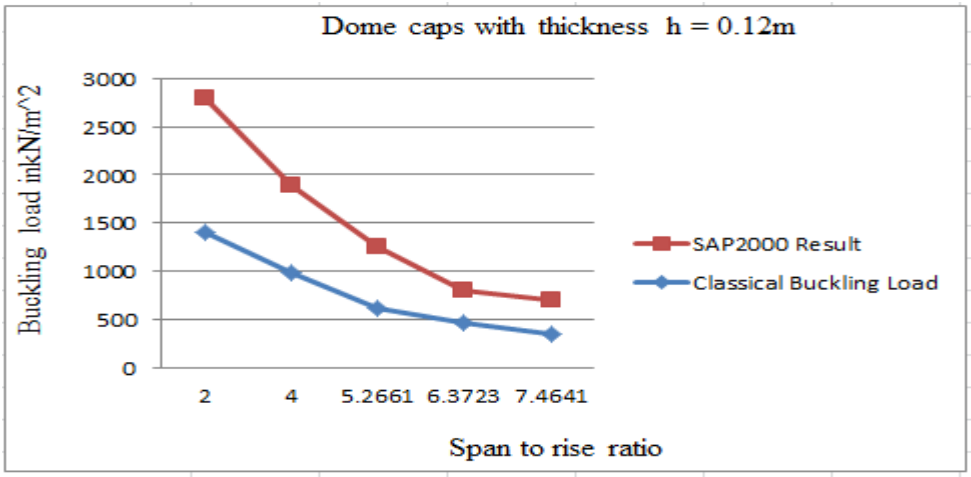

Figure5-7: The effect of span-to-rise ratio at the applied uniform pressure of 4.15kN/m^2

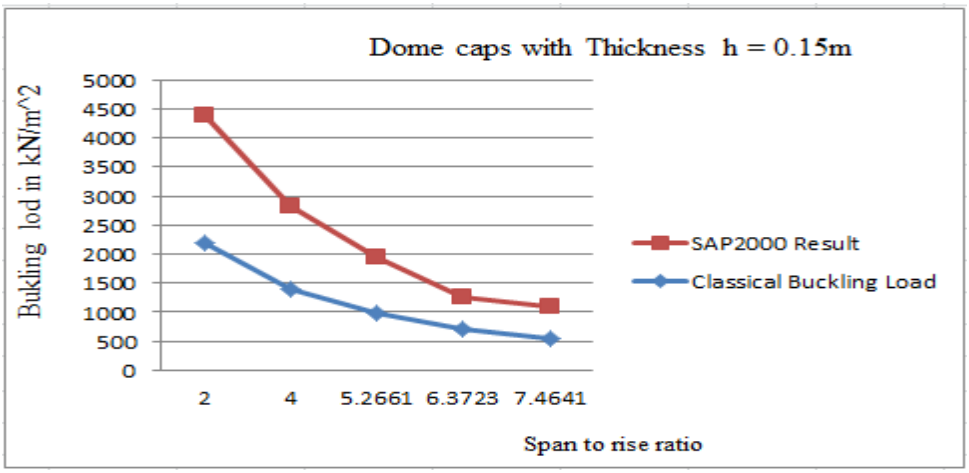

Figure5-8: The effect of span-to-rise ratio at the applied uniform pressure of 4.90kN/m^2

The graphs in Figures 5.5, 5.6, and 5.7 depict the interconnection between the buckling pressure and the span-to-raise (height) ratio of a dome with varying thicknesses; this bonding has shown that the critical buckling load value decreases as the span-to-raise (height) ratio of a concrete shell with constant span increases.

5.4 Effect of Support Conditions

The effect of stability of the support conditions of concrete domes is studied for three cases, taking into account the support condition fixed for rotation and movement (Fixed), fixed for movement and free to rotate (pinned), Dome models with edge ring beams, and only fixed for vertical movement along Z-axis; which is roller support conditions.

The roller support condition has negligible effects on the buckling pressure resulting from the linear analysis, according to realized observations in the fixity of the abutment of concrete dome caps. As a result, the roller support case is excluded from the comparison of support conditions.

Table 5-10: SAP200 results show a comparison of fixed and pinned support conditions for buckling pressures.

Thickness, m	No. Models	Buckling pressure, kN/m^2 at fixed support.	Buckling pressure, kN/m^2 at pinned support.	Percentages (%)
0.1	1	144.8291	141.0053	2.6402
	2	188.0536	180.8117	3.8510
	3	252.9286	238.7339	5.6121
	4	348.6068	320.7300	7.9966
	5	389.6115	334.6840	14.0980
0.12	6	158.0297	153.0071	3.1783
	7	265.1181	255.5620	3.6054
	8	356.5818	337.0727	5.4711
	9	493.8598	453.9459	8.0820
	10	556.1893	472.3401	15.0757
0.15	11	312.5984	303.9970	2.7516
	12	406.7193	391.0219	3.8595
	13	545.0046	516.2439	5.2771
	14	758.8397	695.4488	8.3537
	15	863.4189	726.9131	15.8099

According to the results in Table 5.10, fixed support conditions have a better effect on buckling pressure resulting from linear analysis than pinned support conditions. According to this, Fixed or clamped boundary conditions are superior to other remaining supports in the design of reinforced concrete spherical shell domes. This means that in the case of uniformly distributed loading, fixed supports are better suited for buckling considerations. Why? Because the stiffness of the shell increases near the dome's edge.

5.5 Buckling Analysis of the Effect of a Horizontal Component of Seismic Actions on a Concrete Spherical Shell

To investigate the effect of horizontal action or lateral loading, such as seismic actions, on the maximum stresses that concrete spherical shells can withstand without serious side effects before buckling, the effect of the horizontal component of earthquake loading on the buckling pressure of circular shells is analyzed by applying only seismic action and the combination of dead load with earthquake action. We used the same procedure as described in section 5.1.2 to calculate the linear buckling load. The outcome of these load cases is shown in the table below.

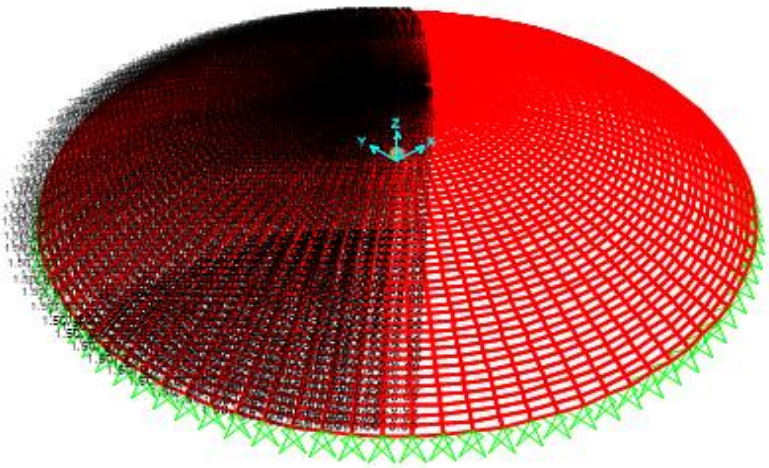

Figure5-9; Sample for seismic action loading on spherical dome models

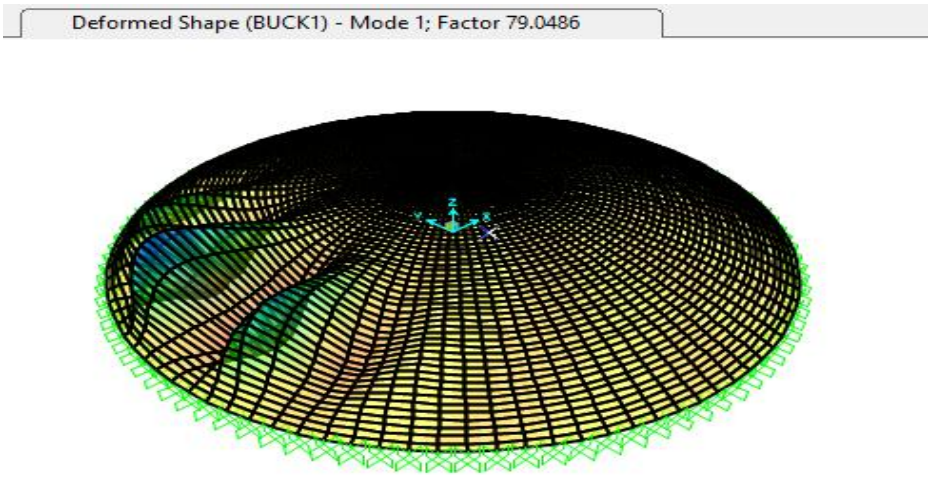

Figure5-10: The buckling load factor in the dome's first mode failure under seismic action (mode one)

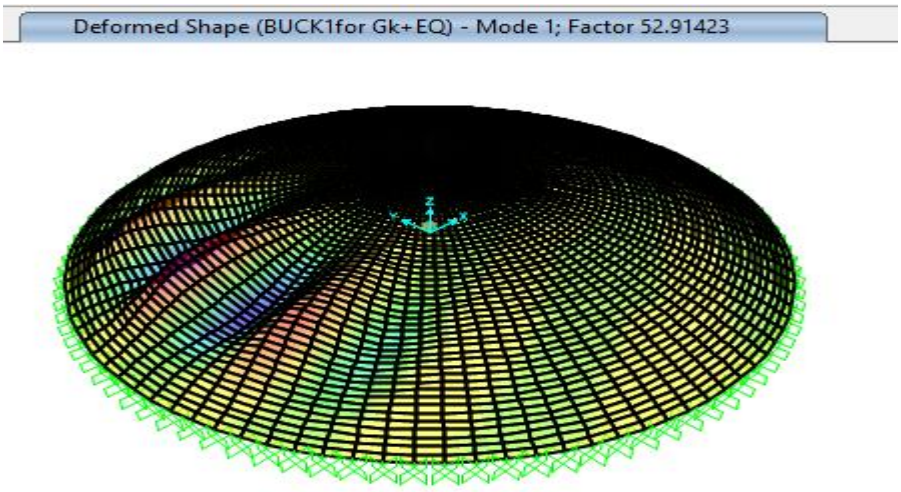

Figure5-11: The eigenvalue buckling load factor in the dome's first mode failure under seismic action and its self-weight (mode one)

Figures 5.10 and 5.11 show the buckling load factors of a concrete dome under only seismic action and the combination of self-weight and seismic action, respectively. The buckling load factor has an inverse relationship with the initially applied loads, which means that as the load increases, the numerical value of the buckling load factor on the same mode decreases and vice versa.

Table 5-11: Comparison of the effect of seismic action alone and earthquake load plus self-weight on the linear buckling load of shells.

Thickness (h) in m	No. models	Buckling load due to(E_X) in (kN/m^2)	Buckling load due to G_K in (kN/m^2) only	Buckling pressure due to ($G_K + E_X$) (kN/m^2)	Percentages (%) difference.
0..1	1	118.5734	243.0656	277.6586	-14.2320
	2	207.3608	317.4735	353.6916	-10.2400
	3	279.4074	432.1167	469.9665	-8.7592
	4	395.6349	622.2480	663.7093	-6.6631
	5	585.9389	972.2625	654.1175	348.6373
0.12	6	228.1409	350.0145	400.1202	-12.5227
	7	305.4555	457.1618	510.3214	-10.4169
	8	404.0660	622.2480	671.8377	-7.3812
	9	571.3502	986.0372	943.1000	4.5528
	10	417.3037	1400.0580	951.3586	47.1641
0.15	11	552.9501	546.8987	628.3341	-12.9605
	12	600.9451	714.3153	627.4289	-1.8480
	13	668.9504	972.2625	1049.9110	-7.3957
	14	743.4378	1400.0580	1456.0196	-3.9047
	15	660.5181	2187.5906	1520.3581	43.8865

Based on the results in Table 5.11, the linear buckling pressures in column five have been decreasing as the load combination has increased when compared to the result of the dome's self-weight.

Concerning the geometrical parameters of the spherical dome, the linear buckling pressure due to the consolidation of more than two types of load has been reduced as the geometric parameters have been expanded (i.e thickness; cutting angle and radius of a circular concrete dome with constant span). According to columns 4 and 5, the numerical buckling load values at the half spheres due to seismic action and dead load have been reduced by 40% to 50% when compared to the outcome of the dome's self-weight.

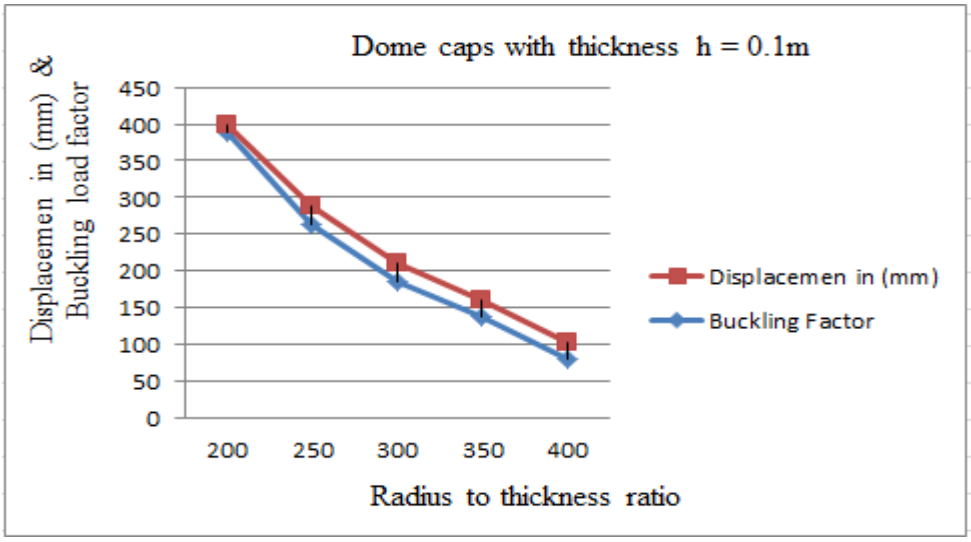

Figure5-12: The effect of radius to thickness ratio at the applied uniform pressure of seismic action of 1.5kN/m^2

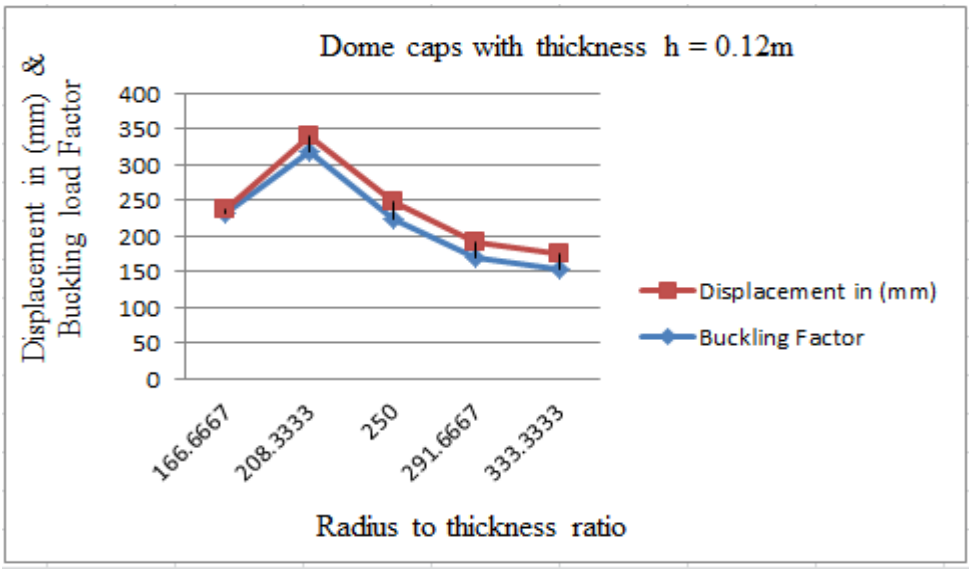

Figure 55-13: The effect of radius to thickness ratio at the applied uniform pressure of seismic action of 1.8kN/m^2

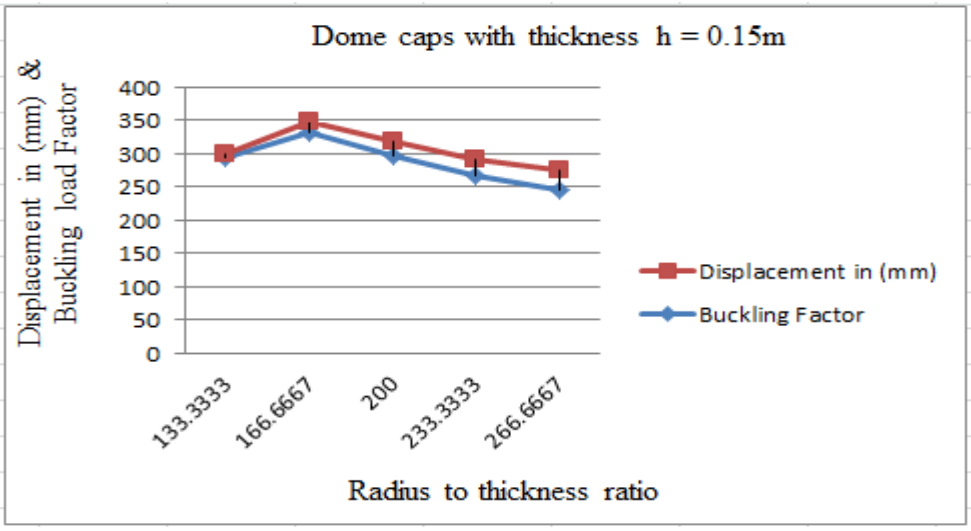

Figure5-14: The effect of radius to thickness ratio at the applied uniform pressure of seismic action of 2.25kN/m^2

The graphs in Figures 5.12, 5.13, and 5.14 show the relationship between the buckling load factor, displacement (deformation), and the corresponding values of the radius-to-thickness ratio; their correlation is inversely proportional when compared to the other. This means that even if the concrete dome caps have the same geometry, the values of the radius-to-thickness ratio increase as the buckling factor and displacement values decrease.

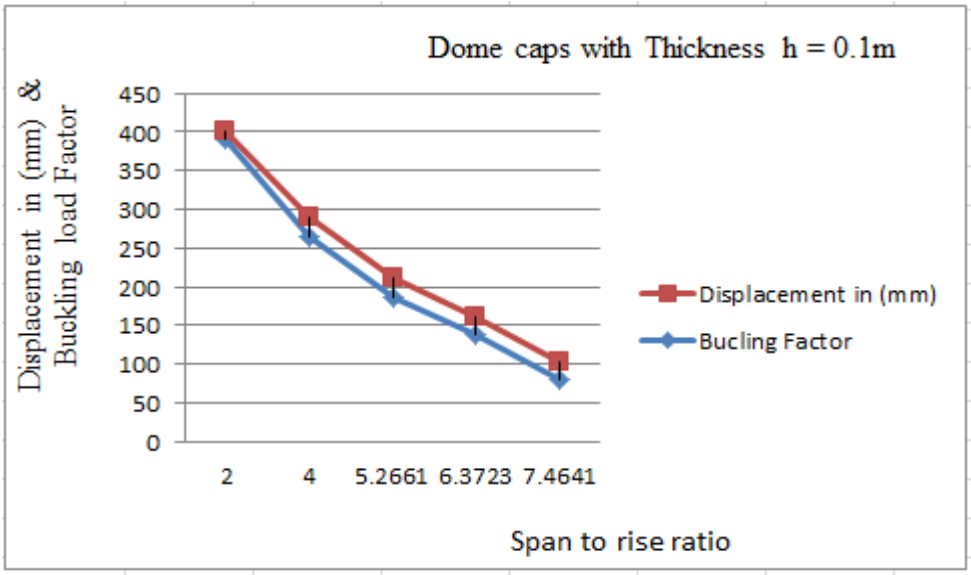

Figure5-15: The effect of span to raise ratio at the applied uniform pressure a seismic action of 1.5kN/m^2

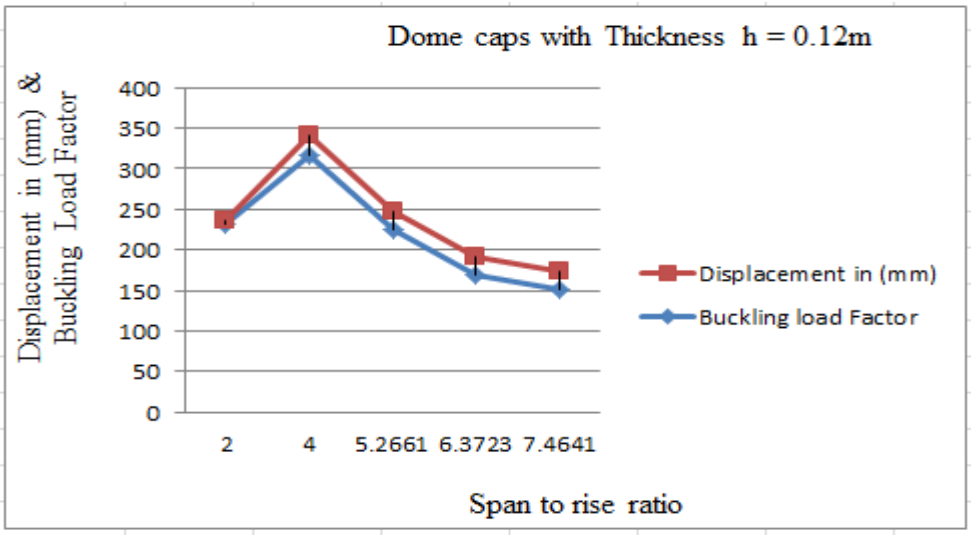

Figure5-16: The effect of span to raise ratio at the applied uniform pressure a seismic action of 1.8kN/m^2

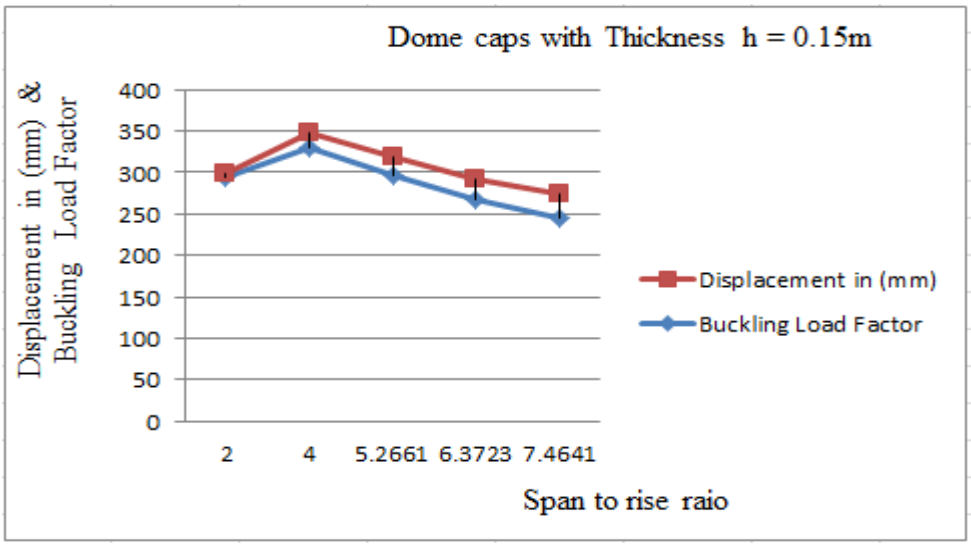

Figure5-17: The effect of span to raise ratio at the applied uniform pressure a seismic action of 2.25 kN/m^2

The graphs in Figures 5.15, 5.16, and 5.17 show the relationship between the buckling load factor, displacement, and the span-to-raise (height) ratio of a circular concrete dome with different thicknesses; this bonding has shown that the buckling load factor and displacement values decrease as the span-to-raise (height) ratio of a concrete shell with constant span increases.

5.6 Effect of Geometric Imperfection

According to Mehdi et al. (1981), the collapse of a spherical cap is greatly dependent on the status of geometrical imperfection and based on the findings of many studies, the minimum withstands a buckling pressure of a spherical cap is one with a shallowness parameter (λ) equal to 4 (Zarghamee and Sarawit, 2020).

Nonlinear buckling analysis is carried out for geometric imperfect circular shells. Corresponding to the cases expressed in an earlier topic in chapter two, an imperfection status parallel to the shallowness parameter of 4 is assumed for all models, as suggested by the span (D) and radius (R imp) at the imperfection region for the shells, respectively. Appendix-A shows all numerical values of the geometrical parameter of the imperfect spherical shell.

Table5-12: Analytical result for linear and nonlinear buckling pressure

Thickness in (m)	Shallowness parameters (λ)	No. models	Linear classical buckling in (kN/m^2)	Nonlinear buckling in (kN/m^2)	Error in %
0.1	4	1	243.0656	68.0625	-71.998
		2	317.4735	88.8998	-72
		3	432.1167	121.0000	-72
		4	622.2480	174.2400	-72
		5	972.2625	272.2500	-72
0.12	4	6	350.0145	98.0100	-72
		7	457.1618	128.031	-71.99
		8	622.2480	174.2400	-72
		9	986.0372	250.9056	-74.55
		10	1400.0580	392.0400	-72
0.15	4	11	546.8987	153.1406	-72
		12	714.3153	200.0204	-72
		13	972.2625	272.2500	-72
		14	1400.0580	392.0400	-72
		15	2187.5906	612.5625	-72

According to the results of Table 5.12, there is a significant reduction in the buckling magnitude of the models where the response of nonlinearity in the presence of geometric imperfection is considered. Based on the results, such a conclusion can result in a 72% reduction in the model's buckling efficiency, demonstrating a discernible difference between the two expressions.

CHAPTER 6 CONCLUSIONS AND RECOMMENDATIONS

6.1 Conclusions

This study tried to forward the following concluding remarks based on the results obtained in chapter five.

- A linear relationship exists between the buckling load factor and the deformation of a concrete shell; however, the relationship between the radius-to-thickness ratio and the span-to-rise (height) ratio of a spherical concrete dome is reciprocal.
- Radiuses of curvature and span (base diameter) of domes have a significant effect on the linear buckling magnitude.
- Linear buckling pressures have been reduced as the load combination has been increased in comparison to the self-weight of the dome.
- In linear buckling load analysis cases, the proposed finite element method agrees well with the analytical results. As a result, in future studies, the P-delta buckling analysis method in SAP2000 could be used.
- The effect of the horizontal component of seismic action on the buckling magnitude of the dome structure increases as the radius-to-thickness ratios decrease; a similar pattern is also observed for low dome rise-to-base diameter (span) ratios; however, in the case of this study, they are linked in most cases to the low radius to thickness ratios, and no conclusive finding is obtained about the effect of this parameter.
- In general, the buckling capacity of spherical shells fixed at the base is greater than that of pinned shells; however, this is not always the case. The acquired variation between the two cases is insignificant, indicating that such an effect is minor.
- Under geometric imperfections, the buckling capacity of the models is reduced by up to 72% when compared to linear buckling efficiencies in circular (spherical) concrete shells with shallowness parameter four.

6.2 Recommendations

Based on the results of this study, some advice and suggestions for future research on the effect of dead load, live load, and the horizontal component of seismic action on the buckling of circular concrete shells are provided.

- The buckling response of circular shells under the combined effect of vertical and horizontal acceleration seismic action can be investigated further to be as close to reality as possible.
- Future research can include the effects of material nonlinearity, such as reinforcement yielding, concrete cracking and crushing, and creep in concrete dome shells.
- Understanding the buckling response of circular shells under the combined effect of wind load, earthquake load, accidental loads, and dead load can be useful for future research.
- The combined effect support conditions; constant cutting angle and radius of curvature can be investigated further to learn about the buckling behaviour of concrete shells of revolution.

REFERENCES

Billington, D.P., 1982. Thin shell concrete structures. McGraw-Hill College.

En, B., 2004. 1-1. Eurocode 2: Design of concrete structures–Part 1-1: General rules and rules for buildings. Eur. Comm. Stand. CEN.

Ethiopia Building Code Standard Based on European Norme, (EBSCEN1998-1: 2004), 'Design of Structures for Earthquake Resistance', Part-1: General Rules, Seismic Actions and Rules for Buildings.

Farnsworth, D.B., 1999. Behavior of shell structures (PhD Thesis). Massachusetts Institute of Technology.

Farshad, M., 2013. Design and analysis of shell structures. Springer Science & Business Media.

Logan, D.L., 2022. First Course in the Finite Element Method, Enhanced Edition, SI Version. Cengage Learning.

Madueno, N.E.M., Moslemi, M., Kianoush, R., 2020. Effect of Horizontal Earthquake on Buckling of Concrete Domes. ACI Struct. J. 117, 243–253.

Mekjavić, I., 2011. Buckling analysis of concrete spherical shells. Teh. Vjesn. 18, 633–639.

Peerdeman, B., 2008. Analysis of thin concrete shells revisited: Opportunities due to innovations in materials and analysis methods Master's thesis-Department of Structural and Building Engineering. Fac. Civ. Eng. Geosci. Delft Univ. Technol.

Rotter, J. Michael, Mackenzie, G., Lee, M., 2016. Spherical dome buckling with edge ring support, in Structures. Elsevier, pp. 264–274.

Rotter, J Michael, Mackenzie, G., Lee, M., 2016. Spherical dome buckling with edge ring support. Presented at the Structures, Elsevier, pp. 264–274.

Varghese, P.C., 2010. Design of reinforced concrete shells and folded plates. PHI Learning Pvt. Ltd.

Verwimp, E., Tysmans, T., Mollaert, M., Berg, S., 2015. Experimental and numerical buckling analysis of a thin TRC dome. Thin-Walled Struct. 94, 89–97.

Wilson, A., 2005. The practical design of concrete shells. Monolithic Dome Institute.

Wilson, E., 2015. CSI analysis reference manual for SAP 2000, ETABS, SAFE and CSI bridge. Berkeley Comput. Struct. Inc.

Zarghamee, M.S., Sarawit, A.T., 2020. Buckling of Shallow Spherical Concrete Domes under Gravity and Earthquake Loads. J. Struct. Eng. 146, 04020053.

Zolqadr, E., An, M., 2017. Buckling of spherical concrete shells. MEng Thesis Dep. Civ. Eng. Ryerson Univ. Tor. Can.

Euro code 0:2001, prEN 1990:2001. Eur-ocode - Basis of structural design.

Euro code 1, EN 1991-1-1:2002 (E). Actions on structures - Part 1-1: General actions - Densities, self-weight, imposed loads for buildings.

Euro code 2:, EN 1992-1-1:2004 (E). Design of concrete structures - Part 1-1: General rules and rules for buildings.

Habtamu Tegegne, 2020. 'Parametric Analysis of Meridional and Hoop Forces Response with Respect to Rise to Radius Ratio of Spherical Concrete Shell'. ADDIS ABABA UNIVERSITY.

APPENDIX A

Classification of spheres based on their corresponding geometric parameters (R; h & ∅) :

$\beta = \sqrt{2\emptyset(^{a}/_{h})}$ → If $\beta < 7$; the spherical cap is called the Shallow sphere

If $\beta \geq 7$; the spherical cap is called the Deep sphere

Where;

α is the radius of curvature of the concrete shell

h is the thickness of the shell

∅ is the cutting (central) angle of the shell in radian measures

The tabulated values of the period (T); fundamental frequencies (F) and angular frequencies (ω) for all cases are shown below.

Table A-1: Fundamental Free vibrational periods and their corresponding frequencies

No. Models	Fundamental period (T) in second	Fundamental Frequencies (1/T)	Fundamental natural frequencies in rad per second (**ω**)
1	0.1761	5.6786	35.6797
2	0.1983	5.0429	31.6855
3	0.2298	4.3516	27.3419
4	0.2812	3.5562	22.3443
5	0.4729	2.1146	13.2864

The tabulated values of horizontal component peak ground acceleration (m/s^2) and seismic load per unit area for all cases are shown below:

Table A-2: For a dome thickness (h) of 0.1m, the horizontal component of earthquake elastic response acceleration and its corresponding seismic load per unit area is given.

No. Models	Fundamental period (T) in second	The horizontal component of peak ground acceleration in $(\frac{\boldsymbol{m}}{\boldsymbol{S^2}})$	Seismic load in $(\frac{\boldsymbol{KN}}{\boldsymbol{m^2}})$
1	0.1761	5.8860	1.5000
2	0.1983	5.8860	1.5000
3	0.2298	5.8860	1.5000
4	0.2812	5.8860	1.5000
5	0.4729	5.8860	1.5000

Table A-3: For a dome thickness (h) of 0.12m, the horizontal component of earthquake elastic response acceleration and its corresponding seismic load per unit area is given.

No. Models	Fundamental period (T) in second	The horizontal component of peak ground acceleration in $(\frac{m}{S^2})$	Seismic load in $(\frac{KN}{m^2})$
1	0.1761	5.8860	1.8000
2	0.1983	5.8860	1.8000
3	0.2298	5.8860	1.8000
4	0.2812	5.8860	1.8000
5	0.4729	5.8860	1.8000

Table A-4: For a dome thickness (h) of 0.15m, the values of the horizontal component of earthquake elastic response acceleration and their corresponding seismic load per unit area are shown.

No. Models	Fundamental period (T) in second	The horizontal component of peak ground acceleration in $(\frac{m}{S^2})$	Seismic load in $(\frac{KN}{m^2})$
1	0.1761	5.8860	2.2500
2	0.1983	5.8860	2.2500
3	0.2298	5.8860	2.2500
4	0.2812	5.8860	2.2500
5	0.4729	5.8860	2.2500

Effect of Geometric Imperfection

The following formulas compute the geometric parameters of imperfect spherical shells.

D = $4.3\sqrt{hxR_{im}}$; Is the diameter of the sphere at the imperfect region.

R_{imp} = 1.4α; Is the radius of curvature of an imperfect shell

α; Is the radius of curvature of a normal spherical shell

h; Is the thickness of shells

For design purposes, the geometric imperfection factor of a spherical cap with shallowness parameter λ = 4 is assumed to be β_{im} = 0.5. As a result, the buckling pressure at the imperfect region with the original radius of curvature (α) and thickness (h) is given by:

$P_{cr} = 0.33E\,(h/R)^2$ .....Equation A-1

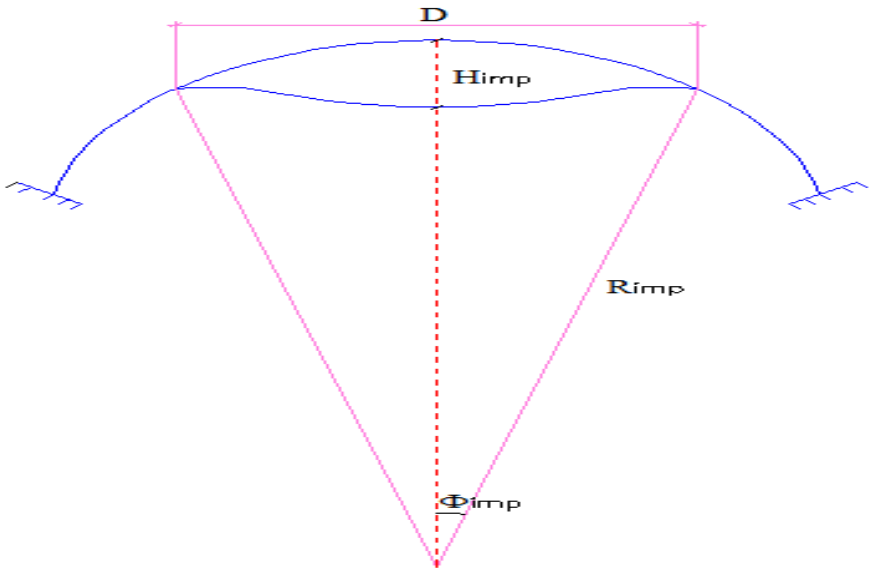

Figure A-1: Geometry of critical imperfection circular shell.

Table A-4: Geometric imperfection parameter values of all modes by assuming their shallowness parameters (λ) = 4

No. Model	Thickness in m	Radius (α) in m	Imperfection radius(R_{im}) (m)	Imperfection Diameter (D) (m)	Half central angle for imperfection	Height for imperfect (m)
1	0.1	40	56	10.18	5.2150	0.2318
2		35	49	9.52	5.5747	0.2318
3		30	42	8.81	6.0203	0.2316
4		25	35	8.05	6.6036	0.2322
5		20	28	7.20	7.3870	0.2324
6	0.12	40	56	11.15	5.7135	0.2782
7		35	49	10.43	6.1095	0.2783
8		30	42	9.65	6.5968	0.2781
9		25	35	8.81	7.2303	0.2783
10		20	28	7.88	8.0892	0.2786
11	0.15	40	56	12.46	12.46	0.3476
12		35	49	11.66	11.66	0.3481
13		30	42	10.79	10.79	0.3479
14		25	35	9.85	9.85	0.3482
15		20	28	8.81	8.81	0.3487

APPENDIX B

Table B- 1:The first 15 modal shapes and their respective load factor in case self-weight.

Modal shapes	Buckling load factors
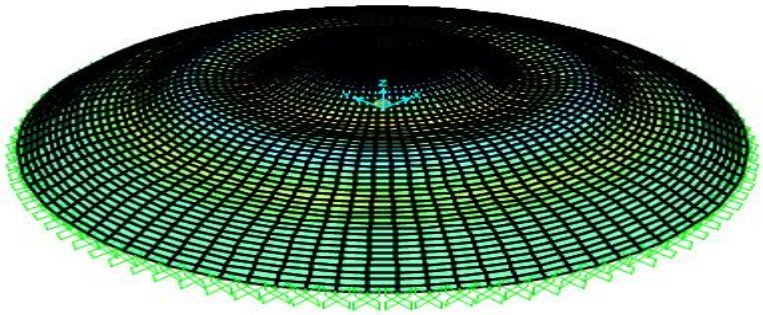	65.8360
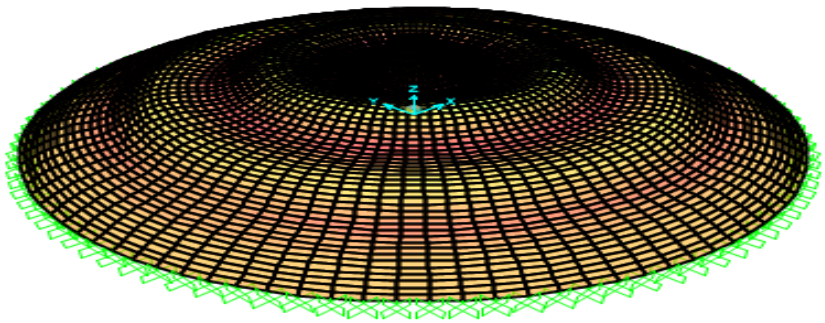	85.7862
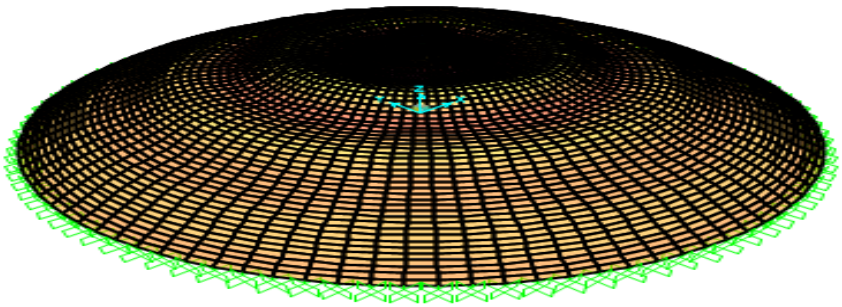	118.6195
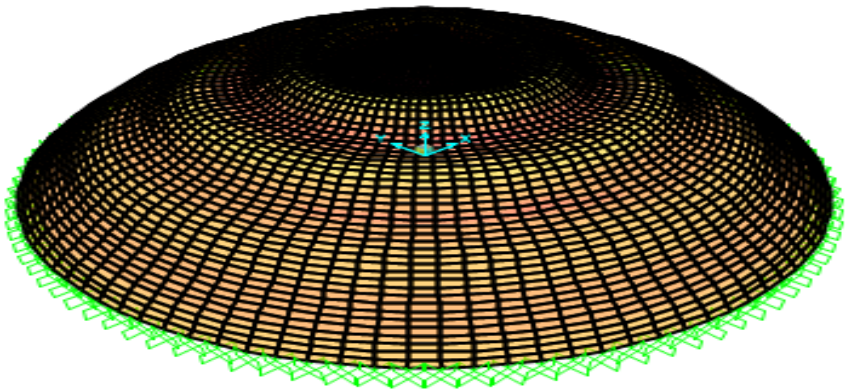	170.8304

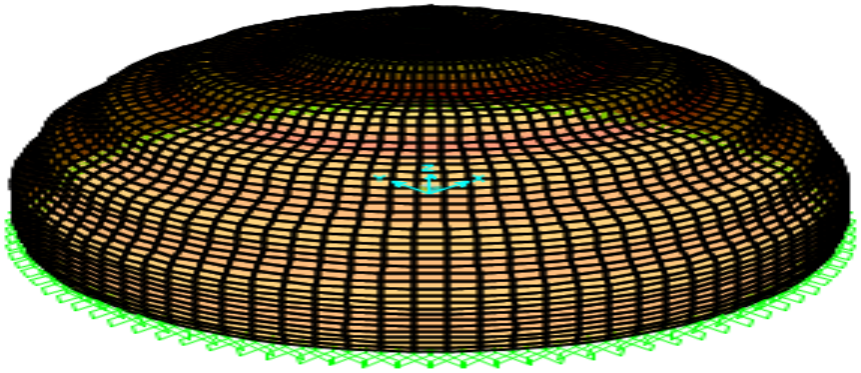	266.3822
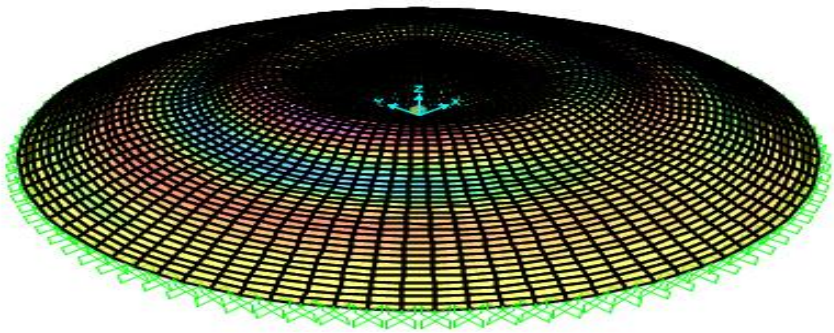	84.8301
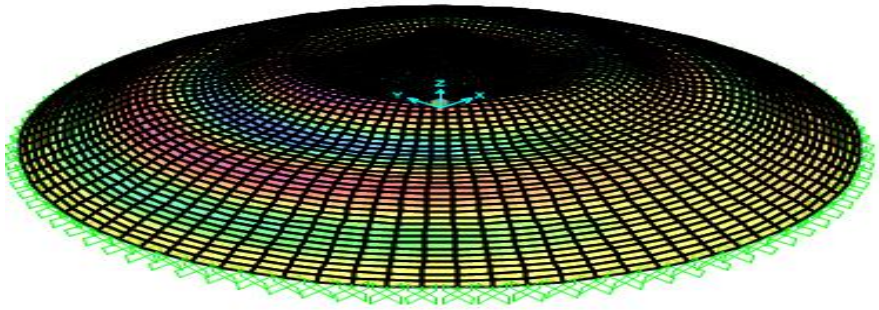	87.1278
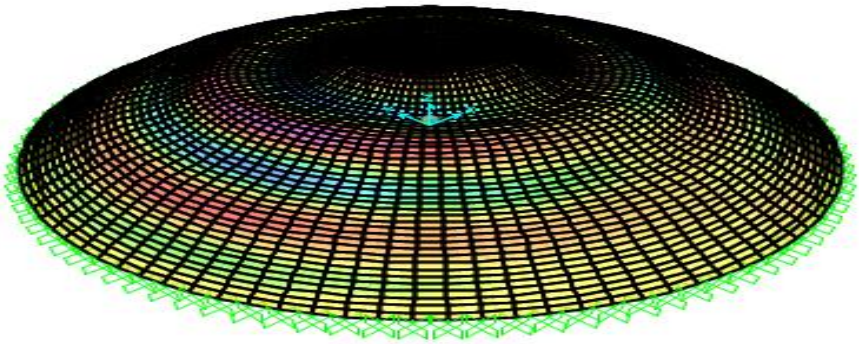	150.6766
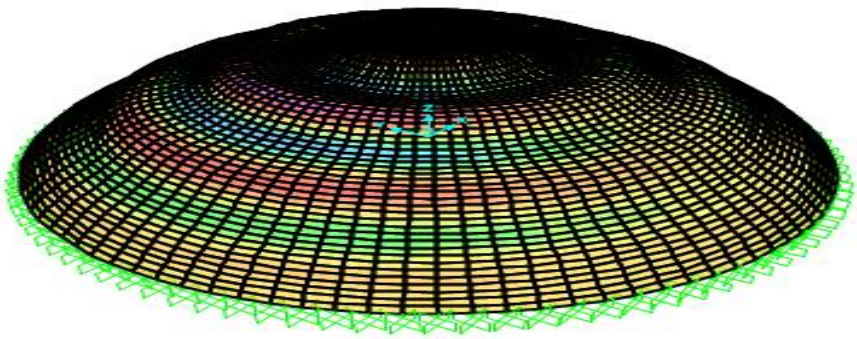	216.7822

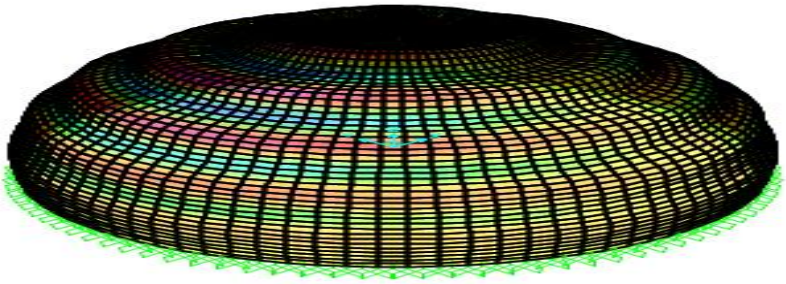	337.7804
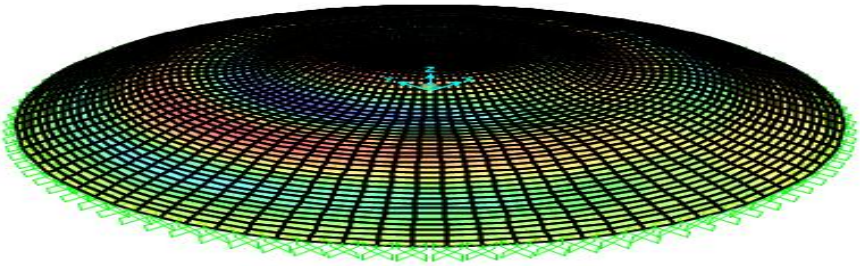	112.7821
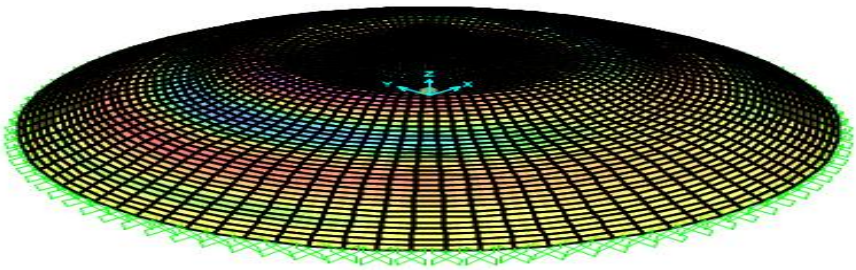	110.8691
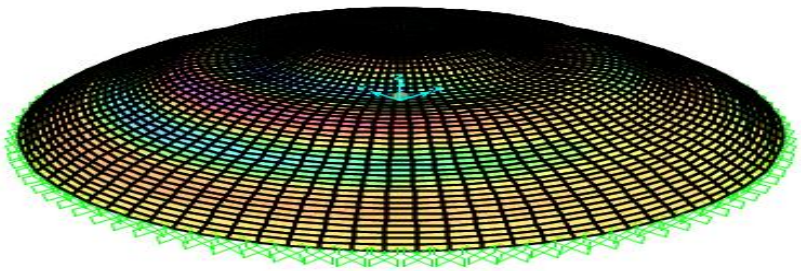	200.1302
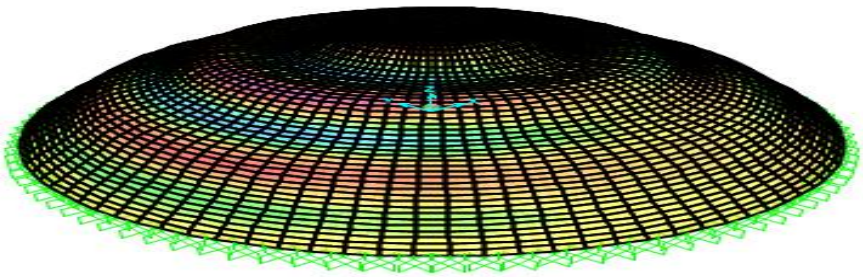	287.6580
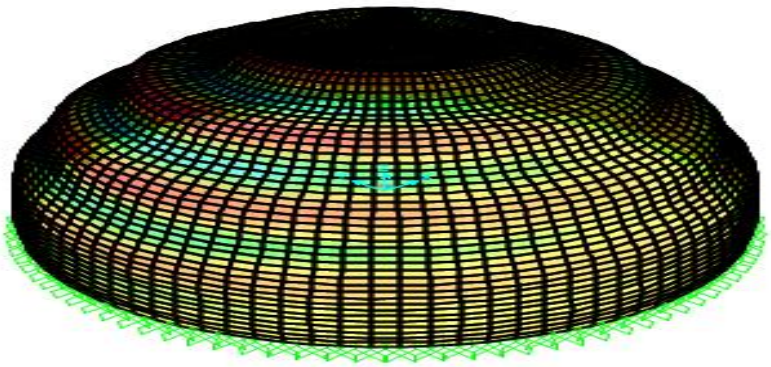	447.8705